



Azimuthal anisotropies of charged particles with high transverse momentum in Pb+Pb collisions at $\sqrt{s_{\text{NN}}} = 5.02$ TeV with the ATLAS detector

The ATLAS Collaboration

A measurement is presented of elliptic (v_2) and triangular (v_3) azimuthal anisotropy coefficients for charged particles produced in Pb+Pb collisions at $\sqrt{s_{\text{NN}}} = 5.02$ TeV using a dataset corresponding to an integrated luminosity of 0.44 nb^{-1} collected with the ATLAS detector at the LHC in 2018. The values of v_2 and v_3 are measured for charged particles over a wide range of transverse momentum (p_{T}), 1–400 GeV, and Pb+Pb collision centrality, 0–60%, using the scalar product and multi-particle cumulant methods. These methods are sensitive to event-by-event fluctuations and non-flow effects in the measurements of azimuthal anisotropies. Positive values of v_2 are observed up to a p_{T} of approximately 100 GeV from both methods across all centrality intervals. Positive values of v_3 are observed up to approximately 25 GeV using both methods, though the application of the three-subevent technique to the multi-particle cumulant method leads to significant changes at the highest p_{T} . At high p_{T} ($p_{\text{T}} \gtrsim 10$ GeV), charged particles are dominantly from jet fragmentation. These jets, and hence the measurements presented here, are sensitive to the path-length dependence of parton energy loss in the quark-gluon plasma produced in Pb+Pb collisions.

1 Introduction

The primary aim of the heavy-ion program at the Large Hadron Collider (LHC) is to produce and study the quark-gluon plasma (QGP), the high-temperature state of matter in which quarks and gluons are no longer confined within protons and neutrons (for a recent review, see Ref. [1]). Measurements of jets originating from hard parton scatterings in the early stages of heavy-ion collisions provide information about the short-distance-scale interactions of high-energy partons with the QGP (for a recent review, see Ref. [2]). The overall rate of jets at a given transverse momentum, p_T , is found to be reduced by approximately a factor of two in central Pb+Pb collisions compared to pp collisions scaled to account for the increased partonic luminosity in Pb+Pb collisions [3–6]. This suppression can be explained by the energy loss of partons propagating through the QGP, and the magnitude of this energy loss depends on the amount of QGP that the parton travels through.

The geometry of the overlap of the two nuclei leads to a shorter average path length if the jet is oriented along the direction of the collision impact parameter¹ than if the jet is oriented in the perpendicular direction. This is expected to lead to a dependence of the jet yield on the azimuthal angle [7–9]. Charged particles with p_T greater than 10 GeV, hereinafter referred to as high- p_T charged particles, are likely to come from jet fragmentation. Therefore, the measurements of azimuthal anisotropies of high- p_T charged particles are useful for investigating the path-length dependence of jet energy loss. An azimuthal modulation of the same direction is also present in the low- p_T charged particles due to the hydrodynamic flow of the QGP. The amplitudes of these anisotropies can be used to constrain the bulk properties of the QGP (for a review, see Ref. [10]).

The azimuthal anisotropies are quantified via the values of Fourier coefficients describing the azimuthal angular distribution of charged particles with respect to the event planes [11]:

$$\frac{dN}{d\phi} \propto 1 + 2 \sum_{n=1}^{\infty} v_n \cos(n(\phi - \Psi_n)),$$

where n is the order of harmonics, Ψ_n is the n -th order event plane angle, and ϕ is the azimuthal angle of charged particles. The order of harmonics in v_n corresponds to the order of eccentricities in the initial geometry of the QGP, such as the ellipticity for v_2 and the triangularity for v_3 . Measurements of v_n also include contributions from non-flow effects, defined as the correlations unrelated to the initial geometry of the QGP, such as resonance decays, global momentum conservation, jet fragmentation, and dijet production. Therefore, various methods have been developed to suppress non-flow effects and applied in v_n measurements at the LHC [12–16] and the Relativistic Heavy Ion Collider (RHIC) [17, 18]. The *scalar-product* (SP) method [17, 19, 20] provides an estimate of $\sqrt{\langle v_n^2 \rangle}$ that is independent of the detector resolution. In addition, the non-flow contributions are mitigated if a pseudorapidity gap is imposed between the correlated particles. Alternatively, lower-order short-distance correlations from particle decays can be effectively suppressed by utilizing genuine multi-particle correlations within the *multi-particle cumulant* (MPC) framework [21, 22], which can be efficiently implemented using the so-called Q -cumulants [23, 24]. Following the convention from this framework, in this paper, correlations, cumulants, and v_n measurements that are integrated in p_T are termed *reference*, in contrast to the *differential* quantities that are differential in p_T . The three-subevent Q -cumulant method extends the standard method by requiring a pseudorapidity gap between some of the correlated particles. This has been shown to reduce further the short-range non-flow effects in measurements of reference v_n [25–27]. The measurements of MPCs used to obtain v_n are

¹ The impact parameter is defined as the distance between the centers of the two colliding nuclei.

conducted over an ensemble of events of similar centralities. It has been observed that the results obtained with the MPC method are also sensitive to the centrality resolution of the event ensemble chosen. Therefore, different strategies of constructing the v_n values in a centrality interval have been investigated [27].

Measurements of the azimuthal anisotropies of jets [13, 14, 28] and charged particles at high- p_T [12, 15, 29] in Pb+Pb collisions have been previously performed. For jets with $p_T > 70$ GeV, positive values of v_2 are measured for all centrality intervals, except the most central, and positive values of v_3 are measured for mid-central collisions [13]. Measurements of v_n using the SP method and the measurements of v_2 using the MPC method have also been performed for charged particles with a p_T up to 100 GeV at the LHC [12, 29]. It has been observed that v_2 values measured with both the SP and the MPC method decrease with p_T for charged particles with a p_T greater than 20 GeV while remaining positive up to a p_T of approximately 80 GeV for the 60% most central collisions. Meanwhile, the values of v_3 measured with the SP method remain positive up to a p_T of approximately 20 GeV for the 40% most central collisions [12]. The positive values of v_n observed in the high- p_T sector suggest that the energy loss of hard-scattered partons is affected by the event-by-event initial geometry of the QGP.

This analysis extends the measurement of v_n values using the SP and MPC methods to higher p_T for charged particles in $\sqrt{s_{NN}} = 5.02$ TeV Pb+Pb collisions. The dataset used corresponds to an integrated luminosity of 0.44 nb^{-1} collected by the ATLAS detector using the innovative partial event building technique. Measurements of v_n were performed in intervals of p_T up to 400 GeV and intervals of centrality spanning the 0–60% most central collisions, and compared between different acceptance ranges and strategies. Measurements of v_n with the SP method, denoted by $v_n\{\text{SP}\}$, were carried out for tracks in three pseudorapidity ranges² $|\eta| < 1.1$, $1.1 < |\eta| < 2.5$ and $|\eta| < 2.5$. And measurements of v_n using the MPC method were performed for four-particle cumulants, denoted by $v_n\{4\}$, for charged particles over the pseudorapidity range of $|\eta| < 2.5$. Furthermore, the three-subevent Q -cumulant method used for reference v_n measurements is expanded to include p_T -differential $v_2\{4\}$ and $v_3\{4\}$. For the MPC method, the cumulants are firstly computed within narrower centrality intervals before combining into wider ones. The differences in the MPC measurements by using different centrality intervals before combining are shown. Finally, results from the SP method and the MPC method are compared with each other.

The paper is organized as follows. Section 2 describes the detector, trigger and datasets, and Section 3 the event and track selections, as well as event combination procedures. Section 4 provides the mathematical framework for the scalar product and multi-particle cumulant methods. The systematic uncertainties are described in Sections 5. Section 6 presents the v_n measurements using the SP and MPC methods. Comparisons of these measurements with existing measurements and between using different strategies and kinematic ranges are also presented. Finally, the conclusions are included in Section 7.

2 ATLAS detector

The ATLAS detector [30] at the LHC covers nearly the entire solid angle around the collision point. It consists of an inner tracking detector surrounded by a thin superconducting solenoid, electromagnetic

² ATLAS uses a right-handed coordinate system with its origin at the nominal IP in the center of the detector, and the z -axis along the beam pipe. The x -axis points from the IP to the center of the LHC ring, and the y -axis points upward. Cylindrical coordinates (r, ϕ) are used in the transverse plane, ϕ being the azimuthal angle around the z -axis. The pseudorapidity is defined in terms of the polar angle θ as $\eta = -\ln \tan(\theta/2)$. The rapidity is defined as $y = 0.5 \ln[(E + p_z)/(E - p_z)]$ where E and p_z are the energy and z -component of the momentum along the beam direction respectively. Transverse momentum and transverse energy are defined as $p_T = p \sin \theta$ and $E_T = E \sin \theta$, respectively.

and hadronic calorimeters, and a muon spectrometer incorporating three large superconducting toroidal magnets.

The inner-detector system (ID) is immersed in a 2 T axial magnetic field and provides charged-particle tracking in the pseudorapidity range $|\eta| < 2.5$. The high-granularity silicon pixel detector covers the vertex region, and is composed of four layers including the insertable B-layer [31, 32]. It is followed by the silicon microstrip tracker (SCT), which usually provides eight measurements per track. These silicon detectors are complemented by the transition radiation tracker (TRT), which enables radially extended track reconstruction up to $|\eta| = 2.0$. The TRT also provides electron identification information based on the fraction of hits (typically 30 in total) above a higher energy-deposit threshold corresponding to transition radiation.

The calorimeter system covers the pseudorapidity range $|\eta| < 4.9$. Within the region $|\eta| < 3.2$, electromagnetic calorimetry is provided by barrel and endcap high-granularity lead/liquid-argon (LAr) electromagnetic calorimeters, with an additional thin LAr presampler covering $|\eta| < 1.8$ to correct for energy loss in material upstream of the calorimeters. The hadronic calorimeters have three sampling layers longitudinal in shower depth in $|\eta| < 1.7$ and four sampling layers in $1.5 < |\eta| < 3.2$, with a slight overlap in η . The solid angle coverage is completed with forward copper/LAr and tungsten/LAr calorimeter modules (FCal) optimized for electromagnetic and hadronic measurements respectively. The FCals cover a pseudorapidity range of $3.2 < |\eta| < 4.9$.

The zero-degree calorimeters (ZDCs) are located symmetrically at $z = \pm 140$ m and cover $|\eta| > 8.3$ during the Pb+Pb data-taking period. The ZDCs use tungsten plates as absorbers and quartz rods sandwiched between the tungsten plates as the active medium. In Pb+Pb collisions the ZDCs primarily measure spectator neutrons. A ZDC coincidence trigger is implemented by requiring the pulse height from each ZDC to be above a threshold set to accept the energy of a single neutron. The luminosity is measured mainly by the LUCID-2 [33] detector that records Cherenkov light produced in the quartz windows of photomultipliers located close to the beampipe.

A two-level trigger system is used to select interesting events [34, 35]. The first-level (L1) trigger is implemented in hardware and uses a subset of detector information, including ZDC coincidences in Pb+Pb collisions, to reduce the event rate to a design value of at most 100 kHz. This is followed by a software-based high-level trigger (HLT) which reduces the event rate to several kHz. A software suite [36] is used in the reconstruction and analysis of real and simulated data, in detector operations, and in the trigger and data acquisition systems of the experiment.

3 Monte Carlo simulation and data selection

3.1 Monte Carlo samples

Monte Carlo (MC) simulations are used in this analysis to evaluate the track reconstruction performance. A minimum-bias sample of Pb+Pb MC events at 5.02 TeV was generated with HIJING [37]. After the generation, the flow harmonics were added to the simulated events using an “afterburner” [11] procedure, which implements the p_T , η , and centrality dependence of the v_n , as measured in the $\sqrt{s_{NN}} = 2.76$ TeV Pb+Pb data [38], by artificially rearranging the ϕ positions of the generated particles. The detector response is simulated with ATLFAST-II [39] for calorimeters and GEANT4 [40, 41] for the ID. The simulated events are then reconstructed using the same algorithms as data events.

3.2 Event selection

The dataset of Pb+Pb collisions at $\sqrt{s_{NN}} = 5.02$ TeV used in this analysis was collected by the ATLAS detector in 2018 and corresponds to an integrated luminosity of 0.44 nb^{-1} after data-quality requirements [42]. Events were required to satisfy one of the three L1 minimum-bias (MB) triggers. The first MB trigger requires an event to have a total transverse energy (ΣE_T^{Cal}) measured in the calorimeter system above 600 GeV. The second MB trigger requires an event to have a ΣE_T^{Cal} above 50 GeV and less than 600 GeV. The third MB trigger will fire when an event is rejected by both of the previous two triggers and satisfies a ZDC coincidence trigger at L1 and have at least one track in the HLT. The MB triggers above have a small prescale³ of approximately 3.95. The small prescale is enabled by a novel strategy known as the partial event building [34], in which data from selected ATLAS subdetectors are used to compose an event, thus enabling higher recording rate and optimized event size. These events contain the ID, FCal and ZDC information required for this analysis as in other events; other information has not been recorded.

For this analysis, events are required to have the z -coordinate of the primary vertex [43] within 100 mm of the nominal interaction point. Events with more than one hadronic interaction from the same bunch crossing are estimated to be less than 0.5% of collisions. These events are suppressed by utilizing the observed anti-correlation, expected from the nuclear geometry, between the total transverse energy deposited in both of the forward calorimeters, ΣE_T^{FCal} , and the energy in the ZDC, with the latter proportional to the number of observed spectator neutrons. Additional hadronic interactions from just before or right after the collision of interest could interfere with calorimeter performance and centrality determinations. Criteria for rejecting these events are determined by the expected strong and linear correlation between charged particle multiplicity and measured ΣE_T^{FCal} . Events with a charged particle multiplicity that falls out of this correlation are rejected. A very stringent criteria is chosen to remove such events, excluding approximately 15% of events nearly independent of centrality. This rejection is made necessary due to the focus of this analysis on measuring correlations of small magnitudes and a smaller bunch spacing used in the ATLAS 2018 Pb+Pb dataset. Whereas the ATLAS 2015 dataset for Pb+Pb collisions at $\sqrt{s_{NN}}=5.02$ TeV used a bunch spacing interval of 100 ns, this analysis uses the ATLAS 2018 dataset where a bunch spacing interval of 75 ns was used for approximately half of the dataset for higher event rate.

The centrality of an event in this analysis is obtained using its ΣE_T^{FCal} energy, and the centrality percentile requirements are determined by using a MC Glauber analysis [44, 45], starting from the most central events, where the collisions have the smallest impact parameter and the highest ΣE_T^{FCal} . In this analysis, results are obtained in seven centrality intervals: 0–5%, 5–10%, 10–20%, 20–30%, 30–40%, 40–50%, and 50–60%.

3.3 Track selection

Tracks of charged particles are reconstructed from hits in the ID using a track reconstruction algorithm that was optimized for the high hit density in heavy-ion collisions [46]. Tracks used in this analysis have $|\eta| < 2.5$ and are required to have at least 10 hits in the silicon detectors. Additionally, a track must have no more than one hole in the SCT, where a hole is defined as the absence of a hit predicted by the track trajectory. All charged-particle tracks used in this analysis are required to have reconstructed transverse

³ A prescale is a number that defines what fraction of events are recorded out of all possible events that would have passed the trigger requirements.

momentum $p_T > 1.0$ GeV. In order to suppress the contribution from secondary particles,⁴ the distance of the closest approach of the track to the primary vertex is required to be less than a p_T -dependent value varying from 0.6 mm at $p_T = 1$ GeV to 0.2 mm at $p_T = 20$ GeV in the transverse plane and less than 1.0 mm in the longitudinal direction [47]. The transverse and longitudinal distances of the closest approach to the primary vertex are denoted by d_0 and z_0 respectively. The significances $|d_0|/\sigma_{d_0}$ and $|z_0 \sin \theta|/\sigma_{z_0 \sin \theta}$ are required to be smaller than 3.0, where θ is the polar angle of the track, and σ_{d_0} and $\sigma_{z_0 \sin \theta}$ are the uncertainties in d_0 and $z_0 \sin \theta$, respectively. The primary vertex is determined using vertex finding and fitting algorithms described in Ref. [48].

The track weight factor in this analysis is denoted by ω_j where j is the track index, and is calculated from the track reconstruction inefficiency and the ID acceptance non-uniformity. The track reconstruction efficiency ϵ for tracks that pass the selections is evaluated as a function of p_T , in intervals of centrality and absolute pseudorapidity $|\eta|$. The charged particle tracks are weighted by $1/\epsilon$ to correct for reconstruction inefficiency in this analysis. In the most central collision interval 0–5% for $|\eta| < 1.1$, ϵ increases from approximately 63% to approximately 70% in the p_T range of 1–20 GeV and reaches a plateau for $p_T > 20$ GeV. For $1.1 < |\eta| < 2.5$ in the same centrality interval, ϵ increases from approximately 43% to approximately 48% in the p_T range of 1–20 GeV, and reaches a plateau for $p_T > 20$ GeV. The efficiency values in other centrality intervals follow the same trend and increase toward peripheral events nearly independent of p_T . The difference in ϵ between the most peripheral centrality interval 50–60% and the most central centrality interval 0–5% is approximately 4% for $|\eta| < 1.1$ and approximately 8% for $1.1 < |\eta| < 2.5$. Reconstructed tracks that are not matched to a generated primary particle in the MC samples are considered “fake” tracks. The fake rate is negligible for tracks that pass the selection criteria for all centrality, p_T , and η ranges used in this analysis, and thus, it is not taken into account. In addition, to correct for non-uniformity in the ID acceptance along azimuthal direction, the tracks are weighted by a factor proportional to $N_{\text{trk}}(\eta)/N_{\text{trk}}(\eta, \phi)$, where $N_{\text{trk}}(\eta)$ is the total number of tracks within a given pseudorapidity interval of 0.1 and $N_{\text{trk}}(\eta, \phi)$ is the number of tracks for a small given pseudorapidity and azimuthal angle interval of 0.1×0.1 [15]. This factor yields a weighted track distribution that is uniform along the azimuthal direction for any given pseudorapidity interval.

4 Analysis method

4.1 Scalar-product method

The SP method is defined in Ref. [17], further discussed in Ref. [19], and results using this method for Pb+Pb and Xe+Xe collisions have been published by ATLAS in Refs. [15, 49]. It uses flow vectors $u_{n,j}$ and Q_n , where the $u_{n,j}$ for each object of interest j , for example, a charged-particle track or energy deposited at a single calorimeter tower, is defined as

$$u_{n,j} = e^{in\phi_j}, \quad (1)$$

and the average flow vector Q_n of a subevent, for example, one side of the FCal, is defined as

$$Q_n = \frac{1}{\sum_j \omega_j} \sum_j \omega_j u_{n,j}, \quad (2)$$

⁴ Primary particles are defined as particles with a mean lifetime $\tau > 0.3 \times 10^{-10}$ s either directly produced in the collisions or from subsequent decays of particles with a shorter lifetime. All other particles are considered to be secondary.

where the summation goes over all objects of interest in the subevent. In this analysis, flow vectors are evaluated separately for the two sides of the FCal and are denoted $Q_n^{N|P}$, where the N and P correspond to a pseudorapidity range of $-4.9 < \eta < -3.2$ and $3.2 < \eta < 4.9$, respectively. In this case, the sum in Eq. 2 runs over the calorimeter towers with approximate granularity of $\Delta\eta \times \Delta\phi = 0.1 \times 0.1$ and the weights ω_j are the transverse energies E_T measured in the towers.

The azimuthal anisotropy coefficients using this method, $v_n\{\text{SP}\}$, are defined for each p_T and centrality interval as,

$$v_n\{\text{SP}\} \equiv Re \frac{\langle u_{n,j} Q_n^{N|P*} \rangle}{\sqrt{\langle Q_n^N Q_n^{P*} \rangle}} = \frac{\langle |u_{n,j}| |Q_n^{N|P}| \cos [n(\phi_j - \Psi_n^{N|P})] \rangle}{\sqrt{\langle |Q_n^N| |Q_n^P| \cos [n(\Psi_n^N - \Psi_n^P)] \rangle}}. \quad (3)$$

The numerator calculates the scalar product of the flow vector of the reference subevent, $Q_n^{N|P}$, and that of each charged-particle track, $u_{n,j}$, where the $\langle \rangle$ denotes an average over all tracks within the particular p_T interval from all events of the given centrality interval. This average is weighted for each track to correct for azimuthal non-uniformity of the detector and track reconstruction inefficiency, as detailed in Section 3.3. The denominator calculates the estimated detector resolutions, as determined using two reference subevents, positive and negative ends of the FCal, of the same event, and the $\langle \rangle$ denotes an average over all events in the given centrality interval. The flow vector Q_n^P (Q_n^N) of the calorimeter is correlated with tracks with $\eta < 0$ ($\eta > 0$). This implementation of the SP method imposes a pseudorapidity gap of at least 3.2 between the reference Q_n and tracks, thus suppressing short-range non-flow correlations, such as those arising from resonance decays and same-jet correlations [20]. The $v_n\{\text{SP}\}$ values are measured for ID pseudorapidity ranges of $|\eta| < 2.5$, $|\eta| < 1.1$, and $1.1 < |\eta| < 2.5$.

4.2 Multi-particle cumulant method

The MPC method using standard Q -cumulants, as applied in this analysis, is based on the generic framework described in Ref. [24]. The three-subevent Q -cumulants method extends this framework and was introduced in Ref. [25] for reference $v_n\{4\}$ measurements. This analysis extends the three-subevent cumulants to p_T -differential $v_n\{4\}$ measurements for high- p_T charged particles in Pb+Pb collisions.

4.2.1 Standard Q -cumulants

For a single event, the n -th order two- and four-particle azimuthal correlators are denoted as $\langle 2 \rangle_n$ and $\langle 4 \rangle_n$, respectively, and defined as [23, 24],

$$\begin{aligned} \langle 2 \rangle_n &\equiv \langle e^{in(\phi_1 - \phi_2)} \rangle, \\ \langle 4 \rangle_n &\equiv \langle e^{in(\phi_1 + \phi_2 - \phi_3 - \phi_4)} \rangle, \end{aligned} \quad (4)$$

where ϕ_i represents the azimuthal angles of distinct charged-particle tracks, and the $\langle \rangle$ denotes an average over all two- or four-particle combinations in the given event. In the standard Q -cumulants, all tracks within the pseudorapidity range of $|\eta| < 2.5$ are used. As it is computationally challenging to calculate four-particle correlations using nested loops, the correlators in this analysis are computed using the

Q -cumulants, following the generic framework from Ref. [24], with the k -th power weighted flow vector $Q_{n,k}$,⁵ defined as

$$Q_{n,k} = \sum_{j=1}^M \omega_j^k u_{n,j}, \quad (5)$$

where M is the charged-particle multiplicity of the event and ω_j is the track weight.

The p_T -integrated reference four-particle cumulants $c_n\{4\}$, computed over reference particles (REF), defined as all charged particles in the soft p_T range of 1–5 GeV, are calculated as,

$$c_n\{4\} \equiv \langle\langle 4 \rangle\rangle_n - 2\langle\langle 2 \rangle\rangle_n^2 = \langle v_n^4 \rangle - 2\langle v_n^2 \rangle^2 = 2\sigma^2(v_n^2) - \langle v_n^4 \rangle = -(v_n\{4\})^4, \quad (6)$$

where $\langle\langle 2 \rangle\rangle_n$ and $\langle\langle 4 \rangle\rangle_n$ are respectively the event-averaged two- and four-particle correlators, with the $\langle\langle \rangle\rangle$ denoting an average of $\langle \rangle$ over all events, and $\sigma^2(v_n^2)$ is the variance of v_n^2 . The corresponding differential cumulants $d_n\{4\}(p_T)$ are defined similarly as,

$$d_n\{4\}(p_T) = \langle\langle 4' \rangle\rangle_n - 2\langle\langle 2' \rangle\rangle_n \langle\langle 2 \rangle\rangle_n, \quad (7)$$

where $\langle\langle 2' \rangle\rangle_n$ and $\langle\langle 4' \rangle\rangle_n$ are calculated using one particle of interest (POI) in a specific p_T bin, while the other particles are REF. The p_T differential $v_n\{4\}$ is computed as,

$$v_n\{4\}(p_T) = \frac{-d_n\{4\}(p_T)}{(-c_n\{4\})^{3/4}}. \quad (8)$$

Depending on the shape of the underlying reference $v_n\{4\}$ distributions, $c_n\{4\}$ could change sign across different centrality ranges. Values of $c_2\{4\}$ have been observed to become positive in the 2% most central collisions, giving an imaginary reference $v_2\{4\}$ [27]. Therefore for this analysis, the centrality interval 0–5% is omitted for the differential $v_2\{4\}$ measurements to ensure that the values of reference $v_2\{4\}$, thus values of the denominator in the differential $v_4\{2\}$ formula, are always real-valued.

4.2.2 Three-subevent Q -cumulants

In the standard Q -cumulants, all of the two or four particles correlated come from the full pseudorapidity range of the ID, $|\eta| < 2.5$. To further suppress the non-flow correlations, rapidity gaps are applied in the MPC method using the three-subevent cumulants [25–27] by requiring the correlated particles in an event to come from different pseudorapidity ranges. The ID acceptance is divided equally into three subevents of non-overlapping pseudorapidity ranges, indexed as a , b and c . The pseudorapidity ranges of these three subevents are as follows,

$$-2.5 < \eta_a < -\frac{2.5}{3}, \quad |\eta_b| < \frac{2.5}{3}, \quad \frac{2.5}{3} < \eta_c < 2.5. \quad (9)$$

The k -th power weighted flow vector for subevent a , $Q_{n,k}^a$, is defined as

$$Q_{n,k}^a = \sum_{j=1}^{M_a} \omega_j^k u_{n,j}, \quad (10)$$

⁵ The notation $Q_{n,k}$ defined for the MPC method by Eq. 5 should be distinguished from the notation Q_n defined for the SP method by Eq. 2. The notation $Q_{n,k}$ is a weighted summation of $u_{n,j}$, whereas Q_n is a weighted average of $u_{n,j}$ computed by the weighted summation of $u_{n,j}$ normalized by the total weight of $u_{n,j}$.

where M_a is the charged-particle multiplicity within subevent a . The three-subevent single-event reference correlators and their corresponding event weights $W_{(2)}$ and $W_{(4)}$, calculated also using flow vectors where $n = 0$, are defined as

$$\langle 2 \rangle_n^{a|b} \equiv \langle e^{in(\phi_a - \phi_b)} \rangle = Re \frac{Q_{n,1}^a Q_{-n,1}^b}{W_{(2)}^{a|b}}, \quad (11)$$

$$W_{(2)}^{a|b} = Q_{0,1}^a Q_{0,1}^b,$$

$$\langle 4 \rangle_n^{a,a|b,c} \equiv \langle e^{in(\phi_a + \phi'_a - \phi_b - \phi_c)} \rangle = Re \frac{[(Q_{n,1}^a)^2 - Q_{2n,2}^a] Q_{-n,1}^b Q_{-n,1}^c}{W_{(4)}^{a,a|b,c}}, \quad (12)$$

$$W_{(4)}^{a,a|b,c} = [(Q_{0,1}^a)^2 - Q_{0,2}^a] Q_{0,1}^b Q_{0,1}^c.$$

where the superscript in event weights $W_{(2)}$ and $W_{(4)}$ corresponds to the track configuration of correlators. Here the prime label on the azimuthal angle ϕ'_a indicates that a second distinct particle is selected from subevent a . The reference cumulants $c_n^{a,a|b,c}\{4\}$ are calculated from the event-averaged correlators as,

$$c_n^{a,a|b,c}\{4\} = \langle\langle 4 \rangle\rangle_n^{a,a|b,c} - 2 \langle\langle 2 \rangle\rangle_n^{a|b} \langle\langle 2 \rangle\rangle_n^{a|c}. \quad (13)$$

To boost the statistics and reduce η -dependent detector bias, the subevent index a is interchanged with b and c to create two additional configurations. The weighted average of these three measurements is used to obtain three-subevent reference cumulants $c_n^{3\text{-sub}}\{4\}$. The formulae for these reference correlators, presented with different notations, are detailed in Ref. [25].

Each subevent configuration of reference correlator $\langle 2 \rangle_n$ is subdivided into two separate configurations of the differential flow correlators by selecting each of the two correlated particles as the POI. Similarly, each reference correlator configuration of $\langle 4 \rangle_n$ is subdivided into four differential correlator configurations. For subevent a , the n -th order harmonic k -th power weighted flow vector using only POIs is denoted by $p_{n,k}^a$, which is defined for a given p_T interval. Similarly, the flow vector made from particles that are both REF and POI for a given p_T interval is denoted by $q_{n,k}^a$ for subevent a . These two flow vectors are calculated similarly to Eq. 10. For $\langle 4 \rangle_n$, two formulae were provided: one for when the POI comes from a subevent within which two particles are selected, as shown in Eq. 15, and the other for when the POI is the only particle from its subevent, as shown in Eq. 16. A prime in the subevent index indicates that the subevent from which the POI of this correlator is selected.

$$\langle 2' \rangle_n^{a'|b} = Re \frac{p_{n,1}^a Q_{-n,1}^b}{W_{(2')}^{a'|b}}, \quad (14)$$

$$W_{(2')}^{a'|b} = p_{0,1}^a Q_{0,1}^b,$$

$$\langle 4' \rangle_n^{a',a|b,c} = \langle 4' \rangle_n^{a,a'|b,c} = Re \frac{(p_{n,1}^a Q_{n,1}^a - q_{2n,2}^a) Q_{-n,1}^b Q_{-n,1}^c}{W_{(4')}^{a',a|b,c}}, \quad (15)$$

$$W_{(4')}^{a',a|b,c} = (p_{0,1}^a Q_{0,1}^a - q_{0,2}^a) Q_{0,1}^b Q_{0,1}^c,$$

$$\langle 4 \rangle_n^{a,a|b',c} = Re \frac{[(Q_{n,1}^a)^2 - Q_{2n,2}^a] p_{-n,1}^b Q_{-n,1}^c}{W_{(4)}^{a,a|b',c}}, \quad (16)$$

$$W_{(4)}^{a,a|b',c} = [(Q_{0,1}^a)^2 - Q_{0,2}^a] p_{0,1}^b Q_{0,1}^c.$$

Other configurations can be written similarly by permuting the subevent indices. Similar to Eq. 13, the differential cumulants are defined as

$$d_n^{a', a|b, c}\{4\}(p_T) = \langle\langle 4' \rangle\rangle_n^{a', a|b, c} - 2\langle\langle 2' \rangle\rangle_n^{a'|b} \langle\langle 2 \rangle\rangle_n^{a|c}. \quad (17)$$

Each of the three configurations for the reference cumulant corresponds to four configurations for the differential cumulant. The three-subevent differential cumulants $d_n^{3\text{-sub}}\{4\}(p_T)$ are calculated as the weighted average from these 12 configurations, and then used for the calculation of three-subevent cumulants $v_n\{4\}$ (as defined in Eq. 8), denoted by $v_n^{3\text{-sub}}\{4\}$.

4.2.3 Event combination procedure

In this analysis, the event-averaged cumulants $c_n\{4\}$ and $d_n\{4\}(p_T)$ are firstly computed in narrower centrality intervals, and then averaged toward wider centrality intervals in which the final results of v_n are presented. The choice of initial centrality intervals in which the cumulants are calculated defines an event combination procedure. The choice of event combination procedure can affect the measured v_n in different ways. High- p_T particle production is biased toward more central events, and therefore, for quantities measured using high- p_T charged particles, an average over a wide centrality interval is biased toward the more central edge of the interval. Also, the event-by-event fluctuations in the underlying azimuthal anisotropy distributions are sensitive to the event combination procedure. Therefore, the choice of the initial centrality intervals in an event combination procedure can be used to test the sensitivity of an observable to the underlying fluctuations and to identify the source of this fluctuation. These fluctuations can stem from the initial state geometry or non-flow effects. It has been shown in measurements of reference v_n that the centrality resolution of the initial centrality intervals affects the MPC measurements of v_n due to fluctuations in non-flow effects [25, 27].

By default, cumulants are calculated within 1% centrality percentiles before combining. For comparison, cumulants are also calculated within 2% centrality percentiles before combining and directly calculated within the quoted centrality intervals for results. Results obtained following these procedures are referred to later as $\langle 1\% \rangle$, $\langle 2\% \rangle$ and $\langle 10\% \rangle$, respectively. The final results are presented in 5% centrality intervals for the most central 10% of events, and in 10% centrality intervals for all other events.

5 Systematic uncertainties

The systematic uncertainties in this analysis arise from the choice of the pseudorapidity ranges used in reference v_n definitions, variation of track selection criteria, detector material uncertainties affecting reconstruction efficiency and overall imperfections in the detector response. These uncertainties are evaluated by first repeating the analysis with alternative pseudorapidity ranges, the varied selection criteria on tracks, or different track reconstruction efficiency corrections, and then calculating the absolute differences in the resulted v_n values from the default results. For each alteration, track weights and other corrections are re-calculated accordingly.

For a detector with perfect azimuthal symmetry, the imaginary part of the scalar product should be zero. Therefore, the imaginary part of the scalar product, referred to as the residual sine term, is used as a systematic uncertainty. The sensitivity of the result to the pseudorapidity range of the FCals used to determine the flow vector is evaluated by using only the inner or outer halves of the FCals, corresponding to

pseudorapidity ranges of $|\eta_{\text{FCal}}| < 4.0$ and $|\eta_{\text{FCal}}| > 4.0$, respectively. Additionally, v_n values are expected to be consistent between the positive and negative halves of ID due to the symmetry of the collision system. Any asymmetry of the results in η is included in the systematic uncertainty, evaluated using $\eta_{\text{trk}} < 0$ and $\eta_{\text{trk}} > 0$. The sensitivity of the result to the track selection is assessed by tightening the track selection criteria, requiring at least 12 hits in the silicon detectors and no holes in the SCT. The default $\Sigma E_{\text{T}}^{\text{FCal}}$ requirements used for the centrality percentile is determined by matching 85% of the Glauber-like dataset to MC events using the Glauber Model [44, 45]. The centrality determination uncertainty is accounted for by up and down varying 1% of data used to match the simulations for alternative $\Sigma E_{\text{T}}^{\text{FCal}}$ requirements. The track reconstruction efficiency used in this analysis is fitted as a function of p_{T} in order to obtain a smooth correction. The difference in the measured v_n between the fitted and binned efficiency is used as a systematic uncertainty. The same systematic uncertainties are evaluated for $v_n\{\text{SP}\}$ results for the three ranges of charged-particle pseudorapidity $|\eta| < 1.1$, $1.1 < |\eta| < 2.5$ and $|\eta| < 2.5$.

In addition to $v_n\{\text{SP}\}$ values, the difference between two $v_n\{\text{SP}\}$ measurements using tracks with non-overlapping pseudorapidity ranges is also calculated. Only contributions of systematic uncertainties that are uncorrelated between the two $v_n\{\text{SP}\}$ measurements of non-overlapping ranges are included in this quantity. For this analysis, the charged-particle η -asymmetry and residual sine term uncertainties use non-overlapping parts of sub-detectors and are therefore considered uncorrelated.

For the MPC method, only a subset of systematic uncertainties that are considered for the SP method is included. No systematic uncertainties related to η -symmetry are included, as evaluating multi-particle correlations within half of the default pseudorapidity range would significantly affect the sensitivity of measurements to physical effects such as non-flow correlations. Systematics related to the FCal are irrelevant for the MPC method. Therefore, the list of systematic uncertainty items used for the MPC method is as follow: the sine residual term in the differential cumulant $d_n\{4\}(p_{\text{T}})$, the centrality determination variations, and the systematic uncertainty from the track reconstruction efficiency.

All sources of systematic uncertainties are taken as uncorrelated, and the total systematic uncertainty is calculated as the quadrature sum of the individual components, separately for positive and negative terms. The magnitudes of systematic uncertainties are summarized in Figure 1 for the SP method and Figure 2 for the MPC method for the selected centrality interval of 10–20%. Systematic uncertainties of the SP method are dominated by the choice of the pseudorapidity range for ID or FCal as well as sine terms, whereas the systematic uncertainties of the MPC method are dominated by the variation in the centrality determination. Similar relative magnitudes of systematic uncertainties are seen in other centrality intervals. The magnitudes of total systematic uncertainties increase toward peripheral events. Systematic uncertainties in $v_n\{\text{SP}\}$ using alternative pseudorapidity ranges $0 < |\eta| < 1.1$ and $1.1 < |\eta| < 2.5$ show similar relative magnitudes among different terms and increased total magnitudes in comparison to the default pseudorapidity range of $0 < |\eta| < 2.5$. The centrality and p_{T} dependence of the total systematic uncertainty are similar for both $v_n\{4\}$ and $v_n^{3\text{-sub}}\{4\}$, with the latter having a larger magnitude especially toward more peripheral events. In both the SP and the MPC methods, the statistical uncertainties dominate over systematic ones, especially toward the high- p_{T} region.

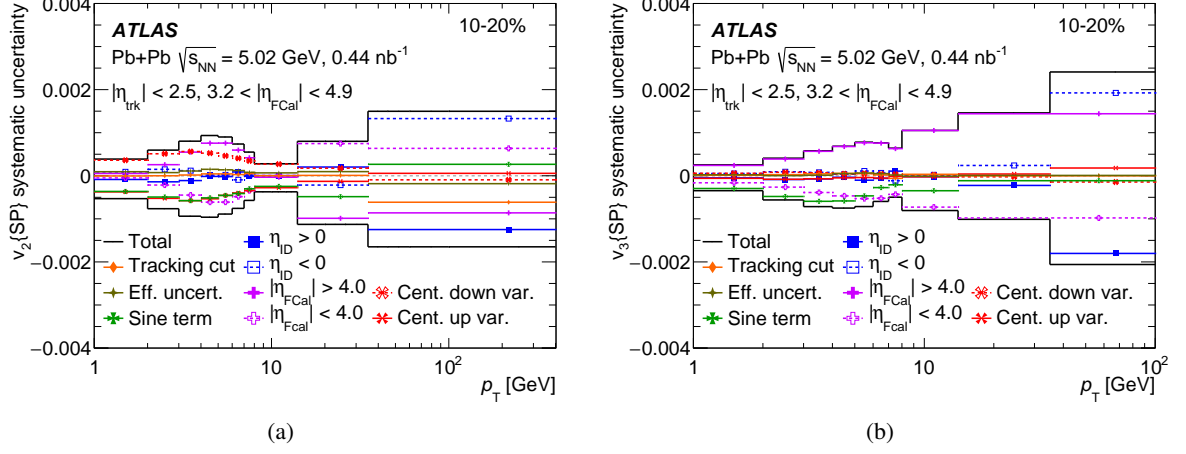


Figure 1: Breakdown of absolute systematic uncertainties as a function of p_T for (a) $v_2\{\text{SP}\}$ and (b) $v_3\{\text{SP}\}$ values in 10–20% central collisions.

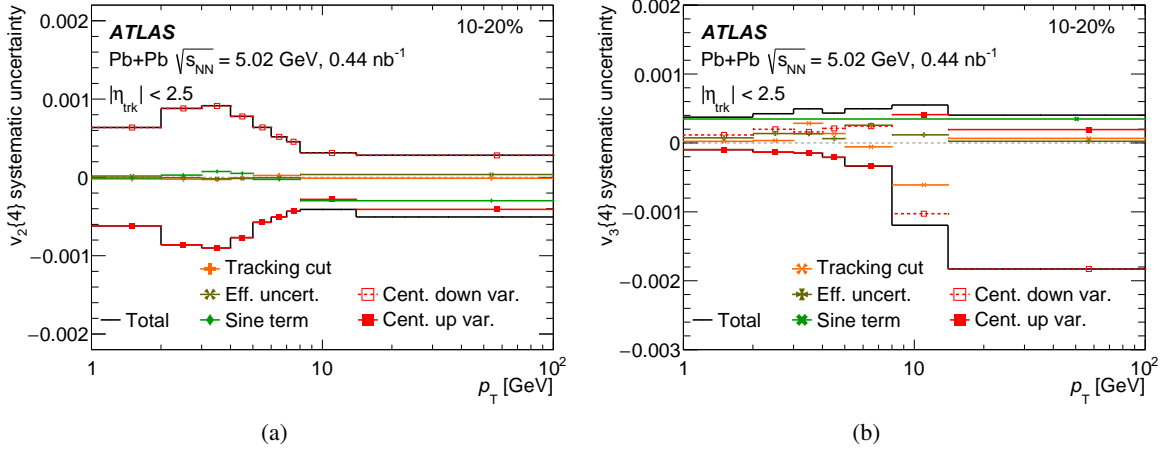


Figure 2: Breakdown of absolute systematic uncertainties as a function of p_T for (a) $v_2\{4\}$ and (b) $v_3\{4\}$ values in 10–20% central collisions.

6 Results

This section presents measurements of v_n using the SP method and the MPC method as a function of the charged-particle p_T for different centrality intervals in Pb+Pb collisions. Comparisons in this section are done for both central and peripheral events, the interval 10–20% for “central events” and the interval 40–50% or 50–60% for “peripheral events”. The former interval is the most central 10%-wide centrality interval, and the latter is the most peripheral centrality interval that is statistically available for the variables concerned. The values are measured over intervals of p_T , and the p_T -position of each data point corresponds to the center of each p_T interval. Additional centrality intervals for some plots are included in Appendix A.

6.1 Scalar product method

Figure 3 shows the $v_2\{\text{SP}\}$ and $v_3\{\text{SP}\}$ values as functions of p_T for the selected centrality intervals. The measured $v_2\{\text{SP}\}$ values are positive for the selected centrality intervals up to a p_T of 100 GeV, and become approximately constant with p_T for $p_T > 50$ GeV. Note that due to decreased statistics, $v_3\{\text{SP}\}$ results in the 50–60% centrality interval use wider p_T intervals toward high p_T than other centrality intervals. The measured $v_3\{\text{SP}\}$ values are positive up to approximately 25 GeV for the selected centrality intervals, except for the 50–60% centrality interval, where values of $v_3\{\text{SP}\}$ become negative and have a downward trend for $p_T > 20$ GeV. Figures 4 and 5 show the consistency of the $v_n\{\text{SP}\}$ measured in Pb+Pb collision at $\sqrt{s_{\text{NN}}} = 5.02$ TeV for the centrality interval 10–20%. Note that in the two figures, two different pseudorapidity ranges are used for the ATLAS 2018 measurements from this analysis. In Figure 4, the reported ATLAS 2015 measurements [15] use the same pseudorapidity ranges of ID and FCal with the ATLAS 2018 measurements, and the two results show good agreement. In Figure 5, the CMS 2015 measurements [12] shown use tracks with pseudorapidity range $|\eta| < 1.0$ and calorimeters in pseudorapidity range $3 < |\eta| < 5$. Overall, good agreement is found between the ATLAS 2018 and the CMS 2015 measurements, except for $v_2\{\text{SP}\}$ in the p_T range of 14–50 GeV, where the CMS 2015 measurements yield higher values than the measurements from this analysis.

In Figures 6 and 7, a comparison is made between the charged-particle $v_n\{\text{SP}\}$ measurements from this analysis and the jet v_n measurements from ATLAS using the event plane method from Ref. [13]. The measured v_n values are qualitatively similar between the jets and charged particles in the quoted high p_T range of 20–400 GeV. These high- p_T charged particles are from jet fragmentation but carry only a fraction of a given jet’s p_T .

Measurements of $v_n\{\text{SP}\}$ using two non-overlapping pseudorapidity ranges of tracks are compared in Figures 8 and 9 in two centrality intervals. The pseudorapidity range $1.1 < |\eta| < 2.5$ corresponds to a greater average pseudorapidity gap between the tracks and correlated reference Q_n than the pseudorapidity range $|\eta| < 1.1$. At $p_T < 10$ GeV for both centrality intervals shown, tracks with the pseudorapidity range $1.1 < |\eta| < 2.5$ yield smaller values of both $v_2\{\text{SP}\}$ and $v_3\{\text{SP}\}$ than tracks with the pseudorapidity range $|\eta| < 1.1$. With a larger pseudorapidity gap imposed, certain non-flow effects are better suppressed, while the longitudinal decorrelation effects in the event plane become stronger [50], both of which reduce the measured values of v_n . For the 10–20% centrality interval, the difference in $v_2\{\text{SP}\}$ between the two pseudorapidity ranges at $10 < p_T < 20$ GeV is similar to that at low- p_T while the difference in $v_3\{\text{SP}\}$ between the two pseudorapidity ranges becomes consistent with zero. For the most peripheral centrality intervals, 50–60% for $v_2\{\text{SP}\}$ and 40–50% for $v_3\{\text{SP}\}$, tracks with the pseudorapidity range

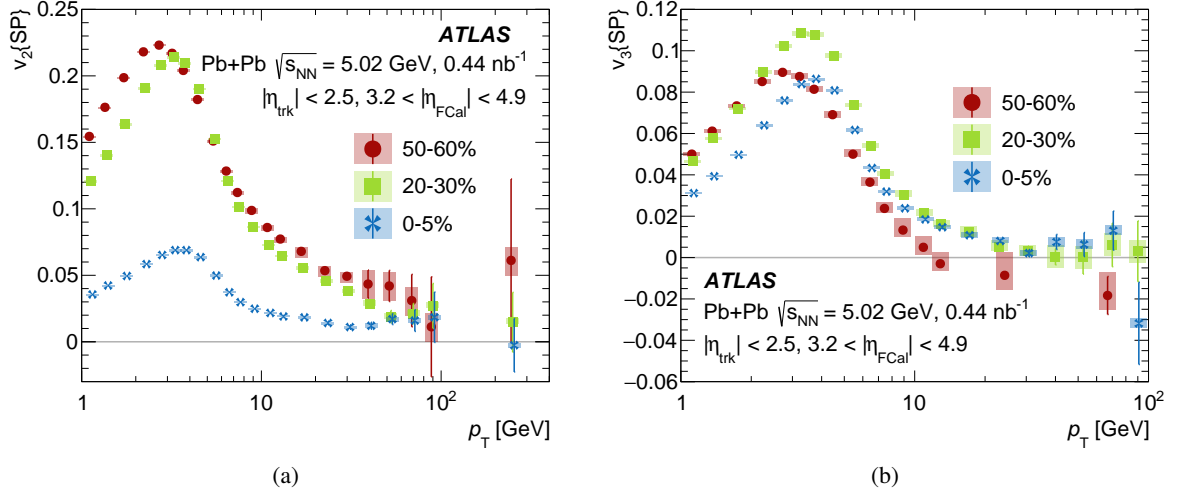


Figure 3: The (a) $v_2\{\text{SP}\}$ and (b) $v_3\{\text{SP}\}$ values as a function of charged-particle p_T for centrality intervals 0–5%, 20–30%, and 50–60%. The statistical uncertainties are shown as error bars and the systematic uncertainties are shown as boxes.

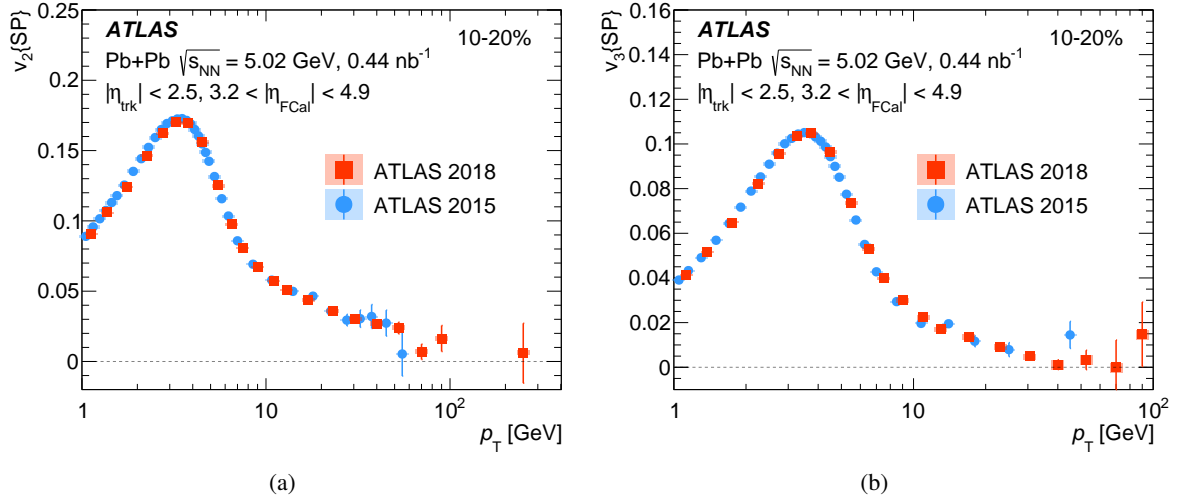


Figure 4: The (a) $v_2\{\text{SP}\}$ and (b) $v_3\{\text{SP}\}$ values as a function of charged-particle p_T , for the 10–20% centrality interval, compared with ATLAS 2015 measurements from Ref. [15] in the same charged particle and calorimeter pseudorapidity ranges. The statistical uncertainties are shown as error bars and the systematic uncertainties are shown as boxes.

$1.1 < |\eta| < 2.5$ yield smaller $v_2\{\text{SP}\}$ values but larger $v_3\{\text{SP}\}$ values than tracks with the pseudorapidity range $|\eta| < 1.1$. In this p_T range, particle production is dominated by jets. The observed contrasting behavior of $v_2\{\text{SP}\}$ and $v_3\{\text{SP}\}$ at high- p_T , especially in peripheral events, is consistent with a non-flow dijet contamination, which contributes positively to even-order harmonics and negatively to odd-order harmonics [26]. At $p_T > 20$ GeV, no similar conclusions can be drawn due to increased statistical uncertainties and fluctuations.

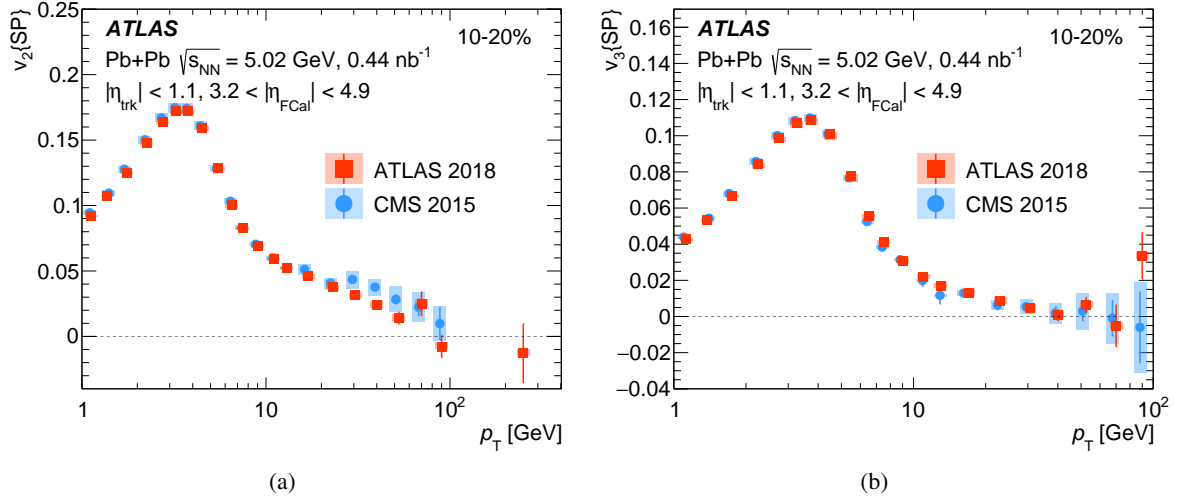


Figure 5: The (a) $v_2\{\text{SP}\}$ and (b) $v_3\{\text{SP}\}$ values as a function of charged-particle p_T , for the 10–20% centrality interval, compared with CMS 2015 measurements from Ref. [12], which uses charged particles with pseudorapidity range $|\eta| < 1.0$ and calorimeter in pseudorapidity range $3 < |\eta| < 5$. The statistical uncertainties are shown as error bars and the systematic uncertainties are shown as boxes.

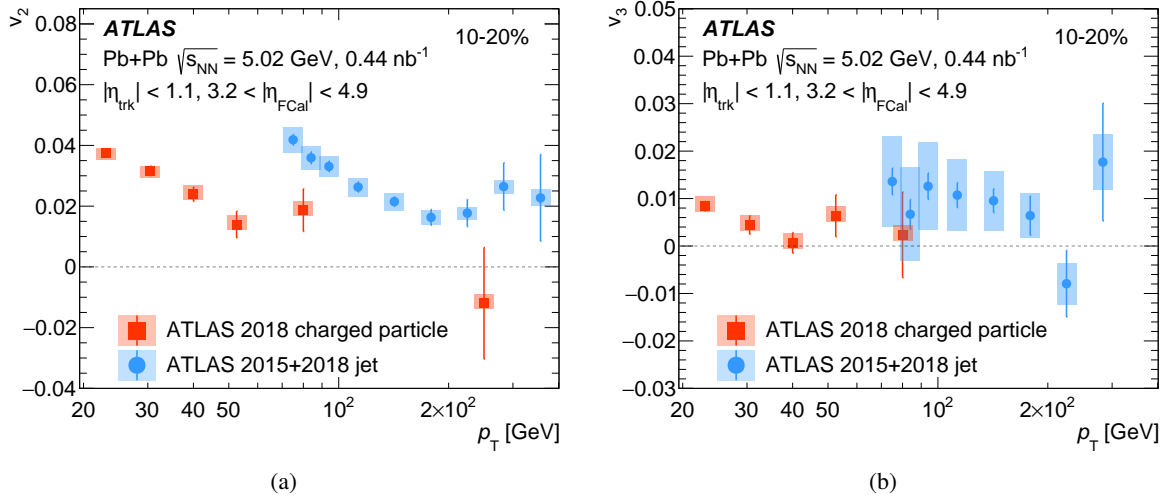


Figure 6: The (a) v_2 and (b) v_3 values as a function of charged particle or jet p_T , for the 10–20% centrality interval, compared with ATLAS jet v_n measurements from Ref. [13]. The statistical uncertainties are shown as error bars and the systematic uncertainties are shown as boxes.

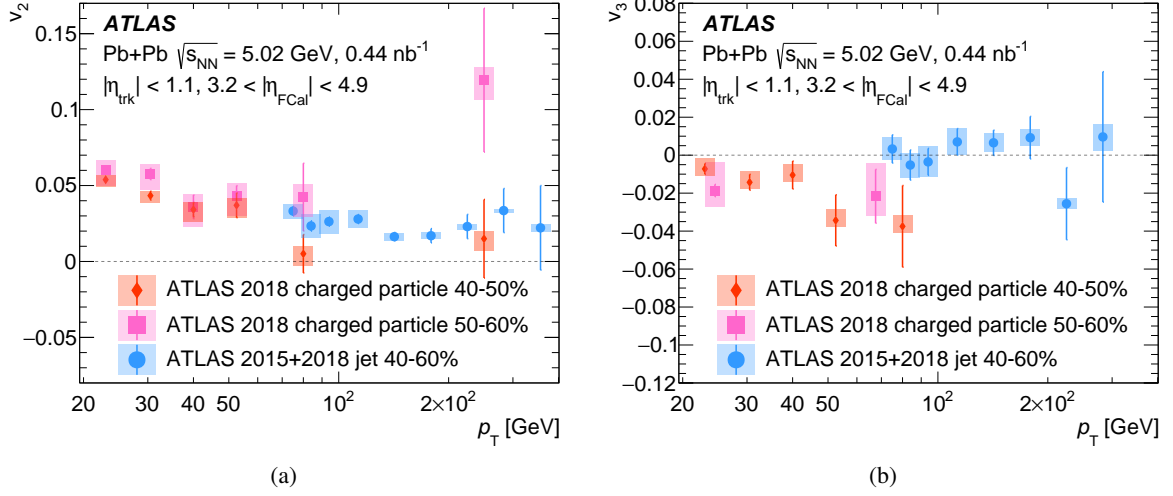


Figure 7: The (a) v_2 and (b) v_3 values as a function of charged particle or jet p_T , for the centrality intervals within 40–60%, compared with ATLAS jet v_n measurements from Ref. [13]. The statistical uncertainties are shown as error bars and the systematic uncertainties are shown as boxes.

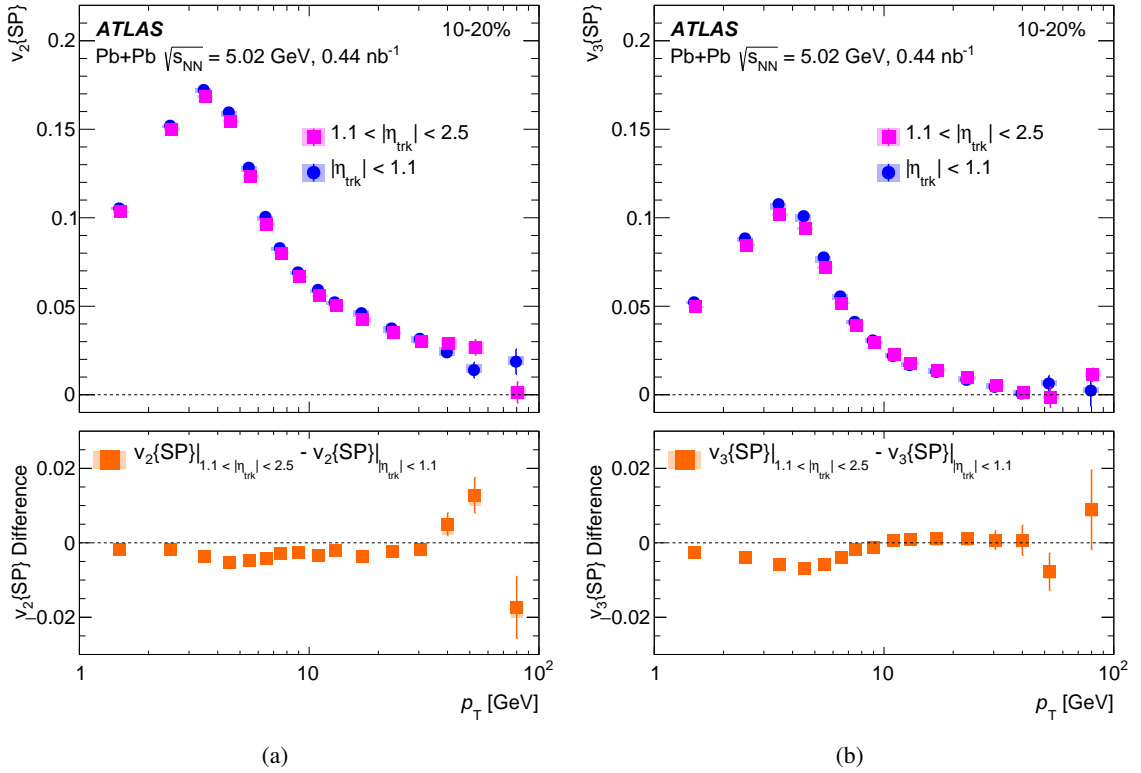


Figure 8: The (a) $v_2\{\text{SP}\}$ and (b) $v_3\{\text{SP}\}$ values as a function of charged-particle p_T in the 10–20% centrality interval for different pseudorapidity ranges. The bottom panel shows the difference in the $v_n\{\text{SP}\}$ measured between the two ranges. The statistical uncertainties are shown as error bars and the systematic uncertainties are shown as boxes.

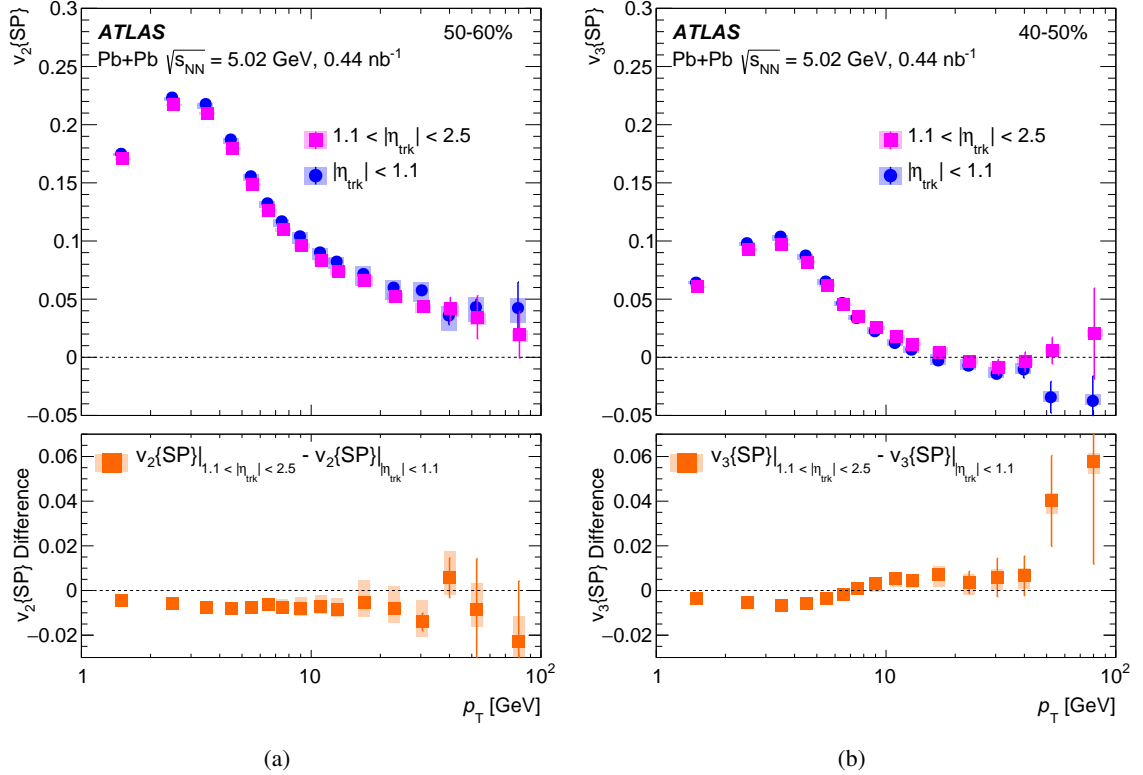


Figure 9: The $v_n\{\text{SP}\}$ values as a function of charged-particle p_T for different pseudorapidity ranges in (a) the 50–60% centrality interval for $v_2\{\text{SP}\}$ and (b) the 40–50% centrality interval for $v_3\{\text{SP}\}$. The bottom panel shows the difference in the $v_n\{\text{SP}\}$ measured between the two ranges. The statistical uncertainties are shown as error bars and the systematic uncertainties are shown as boxes.

6.2 Multi-particle cumulant method

Measurements of $v_n\{4\}$ with the MPC method with standard Q -cumulants using the $\langle 1\% \rangle$ event combination procedure are shown in Figure 10. Due to statistical limitations, $v_3\{4\}$ is measured only up to the 50% most central events. As explained in Section 4.2.1, 0–5% central events are omitted for $v_2\{4\}$ to avoid imaginary-valued reference $v_2\{4\}$. At high p_T , above 10 GeV, the $v_2\{4\}$ values for centrality intervals within the 5–40% most central events decrease with p_T across the measured range. In contrast, for the 40–50% (peripheral events), values of $v_2\{4\}$ decrease with p_T up to approximately 30 GeV and then increase at larger p_T values. Meanwhile, values of $v_3\{4\}$ become approximately constant above 8 GeV, with an upward fluctuation between approximately 8 and 10 GeV for some centrality intervals.

The flattening and slight increase of v_n with p_T in peripheral events could arise from non-flow effects. A comparison is made between the standard Q -cumulant result $v_n\{4\}$ and three-subevent Q -cumulant results $v_n^{3\text{-sub}}\{4\}$ to further understand the role of non-flow effects. Note that $v_n^{3\text{-sub}}\{4\}$ values are only measured up to $p_T = 35$ GeV and the most central 50% collisions due to statistical limitations. As shown in Figure 11, values of $v_n^{3\text{-sub}}\{4\}$ agree with $v_n\{4\}$ for central events, and deviate from $v_n\{4\}$ in peripheral events at high p_T . The p_T and centrality dependence of this deviation is consistent with a suppression of short-range non-flow correlations by the three-subevent cumulants. As has been shown in Ref. [26], these non-flow correlations have a more significant effect in events of smaller charged-particle multiplicity. Different

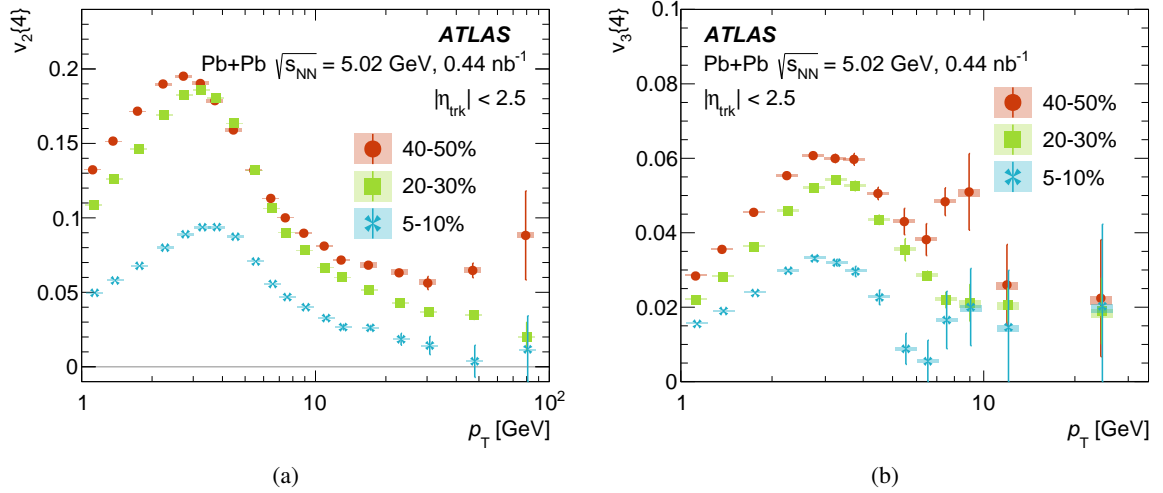


Figure 10: (a) $v_2\{4\}$ and (b) $v_3\{4\}$ using standard Q -cumulants for the centrality intervals 5–10%, 20–30%, and 40–50%. The statistical uncertainties are shown as error bars and the systematic uncertainties are shown as boxes.

behaviors are observed for $v_2^{3\text{-sub}}\{4\}$ and $v_3^{3\text{-sub}}\{4\}$ in the most peripheral centrality intervals available. For $p_T > 20$ GeV, the values of $v_2^{3\text{-sub}}\{4\}$ become nearly constant, whereas the values of $v_3^{3\text{-sub}}\{4\}$ continue to decrease for higher p_T . As in the cases of $v_n\{\text{SP}\}$, the contrasting behavior between v_2 and v_3 in the high- p_T region is consistent with contamination from dijet production, which contributes positively to even-order harmonics and negatively to odd-order harmonics and has a bigger impact in more peripheral events. In these measurements, dijet contributions are more pronounced in the MPC method than the SP method, and can arise from the narrower pseudorapidity range used for the MPC method.

The v_n values measured with four-particle cumulants are sensitive to the mean value as well as fluctuations of the underlying distributions, which includes contributions from both non-flow effects and initial-state geometry [21]. To better understand how the event-by-event distributions of non-flow effects and the initial-state geometry contribute to the measurements of v_n , comparisons of $v_n\{4\}$ using different event combination procedures are shown in Figures 12 and 13. In all centrality and p_T ranges measured, the $\langle 2\% \rangle$ results converge to those obtained with the default $\langle 1\% \rangle$ procedure, indicating that centrality-resolution-related fluctuations are negligible in these measurements when using the $\langle 1\% \rangle$ procedure. Therefore, the $\langle 1\% \rangle$ procedure results serve as an appropriate baseline for comparison. In the low- p_T region, the event combination procedure affects the fluctuation terms but not the mean value of the underlying distribution, whereas in the high- p_T region, computing cumulants directly in a wider centrality interval also biases the mean of measurements toward more central events.

Figure 12 shows that for v_2 the impact of event combination procedure is dependent on centrality, p_T , and less pronounced in three-subevent cumulants. In both of the quoted centrality intervals, the $\langle 10\% \rangle$ procedure shows a greater discrepancy from the $\langle 1\% \rangle$ procedure for $v_2\{4\}$ than for $v_n^{3\text{-sub}}\{4\}$, and the difference between $v_2\{4\}$ and $v_n^{3\text{-sub}}\{4\}$ is more pronounced in peripheral events. With the application of three-subevent cumulants, the discrepancy between event combination procedures is vanishingly small. This discrepancy shows a centrality and p_T dependence, as well as a sensitivity to the three-subevent cumulants similar to that observed for non-flow effects, suggesting the four-particle cumulant v_2 is primarily sensitive to fluctuations in non-flow effects. Similar observations have been made in studies of low- p_T flow [25, 27].

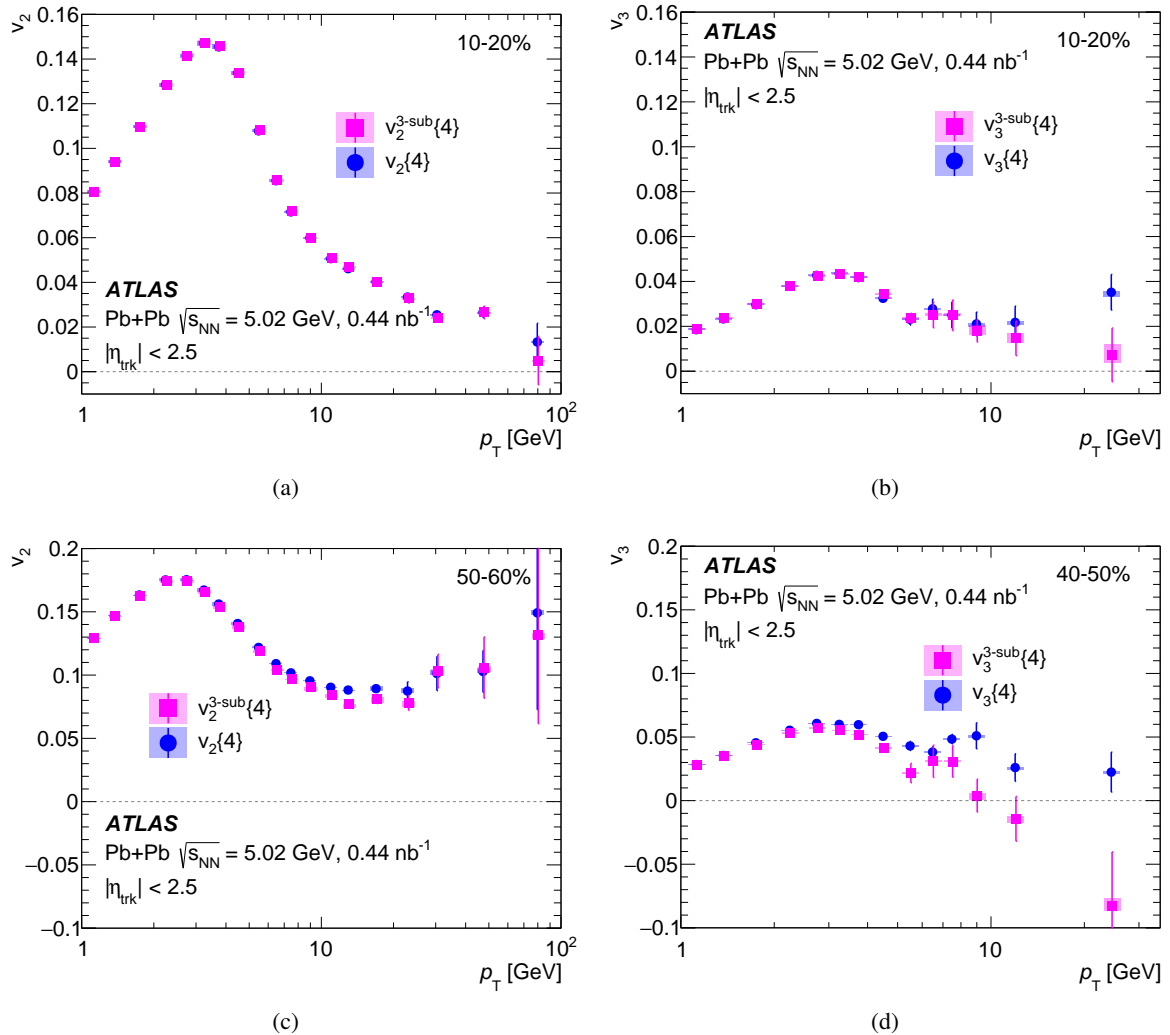


Figure 11: Comparison between standard and three-subevent Q -cumulants for (a) $v_2\{4\}$ and (b) $v_3\{4\}$ in the centrality interval 10–20%, and for (c) $v_2\{4\}$ in the centrality interval 50–60% and (d) $v_3\{4\}$ in the centrality interval 40–50%. The statistical uncertainties are shown as error bars and the systematic uncertainties are shown as boxes.

Figure 13 shows a comparison between different event combination procedures for $v_3\{4\}$ and $v_3^{3\text{-sub}}\{4\}$. It can be seen that the discrepancy between $\langle 10\% \rangle$ and $\langle 1\% \rangle$ is much more substantial than v_2 in the quoted centrality intervals for both the standard and the three-subevent cumulants, the latter of which have been shown to suppress short-range non-flow effects in Figure 11. These observations show that v_3 values are more sensitive to fluctuations in initial geometry than those in non-flow effects. It has been found in the measurements of reference flow that the fluctuations of v_3 are more significant relative to the mean in comparison to v_2 [51]. Results from Figures 12 and 13 suggest that event-by-event fluctuations are more pronounced in the triangularity of the initial geometry than the ellipticity. The discrepancy among event combination procedures decreases in the 40–50% centrality interval, where the centrality dependence of $v_3\{4\}$ has been observed to flatten [27].

Figure 14 shows a comparison between the SP method and the three-subevent Q -cumulant MPC method using the default $\langle 1\% \rangle$ event combination procedure. The $v_3^{3\text{-sub}}\{4\}$ results are truncated at a p_T of 35 GeV

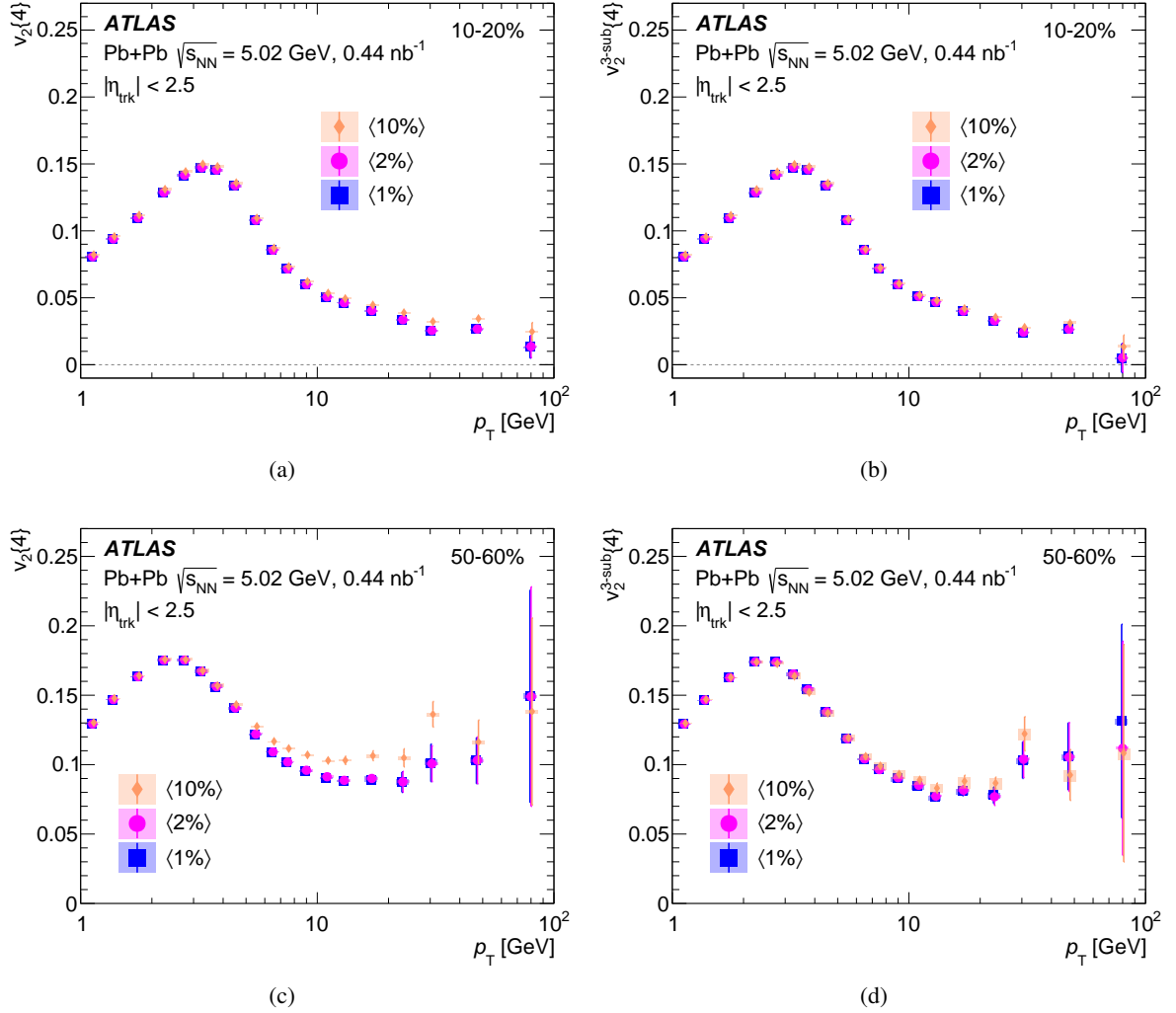


Figure 12: Comparison between the $\langle 1\% \rangle$, $\langle 2\% \rangle$, and $\langle 10\% \rangle$ event combination procedures in the centrality interval 10–20% for (a) $v_2\{4\}$ and (b) $v_2^{3\text{-sub}}\{4\}$, and in the centrality interval 50–60% for (c) $v_2\{4\}$ and (d) $v_2^{3\text{-sub}}\{4\}$. The statistical uncertainties are shown as error bars and the systematic uncertainties are shown as boxes.

due to limited statistics. Values of $v_n\{\text{SP}\}$ are greater than $v_n^{3\text{-sub}}\{4\}$, similar to the comparison observed in v_n measurements in Pb+Pb collisions at $\sqrt{s_{NN}} = 2.76$ TeV [29]. At $p_T > 10$ GeV, the comparison between the two methods contains information about how hard scattered partons respond to the event-by-event distribution of the initial-state QGP geometry. Different behaviors are observed for different centrality intervals. In central events, the relation $v_n\{\text{SP}\} > v_n^{3\text{-sub}}\{4\}$ holds up to p_T of approximately 15 GeV for both v_2 and v_3 . In peripheral events, the two methods converge with increasing p_T and then intersect for v_2 around approximately 15 GeV, above which the two methods diverge with $v_2\{4\} > v_2\{\text{SP}\}$, whereas in v_3 , the methods diverge from each other for $p_T > 10$ GeV, and always exhibiting $v_3\{\text{SP}\} > v_3\{4\}$. This difference between v_2 and v_3 suggests residual non-flow dijet contributions, which have greater impact in peripheral events. It should be noted that multiple effects could contribute to the observed trends in peripheral events, such as other non-flow correlations, the effects of the event combination procedure, and event plane longitudinal decorrelation.

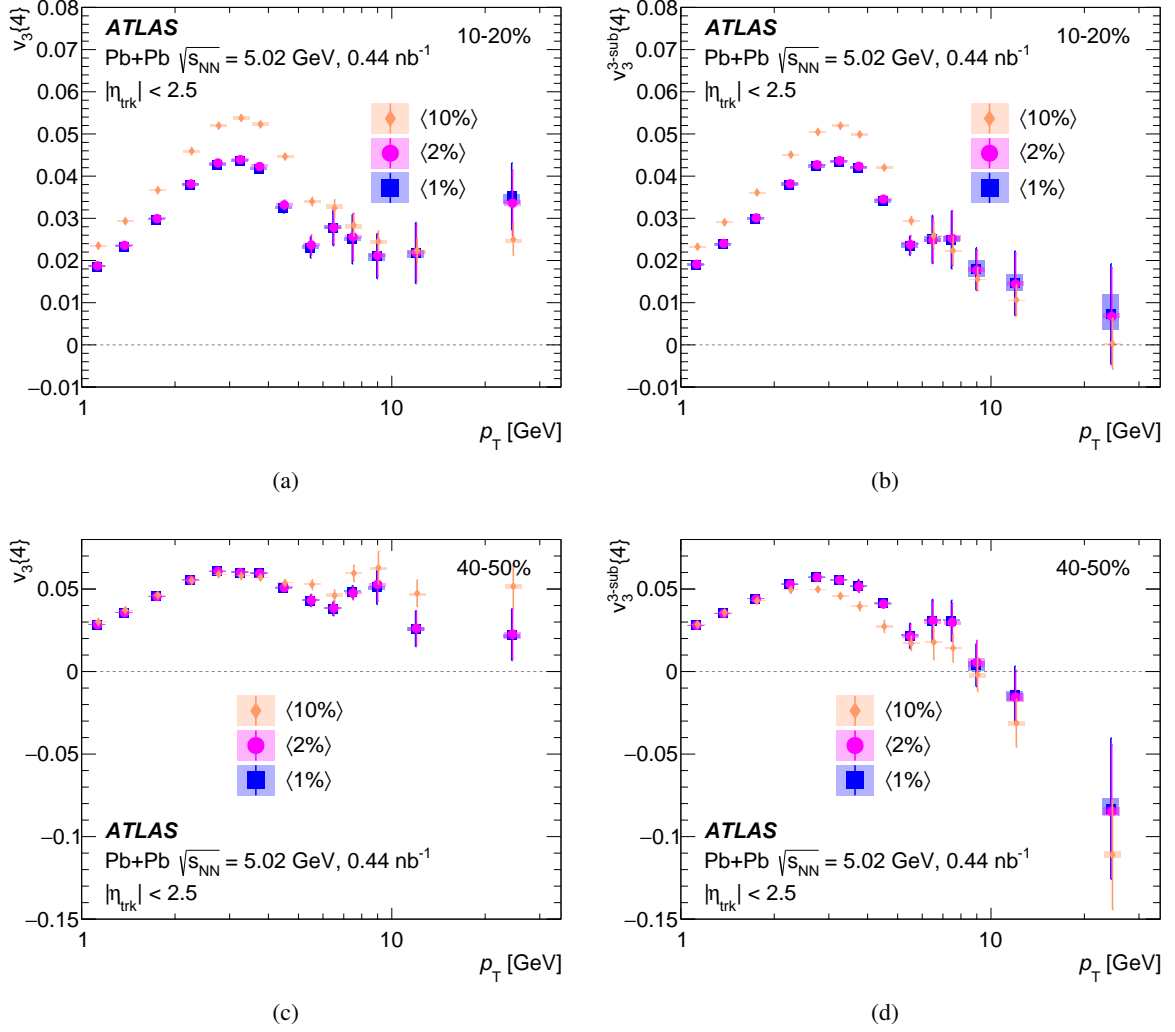


Figure 13: Comparison between the $\langle 1\% \rangle$, $\langle 2\% \rangle$, and $\langle 10\% \rangle$ event combination procedures in the centrality interval 10–20% for (a) $v_3\{4}$ and (b) $v_3^{3\text{-sub}}\{4}$, and in the centrality interval 40–50% for (c) $v_3\{4}$ and (d) $v_3^{3\text{-sub}}\{4}$. The statistical uncertainties are shown as error bars and the systematic uncertainties are shown as boxes.

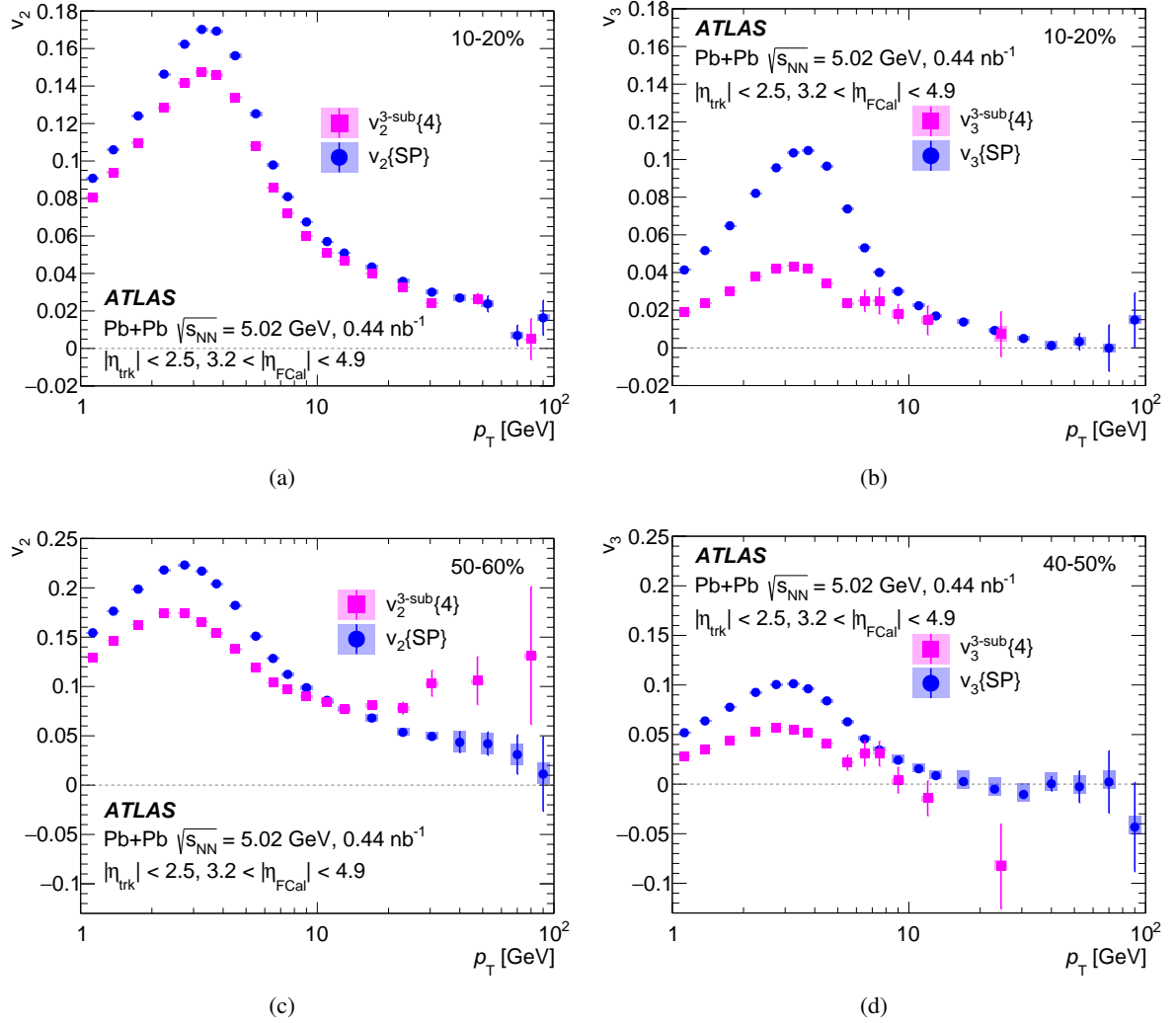


Figure 14: Comparison between the $v_n\{\text{SP}\}$ results and $v_n^{3\text{-sub}}\{4\}$ in centrality intervals 10–20% for (a) $n = 2$ and (b) $n = 3$, and (c) in centrality intervals 50–60% for $n = 2$ and (d) in centrality intervals 40–50% for $n = 3$. The statistical uncertainties are shown as error bars and the systematic uncertainties are shown as boxes.

7 Conclusions

This paper describes the measurements of azimuthal anisotropies of charged particles in Pb+Pb collisions at $\sqrt{s_{\text{NN}}} = 5.02$ TeV, using a dataset corresponding to an integrated luminosity of 0.44 nb^{-1} collected with the ATLAS detector at the LHC in 2018. The azimuthal anisotropy coefficients, v_2 and v_3 , are measured using the scalar product and multi-particle cumulant methods over the charged particles with p_{T} up to 400 GeV in several centrality intervals spanning the 0–60% most central events. Additionally, different pseudorapidity ranges and strategies for v_n values are compared.

The p_{T} -differential $v_n\{\text{SP}\}$ values are measured over a pseudorapidity range $|\eta| < 2.5$ and a p_{T} range of 1–400 GeV in the 0–60% most central collisions. In mid-central collisions, the $v_2\{\text{SP}\}$ values are found to remain positive up to p_{T} of 100 GeV with a value of 1–2%; the $v_3\{\text{SP}\}$ values are found to be positive up to p_{T} of approximately 25 GeV. These results are consistent with previous measurements from the LHC experiments, and the increased luminosity and implemented data taking innovations resulted in a larger dataset that has allowed for improved precision at high p_{T} . Values of $v_n\{\text{SP}\}$ are also measured across two additional pseudorapidity ranges: $|\eta| < 1.1$ and $1.1 < |\eta| < 2.5$, over a p_{T} range of 1–100 GeV. In the low- p_{T} region, a larger pseudorapidity gap between the correlated flow vectors decreases both $v_2\{\text{SP}\}$ and $v_3\{\text{SP}\}$ values, which can arise from decreased non-flow effects and the increased longitudinal decorrelation. By contrast, at high p_{T} , a larger pseudorapidity gap between the correlated flow vectors decreases $v_2\{\text{SP}\}$ but increases $v_3\{\text{SP}\}$ values, suggesting non-flow dijet contributions, especially in peripheral events.

Using the MPC method, the p_{T} -differential $v_2\{4\}$ values are measured over a pseudorapidity range of $|\eta| < 2.5$ and a p_{T} up to 100 GeV in the most central 0–60% events. For $p_{\text{T}} > 10$ GeV, it is observed that the three-subevent technique suppresses short-range non-flow contributions. Meanwhile, non-flow dijet contributions are still observed with the three-subevent technique. Measurements of $v_2\{4\}$ and $v_3\{4\}$ using two additional event combination procedures, $\langle 2\% \rangle$ and $\langle 10\% \rangle$, were also performed and compared to results using the default $\langle 1\% \rangle$ procedure to understand the dominating source of fluctuations in v_n measurements. It is observed that for $v_2\{4\}$, the event combination procedure affects non-flow contributions primarily, whereas, for $v_3\{4\}$, initial geometry contributions are more significantly affected.

The comparison between the SP and MPC methods shows different trends between v_2 and v_3 in peripheral events. For v_2 , the difference between the SP and the MPC methods decreases toward zero up to p_{T} of 15 GeV, then flips sign for $p_{\text{T}} > 15$ GeV. For v_3 , however, this difference continues to increase with p_{T} with the same sign. The contrasting behavior between v_2 and v_3 indicates remaining non-flow dijet contributions, which contribute to the SP and the MPC methods differently.

These results provide comprehensive information on the mechanism and fluctuations of azimuthal anisotropies of hard-scattered particles in the Pb+Pb collision system. The positive v_2 and v_3 values observed suggest that the energy loss of the hard-scattered partons is influenced by the event-by-event distribution of the initial geometry of the QGP, and these values can be used to constrain the path-length dependence of jet quenching. The comparison studies presented provide key insights on the different contributions of the various non-flow sources, as well as revealing the different sources of fluctuations that dominate in v_2 and v_3 .

Acknowledgements

We thank CERN for the very successful operation of the LHC and its injectors, as well as the support staff at CERN and at our institutions worldwide without whom ATLAS could not be operated efficiently.

The crucial computing support from all WLCG partners is acknowledged gratefully, in particular from CERN, the ATLAS Tier-1 facilities at TRIUMF/SFU (Canada), NDGF (Denmark, Norway, Sweden), CC-IN2P3 (France), KIT/GridKA (Germany), INFN-CNAF (Italy), NL-T1 (Netherlands), PIC (Spain), RAL (UK) and BNL (USA), the Tier-2 facilities worldwide and large non-WLCG resource providers. Major contributors of computing resources are listed in Ref. [52].

We gratefully acknowledge the support of ANPCyT, Argentina; YerPhI, Armenia; ARC, Australia; BMWFW and FWF, Austria; ANAS, Azerbaijan; CNPq and FAPESP, Brazil; NSERC, NRC and CFI, Canada; CERN; ANID, Chile; CAS, MOST and NSFC, China; Minciencias, Colombia; MEYS CR, Czech Republic; DNRF and DNSRC, Denmark; IN2P3-CNRS and CEA-DRF/IRFU, France; SRNSFG, Georgia; BMBF, HGF and MPG, Germany; GSRI, Greece; RGC and Hong Kong SAR, China; ICHEP and Academy of Sciences and Humanities, Israel; INFN, Italy; MEXT and JSPS, Japan; CNRST, Morocco; NWO, Netherlands; RCN, Norway; MNiSW, Poland; FCT, Portugal; MNE/IFA, Romania; MSTDI, Serbia; MSSR, Slovakia; ARIS and MVZI, Slovenia; DSI/NRF, South Africa; MICIU/AEI, Spain; SRC and Wallenberg Foundation, Sweden; SERI, SNSF and Cantons of Bern and Geneva, Switzerland; NSTC, Taipei; TENMAK, Türkiye; STFC/UKRI, United Kingdom; DOE and NSF, United States of America.

Individual groups and members have received support from BCKDF, CANARIE, CRC and DRAC, Canada; CERN-CZ, FORTE and PRIMUS, Czech Republic; COST, ERC, ERDF, Horizon 2020, ICSC-NextGenerationEU and Marie Skłodowska-Curie Actions, European Union; Investissements d’Avenir Labex, Investissements d’Avenir Idex and ANR, France; DFG and AvH Foundation, Germany; Herakleitos, Thales and Aristeia programmes co-financed by EU-ESF and the Greek NSRF, Greece; BSF-NSF and MINERVA, Israel; NCN and NAWA, Poland; La Caixa Banking Foundation, CERCA Programme Generalitat de Catalunya and PROMETEO and GenT Programmes Generalitat Valenciana, Spain; Göran Gustafssons Stiftelse, Sweden; The Royal Society and Leverhulme Trust, United Kingdom.

In addition, individual members wish to acknowledge support from Armenia: Yerevan Physics Institute (FAPERJ); CERN: European Organization for Nuclear Research (CERN DOCT); Chile: Agencia Nacional de Investigación y Desarrollo (FONDECYT 1230812, FONDECYT 1230987, FONDECYT 1240864); China: Chinese Ministry of Science and Technology (MOST-2023YFA1605700, MOST-2023YFA1609300), National Natural Science Foundation of China (NSFC - 12175119, NSFC 12275265, NSFC-12075060); Czech Republic: Czech Science Foundation (GACR - 24-11373S), Ministry of Education Youth and Sports (FORTE CZ.02.01.01/00/22_008/0004632), PRIMUS Research Programme (PRIMUS/21/SCI/017); EU: H2020 European Research Council (ERC - 101002463); European Union: European Research Council (ERC - 948254, ERC 101089007, ERC, BARD, 101116429), European Union, Future Artificial Intelligence Research (FAIR-NextGenerationEU PE00000013), Italian Center for High Performance Computing, Big Data and Quantum Computing (ICSC, NextGenerationEU); France: Agence Nationale de la Recherche (ANR-20-CE31-0013, ANR-21-CE31-0013, ANR-21-CE31-0022, ANR-22-EDIR-0002); Germany: Baden-Württemberg Stiftung (BW Stiftung-Postdoc Eliteprogramme), Deutsche Forschungsgemeinschaft (DFG - 469666862, DFG - CR 312/5-2); Italy: Istituto Nazionale di Fisica Nucleare (ICSC, NextGenerationEU), Ministero dell’Università e della Ricerca (PRIN - 20223N7F8K - PNRR M4.C2.1.1); Japan: Japan Society for the Promotion of Science (JSPS KAKENHI JP22H01227, JSPS KAKENHI JP22H04944, JSPS KAKENHI JP22KK0227, JSPS KAKENHI

JP23KK0245); Norway: Research Council of Norway (RCN-314472); Poland: Ministry of Science and Higher Education (IDUB AGH, POB8, D4 no 9722), Polish National Agency for Academic Exchange (PPN/PPO/2020/1/00002/U/00001), Polish National Science Centre (NCN 2021/42/E/ST2/00350, NCN OPUS 2023/51/B/ST2/02507, NCN OPUS nr 2022/47/B/ST2/03059, NCN UMO-2019/34/E/ST2/00393, NCN & H2020 MSCA 945339, UMO-2020/37/B/ST2/01043, UMO-2021/40/C/ST2/00187, UMO-2022/47/O/ST2/00148, UMO-2023/49/B/ST2/04085, UMO-2023/51/B/ST2/00920); Spain: Generalitat Valenciana (Artemisa, FEDER, IDIFEDER/2018/048), Ministry of Science and Innovation (MCIN & NextGenEU PCI2022-135018-2, MICIN & FEDER PID2021-125273NB, RYC2019-028510-I, RYC2020-030254-I, RYC2021-031273-I, RYC2022-038164-I); Sweden: Carl Trygger Foundation (Carl Trygger Foundation CTS 22:2312), Swedish Research Council (Swedish Research Council 2023-04654, VR 2018-00482, VR 2022-03845, VR 2022-04683, VR 2023-03403, VR grant 2021-03651), Knut and Alice Wallenberg Foundation (KAW 2018.0458, KAW 2019.0447, KAW 2022.0358); Switzerland: Swiss National Science Foundation (SNSF - PCEFP2_194658); United Kingdom: Leverhulme Trust (Leverhulme Trust RPG-2020-004), Royal Society (NIF-R1-231091); United States of America: U.S. Department of Energy (ECA DE-AC02-76SF00515), Neubauer Family Foundation.

Appendix

A Measurements and comparisons of v_n in additional centrality intervals

This appendix includes additional centrality intervals for the measurements presented in Section 6. For comparison purposes, the selected centrality intervals are all of 10% width, except in Figures 15 and 18, where the 5% wide centrality intervals are also shown. These additional centrality intervals supplement the transitioning of trends from the central 10–20% interval to the peripheral 40–50% or 50–60% interval shown in Section 6.

Figure 15 shows additional centrality intervals for $v_n\{\text{SP}\}$ results as a function of p_T , where the same centrality and p_T trends shown in Figure 3 can be observed. Figures 16 and 17 show the comparison of different pseudorapidity ranges for $v_2\{\text{SP}\}$ and $v_3\{\text{SP}\}$ results in two mid-central intervals. In these comparisons, the difference between pseudorapidity ranges does not show as strong a dependence on p_T for $v_2\{\text{SP}\}$ as it does for $v_3\{\text{SP}\}$.

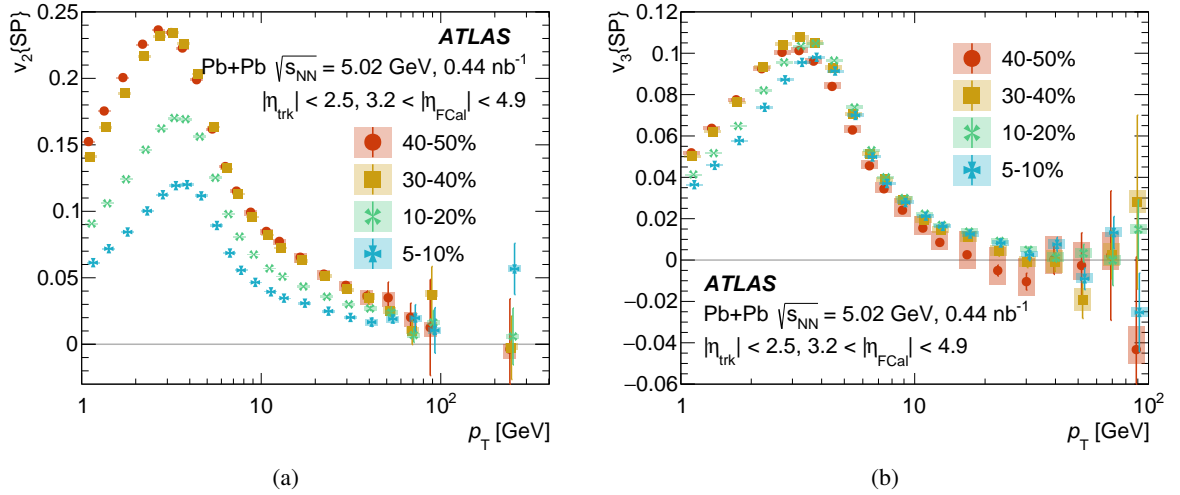


Figure 15: The (a) $v_2\{\text{SP}\}$ and (b) $v_3\{\text{SP}\}$ values as a function of charged-particle p_T for the centrality intervals 5–10%, 10–20%, 30–40%, and 40–50%. The statistical uncertainties are shown as error bars and the systematic uncertainties are shown as boxes.

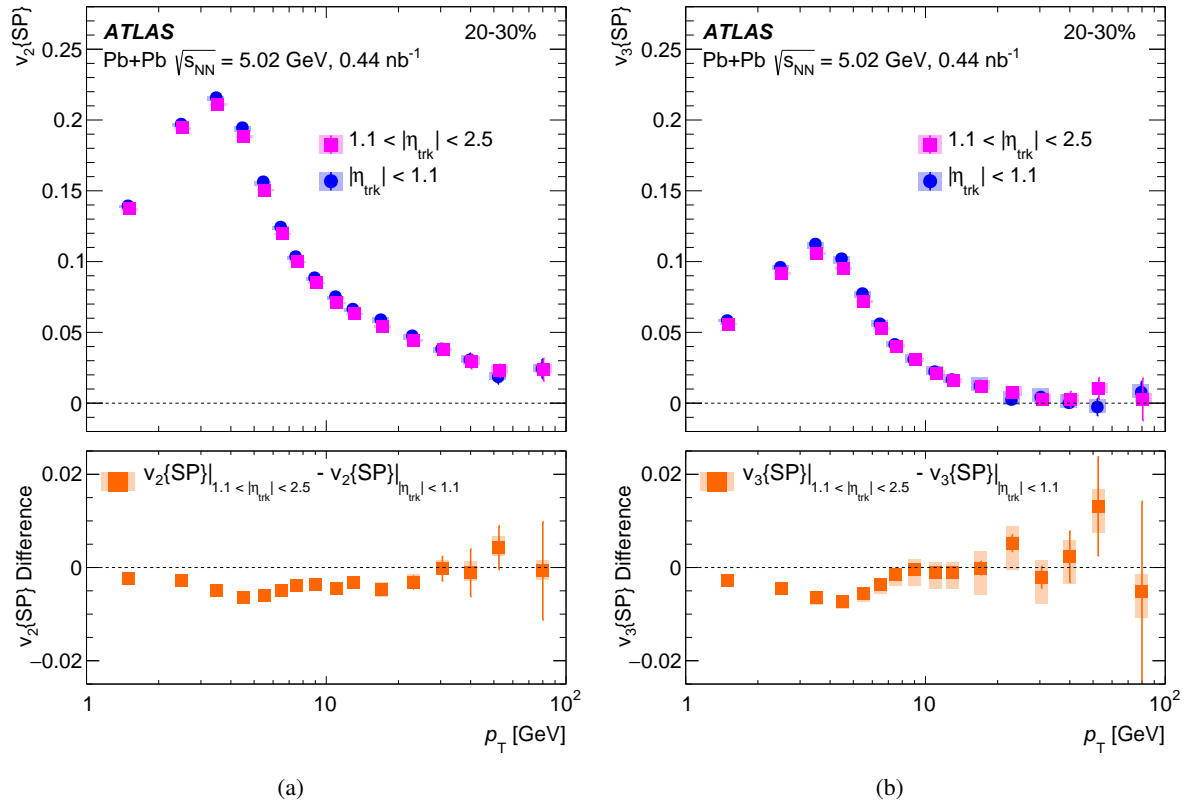


Figure 16: The (a) $v_2\{\text{SP}\}$ and (b) $v_3\{\text{SP}\}$ values as a function of charged-particle p_T in the centrality interval 20–30% for different pseudorapidity ranges. The bottom panel shows the difference in the $v_3\{\text{SP}\}$ measured between the two ranges. The statistical uncertainties are shown as error bars and the systematic uncertainties are shown as boxes.

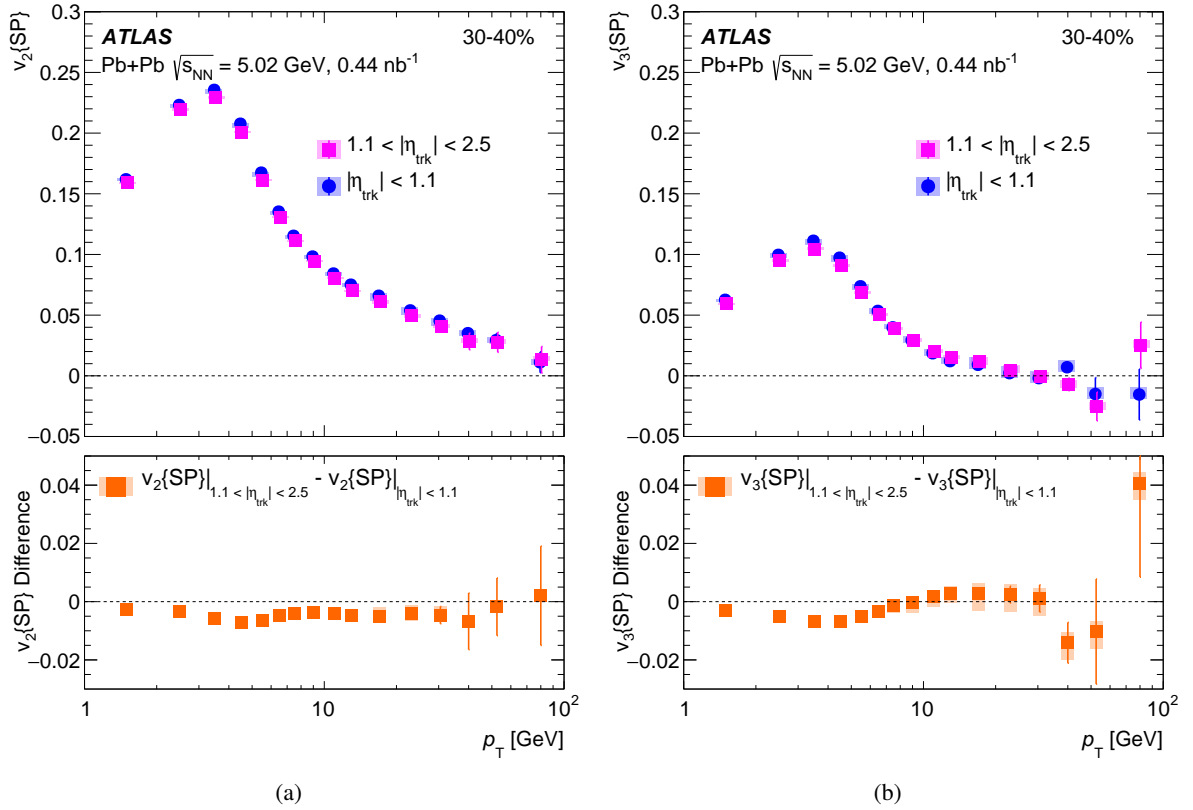


Figure 17: The (a) $v_2\{\text{SP}\}$ and (b) $v_3\{\text{SP}\}$ values as a function of charged-particle p_T in the centrality interval 30–40% for different pseudorapidity ranges. The bottom panel shows the difference in the $v_3\{\text{SP}\}$ measured between the two ranges. The statistical uncertainties are shown as error bars and the systematic uncertainties are shown as boxes.

Figure 18 shows additional centrality intervals for $v_n\{4\}$ results with standard Q -cumulants using the $\langle 1\% \rangle$ event combination procedure as a function of p_T , where a slight increase at high p_T is observed for $v_2\{4\}$ in the 50–60% centrality interval. Figure 19 shows the comparison of standard versus three-subevent cumulants in $v_n\{4\}$ for mid-central events, where a stronger suppression is observed in v_3 than v_2 . Figures 20 and 21 show the event combination procedure comparisons for $v_2\{4\}$ and $v_3\{4\}$, respectively, for both the standard and three-subevent cumulants. The event combination procedure discrepancy is much smaller in v_2 than in v_3 , and is well suppressed by the three-subevent cumulants. In contrast, $v_3^{3\text{-sub}}\{4\}$ still shows a significant discrepancy between different event combination procedures.

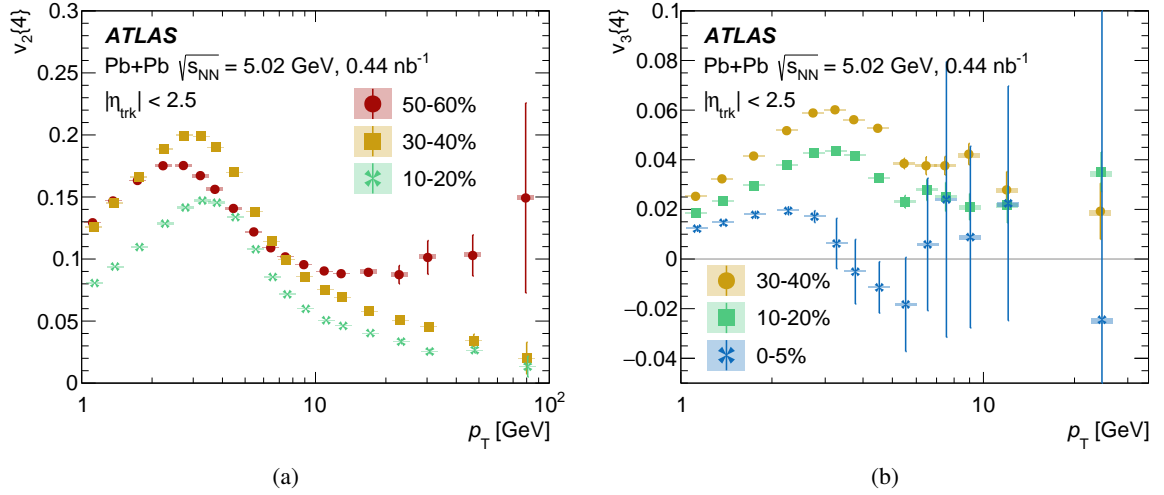


Figure 18: The (a) $v_2\{4\}$ and (b) $v_3\{4\}$ values as a function of charged-particle p_T for different centrality intervals. For $v_2\{4\}$, 10–20%, 30–40% and 50–60% are shown, and for $v_3\{4\}$, 0–5%, 10–20%, and 30–40% are shown. The statistical uncertainties are shown as error bars and the systematic uncertainties are shown as boxes.

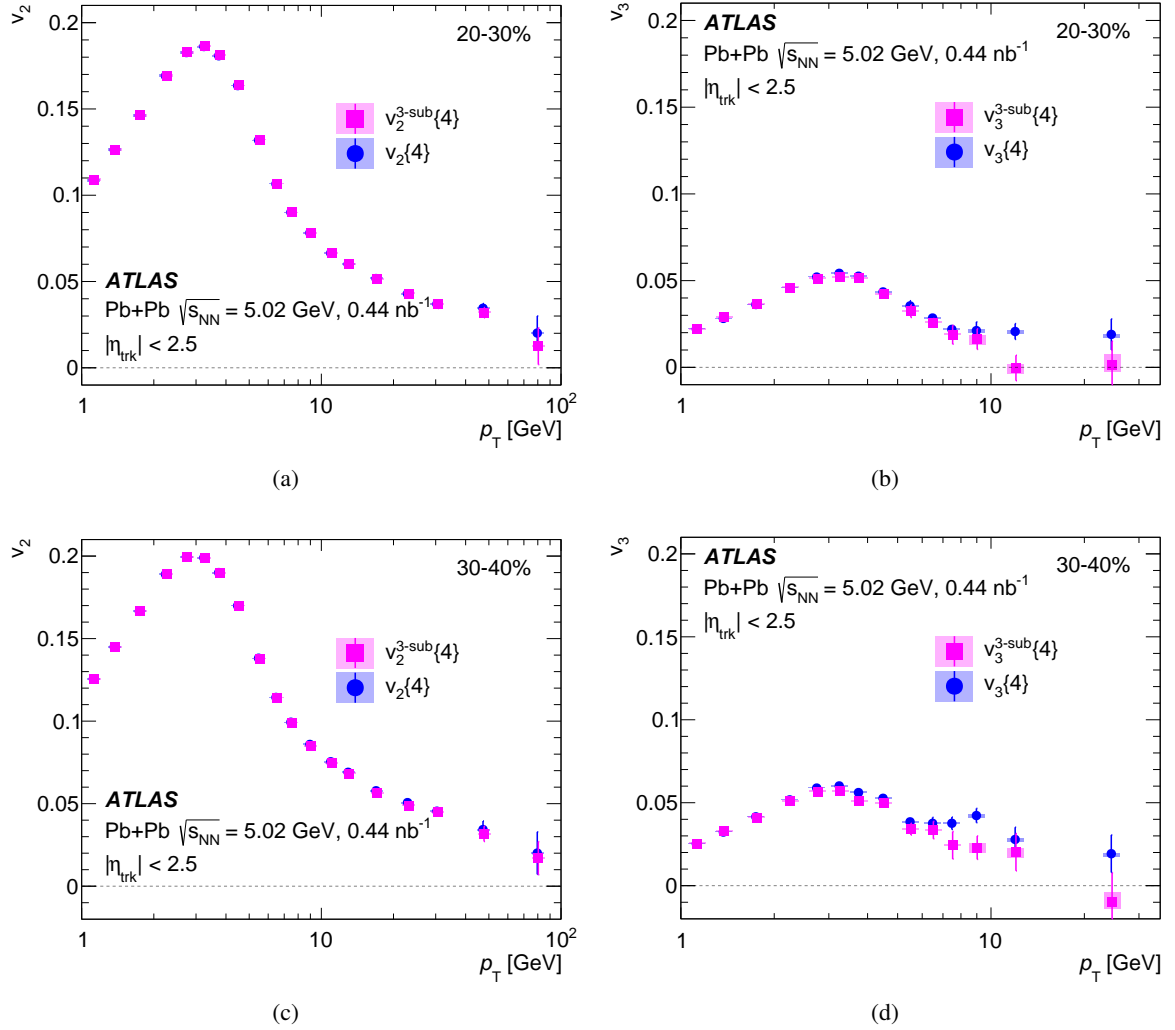


Figure 19: $v_n\{4\}$ comparison between standard and three-subevent Q -cumulants in the centrality interval 20–30% for (a) $v_2\{4\}$ and (b) $v_3\{4\}$, and in the centrality interval 30–40% for (c) $v_2\{4\}$ and (d) $v_3\{4\}$. The statistical uncertainties are shown as error bars and the systematic uncertainties are shown as boxes.

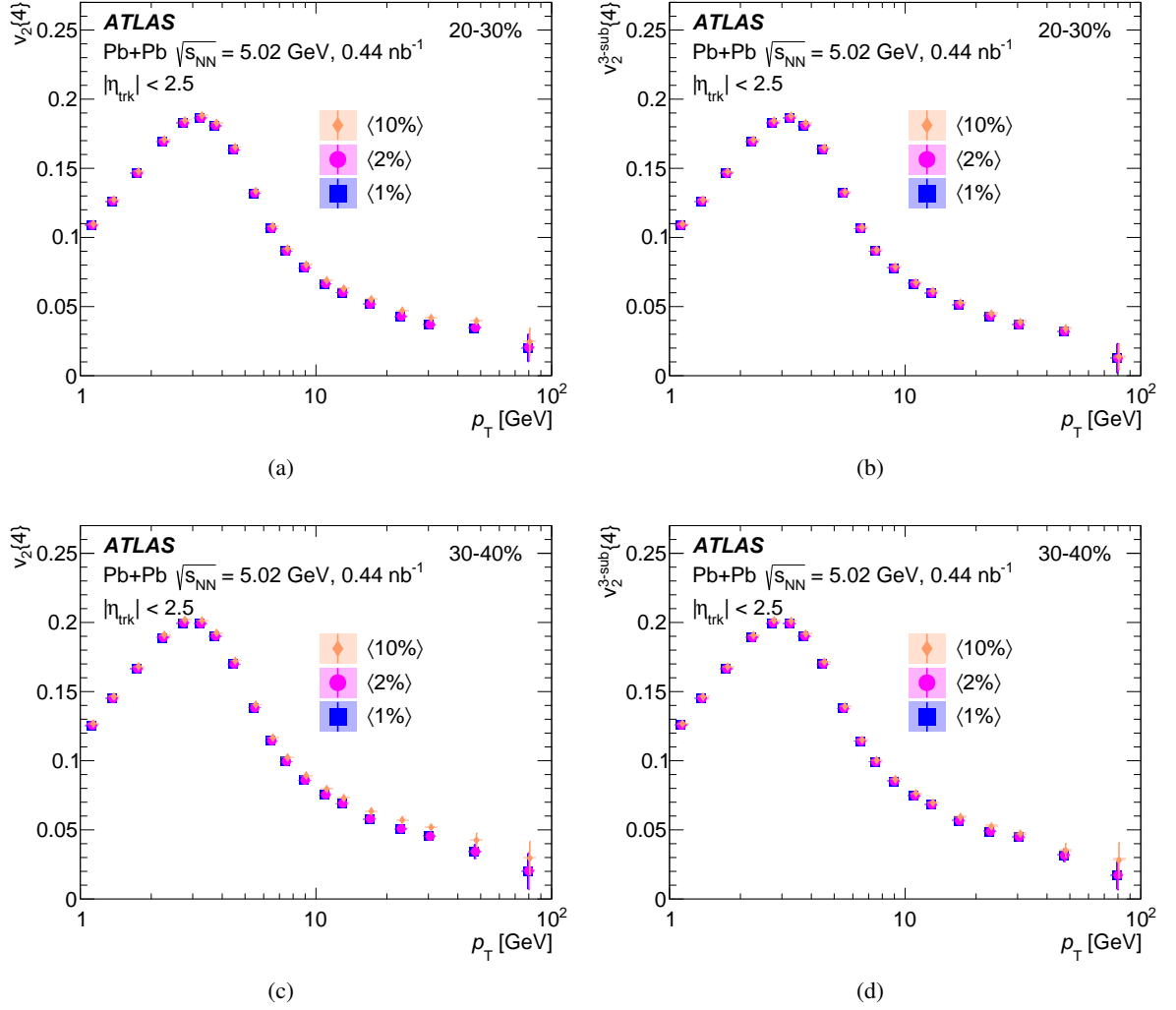


Figure 20: Comparison between $\langle 1\% \rangle$, $\langle 2\% \rangle$ and $\langle 10\% \rangle$ event combination procedures in the centrality intervals 20–30% for (a) $v_2\{4}$ and (b) $v_2^{3\text{-sub}}\{4}$, and in the centrality interval 30–40% for (c) $v_2\{4}$ and (d) $v_2^{3\text{-sub}}\{4}$. The statistical uncertainties are shown as error bars and the systematic uncertainties are shown as boxes.

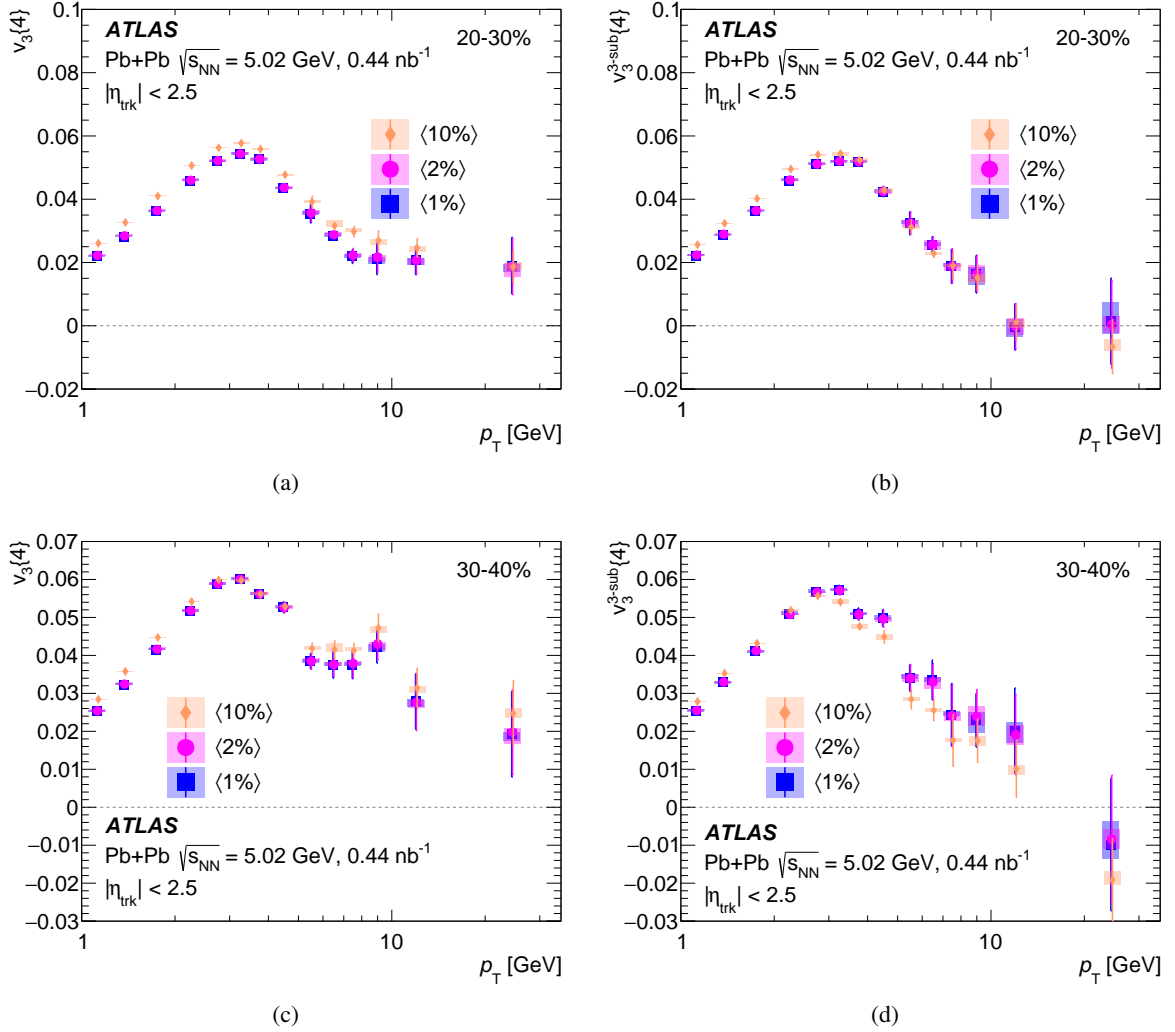


Figure 21: Comparison between $\langle 1\% \rangle$, $\langle 2\% \rangle$ and $\langle 10\% \rangle$ event combination procedures in the centrality interval 20–30% for (a) $v_3\{4\}$ and (b) $v_3^{3\text{-sub}}\{4\}$, and in the centrality interval 30–40% for (c) $v_3\{4\}$ and (d) $v_3^{3\text{-sub}}\{4\}$. The statistical uncertainties are shown as error bars and the systematic uncertainties are shown as boxes.

References

- [1] W. Busza, K. Rajagopal, and W. van der Schee, *Heavy Ion Collisions: The Big Picture, and the Big Questions*, *Ann. Rev. Nucl. Part. Sci.* **68** (2018) 339, arXiv: [1802.04801 \[hep-ph\]](#).
- [2] L. Cunqueiro and A. M. Sickles, *Studying the QGP with Jets at the LHC and RHIC*, *Prog. Part. Nucl. Phys.* **124** (2022) 103940, arXiv: [2110.14490 \[nucl-ex\]](#).
- [3] ATLAS Collaboration, *Measurement of the nuclear modification factor for inclusive jets in Pb+Pb collisions at $\sqrt{s_{NN}} = 5.02$ TeV with the ATLAS detector*, *Phys. Lett. B* **790** (2019) 108, arXiv: [1805.05635 \[nucl-ex\]](#).
- [4] CMS Collaboration, *First measurement of large area jet transverse momentum spectra in heavy-ion collisions*, *JHEP* **05** (2021) 284, arXiv: [2102.13080 \[hep-ex\]](#).
- [5] ATLAS Collaboration, *Measurement of Suppression of Large-Radius Jets and Its Dependence on Substructure in Pb+Pb Collisions at $\sqrt{s_{NN}} = 5.02$ TeV with the ATLAS Detector*, *Phys. Rev. Lett.* **131** (2023) 172301, arXiv: [2301.05606 \[nucl-ex\]](#).
- [6] ALICE Collaboration, *Measurements of inclusive jet spectra in pp and central Pb-Pb collisions at $\sqrt{s_{NN}} = 5.02$ TeV*, *Phys. Rev. C* **101** (2020) 034911, arXiv: [1909.09718 \[nucl-ex\]](#).
- [7] X.-N. Wang, *Jet quenching and azimuthal anisotropy of large p_T spectra in noncentral high-energy heavy ion collisions*, *Phys. Rev. C* **63** (2001) 054902, arXiv: [nucl-th/0009019](#).
- [8] M. Gyulassy, I. Vitev, and X. N. Wang, *High p_T azimuthal asymmetry in noncentral A+A at RHIC*, *Phys. Rev. Lett.* **86** (2001) 2537, arXiv: [nucl-th/0012092](#).
- [9] E. V. Shuryak, *The Azimuthal asymmetry at large p_T seem to be too large for a “jet quenching”*, *Phys. Rev. C* **66** (2002) 027902, arXiv: [nucl-th/0112042](#).
- [10] U. Heinz and R. Snellings, *Collective flow and viscosity in relativistic heavy-ion collisions*, *Ann. Rev. Nucl. Part. Sci.* **63** (2013) 123, arXiv: [1301.2826 \[nucl-th\]](#).
- [11] A. M. Poskanzer and S. A. Voloshin, *Methods for analyzing anisotropic flow in relativistic nuclear collisions*, *Phys. Rev. C* **58** (1998) 1671, arXiv: [nucl-ex/9805001](#).
- [12] CMS Collaboration, *Azimuthal anisotropy of charged particles with transverse momentum up to 100 GeV/c in PbPb collisions at $\sqrt{s_{NN}} = 5.02$ TeV*, *Phys. Lett. B* **776** (2018) 195, arXiv: [1702.00630 \[hep-ex\]](#).
- [13] ATLAS Collaboration, *Measurements of azimuthal anisotropies of jet production in Pb+Pb collisions at $\sqrt{s_{NN}} = 5.02$ TeV with the ATLAS detector*, *Phys. Rev. C* **105** (2022) 064903, arXiv: [2111.06606 \[nucl-ex\]](#).
- [14] ATLAS Collaboration, *Measurement of the Azimuthal Angle Dependence of Inclusive Jet Yields in Pb+Pb Collisions at $\sqrt{s_{NN}} = 2.76$ TeV with the ATLAS detector*, *Phys. Rev. Lett.* **111** (2013) 152301, arXiv: [1306.6469 \[hep-ex\]](#).
- [15] ATLAS Collaboration, *Measurement of the azimuthal anisotropy of charged particles produced in $\sqrt{s_{NN}} = 5.02$ TeV Pb+Pb collisions with the ATLAS detector*, *Eur. Phys. J. C* **78** (2018) 997, arXiv: [1808.03951 \[nucl-ex\]](#).

- [16] ALICE Collaboration, *Investigations of Anisotropic Flow Using Multiparticle Azimuthal Correlations in pp, p-Pb, Xe-Xe, and Pb-Pb Collisions at the LHC*, [Phys. Rev. Lett. **123** \(2019\) 142301](#), arXiv: [1903.01790 \[nucl-ex\]](#).
- [17] STAR Collaboration, *Elliptic flow from two and four particle correlations in Au+Au collisions at $\sqrt{s_{NN}} = 130$ GeV*, [Phys. Rev. C **66** \(2002\) 034904](#), arXiv: [nucl-ex/0206001](#).
- [18] PHENIX Collaboration, *Multiparticle azimuthal correlations for extracting event-by-event elliptic and triangular flow in Au+Au collisions at $\sqrt{s_{NN}} = 200$ GeV*, [Phys. Rev. C **99** \(2019\) 024903](#), arXiv: [1804.10024 \[nucl-ex\]](#).
- [19] S. A. Voloshin, A. M. Poskanzer, and R. Snellings, *Collective phenomena in non-central nuclear collisions*, [Landolt-Bornstein **23** \(2010\) 293](#), ed. by R. Stock, arXiv: [0809.2949 \[nucl-ex\]](#).
- [20] M. Luzum and J.-Y. Ollitrault, *Eliminating experimental bias in anisotropic-flow measurements of high-energy nuclear collisions*, [Phys. Rev. C **87** \(2013\) 044907](#), arXiv: [1209.2323 \[nucl-ex\]](#).
- [21] N. Borghini, P. M. Dinh, and J.-Y. Ollitrault, *Flow analysis from multiparticle azimuthal correlations*, [Phys. Rev. C **64** \(2001\) 054901](#), arXiv: [nucl-th/0105040](#).
- [22] N. Borghini, P. M. Dinh, and J.-Y. Ollitrault, *A New method for measuring azimuthal distributions in nucleus-nucleus collisions*, [Phys. Rev. C **63** \(2001\) 054906](#), arXiv: [nucl-th/0007063](#).
- [23] A. Bilandzic, R. Snellings, and S. Voloshin, *Flow analysis with cumulants: Direct calculations*, [Phys. Rev. C **83** \(2011\) 044913](#), arXiv: [1010.0233 \[nucl-ex\]](#).
- [24] A. Bilandzic, C. H. Christensen, K. Gulbrandsen, A. Hansen, and Y. Zhou, *Generic framework for anisotropic flow analyses with multiparticle azimuthal correlations*, [Phys. Rev. C **89** \(2014\) 064904](#), arXiv: [1312.3572 \[nucl-ex\]](#).
- [25] J. Jia, M. Zhou, and A. Trzupek, *Revealing long-range multiparticle collectivity in small collision systems via subevent cumulants*, [Phys. Rev. C **96** \(2017\) 034906](#), arXiv: [1701.03830 \[nucl-th\]](#).
- [26] P. Huo, K. Gajdošová, J. Jia, and Y. Zhou, *Importance of non-flow in mixed-harmonic multi-particle correlations in small collision systems*, [Phys. Lett. B **777** \(2018\) 201](#), arXiv: [1710.07567 \[nucl-ex\]](#).
- [27] ATLAS Collaboration, *Fluctuations of anisotropic flow in Pb+Pb collisions at $\sqrt{s_{NN}} = 5.02$ TeV with the ATLAS detector*, [JHEP **01** \(2020\) 051](#), arXiv: [1904.04808 \[nucl-ex\]](#).
- [28] ALICE Collaboration, *Azimuthal anisotropy of charged jet production in $\sqrt{s_{NN}} = 2.76$ TeV Pb–Pb collisions*, [Phys. Lett. B **753** \(2016\) 511](#), arXiv: [1509.07334 \[nucl-ex\]](#).
- [29] ATLAS Collaboration, *Measurement of flow harmonics with multi-particle cumulants in Pb+Pb collisions at $\sqrt{s_{NN}} = 2.76$ TeV with the ATLAS detector*, [Eur. Phys. J. C **74** \(2014\) 3157](#), arXiv: [1408.4342 \[hep-ex\]](#).
- [30] ATLAS Collaboration, *The ATLAS Experiment at the CERN Large Hadron Collider*, [JINST **3** \(2008\) S08003](#).

- [31] ATLAS Collaboration, *ATLAS Insertable B-Layer: Technical Design Report*, ATLAS-TDR-19; CERN-LHCC-2010-013, 2010, URL: <https://cds.cern.ch/record/1291633>, Addendum: ATLAS-TDR-19-ADD-1; CERN-LHCC-2012-009, 2012, URL: <https://cds.cern.ch/record/1451888>.
- [32] B. Abbott et al., *Production and integration of the ATLAS Insertable B-Layer*, *JINST* **13** (2018) T05008, arXiv: [1803.00844](https://arxiv.org/abs/1803.00844) [[physics.ins-det](#)].
- [33] G. Avoni et al., *The new LUCID-2 detector for luminosity measurement and monitoring in ATLAS*, *JINST* **13** (2018) P07017.
- [34] ATLAS Collaboration, *Performance of the ATLAS trigger system in 2015*, *Eur. Phys. J. C* **77** (2017) 317, arXiv: [1611.09661](https://arxiv.org/abs/1611.09661) [[hep-ex](#)].
- [35] ATLAS Collaboration, *Operation of the ATLAS trigger system in Run 2*, *JINST* **15** (2020) P10004, arXiv: [2007.12539](https://arxiv.org/abs/2007.12539) [[physics.ins-det](#)].
- [36] ATLAS Collaboration, *Software and computing for Run 3 of the ATLAS experiment at the LHC*, (2024), arXiv: [2404.06335](https://arxiv.org/abs/2404.06335) [[hep-ex](#)].
- [37] M. Gyulassy and X.-N. Wang, *HIJING 1.0: A Monte Carlo program for parton and particle production in high-energy hadronic and nuclear collisions*, *Comput. Phys. Commun.* **83** (1994) 307, arXiv: [nuc1-th/9502021](https://arxiv.org/abs/nuc1-th/9502021).
- [38] ATLAS Collaboration, *Measurement of the azimuthal anisotropy for charged particle production in $\sqrt{s_{NN}} = 2.76$ TeV lead-lead collisions with the ATLAS detector*, *Phys. Rev. C* **86** (2012) 014907, arXiv: [1203.3087](https://arxiv.org/abs/1203.3087) [[hep-ex](#)].
- [39] ATLAS Collaboration, *The ATLAS Simulation Infrastructure*, *Eur. Phys. J. C* **70** (2010) 823, arXiv: [1005.4568](https://arxiv.org/abs/1005.4568) [[physics.ins-det](#)].
- [40] S. Agostinelli et al., *GEANT4 – a simulation toolkit*, *Nucl. Instrum. Meth. A* **506** (2003) 250.
- [41] ATLAS Collaboration, *The ATLAS Simulation Infrastructure*, *Eur. Phys. J. C* **70** (2010) 823, arXiv: [1005.4568](https://arxiv.org/abs/1005.4568) [[physics.ins-det](#)].
- [42] ATLAS Collaboration, *ATLAS data quality operations and performance for 2015–2018 data-taking*, *JINST* **15** (2020) P04003, arXiv: [1911.04632](https://arxiv.org/abs/1911.04632) [[physics.ins-det](#)].
- [43] ATLAS Collaboration, *Vertex Reconstruction Performance of the ATLAS Detector at $\sqrt{s} = 13$ TeV*, ATL-PHYS-PUB-2015-026, 2015, URL: <https://cds.cern.ch/record/2037717>.
- [44] M. L. Miller, K. Reygers, S. J. Sanders, and P. Steinberg, *Glauber modeling in high energy nuclear collisions*, *Ann. Rev. Nucl. Part. Sci.* **57** (2007) 205, arXiv: [nuc1-ex/0701025](https://arxiv.org/abs/nuc1-ex/0701025).
- [45] ATLAS Collaboration, *Measurement of the centrality dependence of the charged particle pseudorapidity distribution in lead-lead collisions at $\sqrt{s_{NN}} = 2.76$ TeV with the ATLAS detector*, *Phys. Lett. B* **710** (2012) 363, arXiv: [1108.6027](https://arxiv.org/abs/1108.6027) [[hep-ex](#)].
- [46] ATLAS Collaboration, *Performance of the ATLAS Track Reconstruction Algorithms in Dense Environments in LHC Run 2*, *Eur. Phys. J. C* **77** (2017) 673, arXiv: [1704.07983](https://arxiv.org/abs/1704.07983) [[hep-ex](#)].
- [47] ATLAS Collaboration, *Measurement of jet fragmentation in Pb+Pb and pp collisions at $\sqrt{s_{NN}} = 5.02$ TeV with the ATLAS detector*, *Phys. Rev. C* **98** (2018) 024908, arXiv: [1805.05424](https://arxiv.org/abs/1805.05424) [[nucl-ex](#)].

- [48] ATLAS Collaboration, *Vertex Reconstruction Performance of the ATLAS Detector at $\sqrt{s} = 13$ TeV*, ATL-PHYS-PUB-2015-026, 2015, URL: <https://cds.cern.ch/record/2037717>.
- [49] ATLAS Collaboration, *Measurement of the azimuthal anisotropy of charged-particle production in Xe + Xe collisions at $\sqrt{s_{NN}} = 5.44$ TeV with the ATLAS detector*, *Phys. Rev. C* **101** (2020) 024906, arXiv: [1911.04812](https://arxiv.org/abs/1911.04812) [[nucl-ex](#)].
- [50] ATLAS Collaboration, *Measurement of longitudinal flow decorrelations in Pb+Pb collisions at $\sqrt{s_{NN}} = 2.76$ and 5.02 TeV with the ATLAS detector*, *Eur. Phys. J. C* **78** (2018) 142, arXiv: [1709.02301](https://arxiv.org/abs/1709.02301) [[nucl-ex](#)].
- [51] ATLAS Collaboration, *Measurement of the distributions of event-by-event flow harmonics in lead-lead collisions at $\sqrt{s_{NN}} = 2.76$ TeV with the ATLAS detector at the LHC*, *JHEP* **11** (2013) 183, arXiv: [1305.2942](https://arxiv.org/abs/1305.2942) [[hep-ex](#)].
- [52] ATLAS Collaboration, *ATLAS Computing Acknowledgements*, ATL-SOFT-PUB-2023-001, 2023, URL: <https://cds.cern.ch/record/2869272>.

The ATLAS Collaboration

G. Aad ¹⁰⁵, E. Aakvaag ¹⁷, B. Abbott ¹²⁴, S. Abdelhameed ^{120a}, K. Abeling ⁵⁶, N.J. Abicht ⁵⁰, S.H. Abidi ³⁰, M. Aboeela ⁴⁶, A. Aboulhorma ^{36e}, H. Abramowicz ¹⁵⁸, Y. Abulaiti ¹²¹, B.S. Acharya ^{70a,70b,n}, A. Ackermann ^{64a}, C. Adam Bourdarios ⁴, L. Adamczyk ^{87a}, S.V. Addepalli ¹⁵⁰, M.J. Addison ¹⁰⁴, J. Adelman ¹¹⁹, A. Adiguzel ^{22c}, T. Adye ¹³⁸, A.A. Affolder ¹⁴⁰, Y. Afik ⁴¹, M.N. Agaras ¹³, A. Aggarwal ¹⁰³, C. Agheorghiesei ^{28c}, F. Ahmadov ^{40,ac}, S. Ahuja ⁹⁸, X. Ai ^{144b}, G. Aielli ^{77a,77b}, A. Aikot ¹⁷⁰, M. Ait Tamlihat ^{36e}, B. Aitbenkikh ^{36a}, M. Akbiyik ¹⁰³, T.P.A. Åkesson ¹⁰¹, A.V. Akimov ¹⁵², D. Akiyama ¹⁷⁵, N.N. Akolkar ²⁵, S. Aktas ^{22a}, G.L. Alberghi ^{24b}, J. Albert ¹⁷², P. Albicocco ⁵⁴, G.L. Albouy ⁶¹, S. Alderweireldt ⁵³, Z.L. Alegria ¹²⁵, M. Aleksa ³⁷, I.N. Aleksandrov ⁴⁰, C. Alexa ^{28b}, T. Alexopoulos ¹⁰, F. Alfonsi ^{24b}, M. Algren ⁵⁷, M. Alhroob ¹⁷⁴, B. Ali ¹³⁶, H.M.J. Ali ^{94,w}, S. Ali ³², S.W. Alibocus ⁹⁵, M. Aliev ^{34c}, G. Alimonti ^{72a}, W. Alkahi ⁵⁶, C. Allaire ⁶⁷, B.M.M. Allbrooke ¹⁵³, J.S. Allen ¹⁰⁴, J.F. Allen ⁵³, P.P. Allport ²¹, A. Aloisio ^{73a,73b}, F. Alonso ⁹³, C. Alpigiani ¹⁴³, Z.M.K. Alsolami ⁹⁴, A. Alvarez Fernandez ¹⁰³, M. Alves Cardoso ⁵⁷, M.G. Alviggi ^{73a,73b}, M. Aly ¹⁰⁴, Y. Amaral Coutinho ^{84b}, A. Ambler ¹⁰⁷, C. Amelung ³⁷, M. Amerl ¹⁰⁴, C.G. Ames ¹¹², D. Amidei ¹⁰⁹, B. Amini ⁵⁵, K.J. Amirie ¹⁶², A. Amirkhanov ⁴⁰, S.P. Amor Dos Santos ^{134a}, K.R. Amos ¹⁷⁰, D. Amperiadou ¹⁵⁹, S. An ⁸⁵, V. Ananiev ¹²⁹, C. Anastopoulos ¹⁴⁶, T. Andeen ¹¹, J.K. Anders ⁹⁵, A.C. Anderson ⁶⁰, A. Andreazza ^{72a,72b}, S. Angelidakis ⁹, A. Angerami ⁴³, A.V. Anisenkov ⁴⁰, A. Annovi ^{75a}, C. Antel ⁵⁷, E. Antipov ¹⁵², M. Antonelli ⁵⁴, F. Anulli ^{76a}, M. Aoki ⁸⁵, T. Aoki ¹⁶⁰, M.A. Aparo ¹⁵³, L. Aperio Bella ⁴⁹, C. Appelt ¹⁵⁸, A. Apyan ²⁷, S.J. Arbiol Val ⁸⁸, C. Arcangeletti ⁵⁴, A.T.H. Arce ⁵², J-F. Arguin ¹¹¹, S. Argyropoulos ¹⁵⁹, J.-H. Arling ⁴⁹, O. Arnaez ⁴, H. Arnold ¹⁵², G. Artoni ^{76a,76b}, H. Asada ¹¹⁴, K. Asai ¹²², S. Asai ¹⁶⁰, N.A. Asbah ³⁷, R.A. Ashby Pickering ¹⁷⁴, A.M. Aslam ⁹⁸, K. Assamagan ³⁰, R. Astalos ^{29a}, K.S.V. Astrand ¹⁰¹, S. Atashi ¹⁶⁶, R.J. Atkin ^{34a}, H. Atmani ^{36f}, P.A. Atlasiddha ¹³², K. Augsten ¹³⁶, A.D. Auriol ⁴², V.A. Austrup ¹⁰⁴, G. Avolio ³⁷, K. Axiotis ⁵⁷, G. Azuelos ^{111,ag}, D. Babal ^{29b}, H. Bachacou ¹³⁹, K. Bachas ^{159,r}, A. Bachiu ³⁵, E. Bachmann ⁵¹, M.J. Backes ^{64a}, A. Badea ⁴¹, T.M. Baer ¹⁰⁹, P. Bagnaia ^{76a,76b}, M. Bahmani ¹⁹, D. Bahner ⁵⁵, K. Bai ¹²⁷, J.T. Baines ¹³⁸, L. Baines ⁹⁷, O.K. Baker ¹⁷⁹, E. Bakos ¹⁶, D. Bakshi Gupta ⁸, L.E. Balabram Filho ^{84b}, V. Balakrishnan ¹²⁴, R. Balasubramanian ⁴, E.M. Baldin ³⁹, P. Balek ^{87a}, E. Ballabene ^{24b,24a}, F. Balli ¹³⁹, L.M. Baltes ^{64a}, W.K. Balunas ³³, J. Balz ¹⁰³, I. Bamwidhi ^{120b}, E. Banas ⁸⁸, M. Bandieramonte ¹³³, A. Bandyopadhyay ²⁵, S. Bansal ²⁵, L. Barak ¹⁵⁸, M. Barakat ⁴⁹, E.L. Barberio ¹⁰⁸, D. Barberis ^{58b,58a}, M. Barbero ¹⁰⁵, M.Z. Barel ¹¹⁸, T. Barillari ¹¹³, M-S. Barisits ³⁷, T. Barklow ¹⁵⁰, P. Baron ¹²⁶, D.A. Baron Moreno ¹⁰⁴, A. Baroncelli ⁶³, A.J. Barr ¹³⁰, J.D. Barr ⁹⁹, F. Barreiro ¹⁰², J. Barreiro Guimarães da Costa ¹⁴, M.G. Barros Teixeira ^{134a}, S. Barsov ³⁹, F. Bartels ^{64a}, R. Bartoldus ¹⁵⁰, A.E. Barton ⁹⁴, P. Bartos ^{29a}, A. Basan ¹⁰³, M. Baselga ⁵⁰, S. Bashiri ⁸⁸, A. Bassalat ^{67,b}, M.J. Basso ^{163a}, S. Bataju ⁴⁶, R. Bate ¹⁷¹, R.L. Bates ⁶⁰, S. Batlamous ¹⁰², M. Battaglia ¹⁴⁰, D. Battulga ¹⁹, M. Baucé ^{76a,76b}, M. Bauer ⁸⁰, P. Bauer ²⁵, L.T. Bayer ⁴⁹, L.T. Bazzano Hurrell ³¹, J.B. Beacham ¹¹³, T. Beau ¹³¹, J.Y. Beaucamp ⁹³, P.H. Beauchemin ¹⁶⁵, P. Bechtel ²⁵, H.P. Beck ^{20,q}, K. Becker ¹⁷⁴, A.J. Beddall ⁸³, V.A. Bednyakov ⁴⁰, C.P. Bee ¹⁵², L.J. Beemster ¹⁶, M. Begalli ^{84d}, M. Begel ³⁰, J.K. Behr ⁴⁹, J.F. Beirer ³⁷, F. Beisiegel ²⁵, M. Belfkir ^{120b}, G. Bella ¹⁵⁸, L. Bellagamba ^{24b}, A. Bellerive ³⁵, P. Bellos ²¹, K. Beloborodov ³⁹, D. Benchebroun ^{36a}, F. Bendebba ^{36a}, Y. Benhammou ¹⁵⁸, K.C. Benkendorfer ⁶², L. Beresford ⁴⁹, M. Beretta ⁵⁴, E. Bergeas Kuutmann ¹⁶⁸, N. Berger ⁴,

B. Bergmann [ID136](#), J. Beringer [ID18a](#), G. Bernardi [ID5](#), C. Bernius [ID150](#), F.U. Bernlochner [ID25](#),
 F. Bernon [ID37](#), A. Berrocal Guardia [ID13](#), T. Berry [ID98](#), P. Berta [ID137](#), A. Berthold [ID51](#), S. Bethke [ID113](#),
 A. Betti [ID76a,76b](#), A.J. Bevan [ID97](#), L. Bezio [ID57](#), N.K. Bhalla [ID55](#), S. Bharthuar [ID113](#), S. Bhatta [ID152](#),
 D.S. Bhattacharya [ID173](#), P. Bhattarai [ID150](#), Z.M. Bhatti [ID121](#), K.D. Bhide [ID55](#), V.S. Bhopatkar [ID125](#),
 R.M. Bianchi [ID133](#), G. Bianco [ID24b,24a](#), O. Biebel [ID112](#), M. Biglietti [ID78a](#), C.S. Billingsley [ID46](#),
 Y. Bimgdi [ID36f](#), M. Bindi [ID56](#), A. Bingham [ID178](#), A. Bingul [ID22b](#), C. Bini [ID76a,76b](#), G.A. Bird [ID33](#),
 M. Birman [ID176](#), M. Biros [ID137](#), S. Biryukov [ID153](#), T. Bisanz [ID50](#), E. Bisceglie [ID24b,24a](#), J.P. Biswal [ID138](#),
 D. Biswas [ID148](#), I. Bloch [ID49](#), A. Blue [ID60](#), U. Blumenschein [ID97](#), J. Blumenthal [ID103](#),
 V.S. Bobrovnikov [ID40](#), M. Boehler [ID55](#), B. Boehm [ID173](#), D. Bogavac [ID37](#), A.G. Bogdanchikov [ID39](#),
 L.S. Boggia [ID131](#), V. Boisvert [ID98](#), P. Bokan [ID37](#), T. Bold [ID87a](#), M. Bomben [ID5](#), M. Bona [ID97](#),
 M. Boonekamp [ID139](#), A.G. Borbély [ID60](#), I.S. Bordulev [ID39](#), G. Borissov [ID94](#), D. Bortoletto [ID130](#),
 D. Boscherini [ID24b](#), M. Bosman [ID13](#), K. Bouaouda [ID36a](#), N. Bouchhar [ID170](#), L. Boudet [ID4](#),
 J. Boudreau [ID133](#), E.V. Bouhova-Thacker [ID94](#), D. Boumediene [ID42](#), R. Bouquet [ID58b,58a](#), A. Boveia [ID123](#),
 J. Boyd [ID37](#), D. Boye [ID30](#), I.R. Boyko [ID40](#), L. Bozianu [ID57](#), J. Bracinek [ID21](#), N. Brahimi [ID4](#),
 G. Brandt [ID178](#), O. Brandt [ID33](#), B. Brau [ID106](#), J.E. Brau [ID127](#), R. Brener [ID176](#), L. Brenner [ID118](#),
 R. Brenner [ID168](#), S. Bressler [ID176](#), G. Brianti [ID79a,79b](#), D. Britton [ID60](#), D. Britzger [ID113](#), I. Brock [ID25](#),
 R. Brock [ID110](#), G. Brooijmans [ID43](#), A.J. Brooks [ID69](#), E.M. Brooks [ID163b](#), E. Brost [ID30](#), L.M. Brown [ID172](#),
 L.E. Bruce [ID62](#), T.L. Bruckler [ID130](#), P.A. Bruckman de Renstrom [ID88](#), B. Brüers [ID49](#), A. Bruni [ID24b](#),
 G. Bruni [ID24b](#), D. Brunner [ID48a,48b](#), M. Bruschi [ID24b](#), N. Bruscinò [ID76a,76b](#), T. Buanes [ID17](#), Q. Buat [ID143](#),
 D. Buchin [ID113](#), A.G. Buckley [ID60](#), O. Bulekov [ID39](#), B.A. Bullard [ID150](#), S. Burdin [ID95](#), C.D. Burgard [ID50](#),
 A.M. Burger [ID37](#), B. Burghgrave [ID8](#), O. Burlayenko [ID55](#), J. Burleson [ID169](#), J.T.P. Burr [ID33](#),
 J.C. Burzynski [ID149](#), E.L. Busch [ID43](#), V. Büscher [ID103](#), P.J. Bussey [ID60](#), J.M. Butler [ID26](#), C.M. Buttar [ID60](#),
 J.M. Butterworth [ID99](#), W. Buttinger [ID138](#), C.J. Buxo Vazquez [ID110](#), A.R. Buzykaev [ID40](#),
 S. Cabrera Urbán [ID170](#), L. Cadamuro [ID67](#), D. Caforio [ID59](#), H. Cai [ID133](#), Y. Cai [ID24b,115c,24a](#), Y. Cai [ID115a](#),
 V.M.M. Cairo [ID37](#), O. Cakir [ID3a](#), N. Calace [ID37](#), P. Calafiura [ID18a](#), G. Calderini [ID131](#), P. Calfayan [ID35](#),
 G. Callea [ID60](#), L.P. Caloba [ID84b](#), D. Calvet [ID42](#), S. Calvet [ID42](#), R. Camacho Toro [ID131](#), S. Camarda [ID37](#),
 D. Camarero Munoz [ID27](#), P. Camarri [ID77a,77b](#), M.T. Camerlingo [ID73a,73b](#), D. Cameron [ID37](#),
 C. Camincher [ID172](#), M. Campanelli [ID99](#), A. Camplani [ID44](#), V. Canale [ID73a,73b](#), A.C. Canbay [ID3a](#),
 E. Canonero [ID98](#), J. Cantero [ID170](#), Y. Cao [ID169](#), F. Capocasa [ID27](#), M. Capua [ID45b,45a](#), A. Carbone [ID72a,72b](#),
 R. Cardarelli [ID77a](#), J.C.J. Cardenas [ID8](#), M.P. Cardiff [ID27](#), G. Carducci [ID45b,45a](#), T. Carli [ID37](#),
 G. Carlino [ID73a](#), J.I. Carlotto [ID13](#), B.T. Carlson [ID133,s](#), E.M. Carlson [ID172](#), J. Carmignani [ID95](#),
 L. Carminati [ID72a,72b](#), A. Carnelli [ID139](#), M. Carnesale [ID37](#), S. Caron [ID117](#), E. Carquin [ID141f](#),
 I.B. Carr [ID108](#), S. Carrá [ID72a](#), G. Carratta [ID24b,24a](#), A.M. Carroll [ID127](#), M.P. Casado [ID13,i](#), M. Caspar [ID49](#),
 F.L. Castillo [ID4](#), L. Castillo Garcia [ID13](#), V. Castillo Gimenez [ID170](#), N.F. Castro [ID134a,134e](#),
 A. Catinaccio [ID37](#), J.R. Catmore [ID129](#), T. Cavaliere [ID4](#), V. Cavaliere [ID30](#), L.J. Caviedes Betancourt [ID23b](#),
 Y.C. Cekmecelioglu [ID49](#), E. Celebi [ID83](#), S. Cella [ID37](#), V. Cepaitis [ID57](#), K. Cerny [ID126](#),
 A.S. Cerqueira [ID84a](#), A. Cerri [ID75a,75b](#), L. Cerrito [ID77a,77b](#), F. Cerutti [ID18a](#), B. Cervato [ID148](#),
 A. Cervelli [ID24b](#), G. Cesarini [ID54](#), S.A. Cetin [ID83](#), P.M. Chabrilat [ID131](#), J. Chan [ID18a](#), W.Y. Chan [ID160](#),
 J.D. Chapman [ID33](#), E. Chapon [ID139](#), B. Chargeishvili [ID156b](#), D.G. Charlton [ID21](#), C. Chauhan [ID137](#),
 Y. Che [ID115a](#), S. Chekanov [ID6](#), S.V. Chekulaev [ID163a](#), G.A. Chelkov [ID40,a](#), B. Chen [ID158](#), B. Chen [ID172](#),
 H. Chen [ID115a](#), H. Chen [ID30](#), J. Chen [ID145a](#), J. Chen [ID149](#), M. Chen [ID130](#), S. Chen [ID90](#), S.J. Chen [ID115a](#),
 X. Chen [ID145a](#), X. Chen [ID15.af](#), C.L. Cheng [ID177](#), H.C. Cheng [ID65a](#), S. Cheong [ID150](#), A. Cheplakov [ID40](#),
 E. Cheremushkina [ID49](#), E. Cherepanova [ID118](#), R. Cherkaoui El Moursli [ID36e](#), E. Cheu [ID7](#), K. Cheung [ID66](#),
 L. Chevalier [ID139](#), V. Chiarella [ID54](#), G. Chiarelli [ID75a](#), N. Chiedde [ID105](#), G. Chiodini [ID71a](#),
 A.S. Chisholm [ID21](#), A. Chitan [ID28b](#), M. Chitishvili [ID170](#), M.V. Chizhov [ID40,t](#), K. Choi [ID11](#), Y. Chou [ID143](#),
 E.Y.S. Chow [ID117](#), K.L. Chu [ID176](#), M.C. Chu [ID65a](#), X. Chu [ID14,115c](#), Z. Chubinidze [ID54](#), J. Chudoba [ID135](#),
 J.J. Chwastowski [ID88](#), D. Cieri [ID113](#), K.M. Ciesla [ID87a](#), V. Cindro [ID96](#), A. Ciocio [ID18a](#), F. Ciroto [ID73a,73b](#),

Z.H. Citron ¹⁷⁶, M. Citterio ^{72a}, D.A. Ciubotaru ^{28b}, A. Clark ⁵⁷, P.J. Clark ⁵³, N. Clarke Hall ⁹⁹, C. Clarry ¹⁶², S.E. Clawson ⁴⁹, C. Clement ^{48a,48b}, Y. Coadou ¹⁰⁵, M. Cobal ^{70a,70c}, A. Coccaro ^{58b}, R.F. Coelho Barrue ^{134a}, R. Coelho Lopes De Sa ¹⁰⁶, S. Coelli ^{72a}, L.S. Colangeli ¹⁶², B. Cole ⁴³, P. Collado Soto ¹⁰², J. Collot ⁶¹, P. Conde Muiño ^{134a,134g}, M.P. Connell ^{34c}, S.H. Connell ^{34c}, E.I. Conroy ¹³⁰, F. Conventi ^{73a,ah}, H.G. Cooke ²¹, A.M. Cooper-Sarkar ¹³⁰, F.A. Corchia ^{24b,24a}, A. Cordeiro Oudot Choi ¹³¹, L.D. Corpe ⁴², M. Corradi ^{76a,76b}, F. Corriveau ^{107,ab}, A. Cortes-Gonzalez ¹⁹, M.J. Costa ¹⁷⁰, F. Costanza ⁴, D. Costanzo ¹⁴⁶, B.M. Cote ¹²³, J. Couthures ⁴, G. Cowan ⁹⁸, K. Cranmer ¹⁷⁷, L. Cremer ⁵⁰, D. Cremonini ^{24b,24a}, S. Crépe-Renaudin ⁶¹, F. Crescioli ¹³¹, M. Cristinziani ¹⁴⁸, M. Cristoforetti ^{79a,79b}, V. Croft ¹¹⁸, J.E. Crosby ¹²⁵, G. Crosetti ^{45b,45a}, A. Cueto ¹⁰², H. Cui ⁹⁹, Z. Cui ⁷, W.R. Cunningham ⁶⁰, F. Curcio ¹⁷⁰, J.R. Curran ⁵³, P. Czodrowski ³⁷, M.J. Da Cunha Sargedas De Sousa ^{58b,58a}, J.V. Da Fonseca Pinto ^{84b}, C. Da Via ¹⁰⁴, W. Dabrowski ^{87a}, T. Dado ³⁷, S. Dahbi ¹⁵⁵, T. Dai ¹⁰⁹, D. Dal Santo ²⁰, C. Dallapiccola ¹⁰⁶, M. Dam ⁴⁴, G. D'amen ³⁰, V. D'Amico ¹¹², J. Damp ¹⁰³, J.R. Dandoy ³⁵, D. Dannheim ³⁷, M. Danninger ¹⁴⁹, V. Dao ¹⁵², G. Darbo ^{58b}, S.J. Das ³⁰, F. Dattola ⁴⁹, S. D'Auria ^{72a,72b}, A. D'Avanzo ^{73a,73b}, T. Davidek ¹³⁷, I. Dawson ⁹⁷, H.A. Day-hall ¹³⁶, K. De ⁸, C. De Almeida Rossi ¹⁶², R. De Asmundis ^{73a}, N. De Biase ⁴⁹, S. De Castro ^{24b,24a}, N. De Groot ¹¹⁷, P. de Jong ¹¹⁸, H. De la Torre ¹¹⁹, A. De Maria ^{115a}, A. De Salvo ^{76a}, U. De Sanctis ^{77a,77b}, F. De Santis ^{71a,71b}, A. De Santo ¹⁵³, J.B. De Vivie De Regie ⁶¹, J. Debevc ⁹⁶, D.V. Dedovich ⁴⁰, J. Degens ⁹⁵, A.M. Deiana ⁴⁶, J. Del Peso ¹⁰², L. Delagrangé ¹³¹, F. Deliot ¹³⁹, C.M. Delitzsch ⁵⁰, M. Della Pietra ^{73a,73b}, D. Della Volpe ⁵⁷, A. Dell'Acqua ³⁷, L. Dell'Asta ^{72a,72b}, M. Delmastro ⁴, C.C. Delogu ¹⁰³, P.A. Delsart ⁶¹, S. Demers ¹⁷⁹, M. Demichev ⁴⁰, S.P. Denisov ³⁹, H. Denizli ^{22a,1}, L. D'Eramo ⁴², D. Derendarz ⁸⁸, F. Derue ¹³¹, P. Dervan ⁹⁵, K. Desch ²⁵, C. Deutsch ²⁵, F.A. Di Bello ^{58b,58a}, A. Di Ciaccio ^{77a,77b}, L. Di Ciaccio ⁴, A. Di Domenico ^{76a,76b}, C. Di Donato ^{73a,73b}, A. Di Girolamo ³⁷, G. Di Gregorio ³⁷, A. Di Luca ^{79a,79b}, B. Di Micco ^{78a,78b}, R. Di Nardo ^{78a,78b}, K.F. Di Petrillo ⁴¹, M. Diamantopoulou ³⁵, F.A. Dias ¹¹⁸, T. Dias Do Vale ¹⁴⁹, M.A. Diaz ^{141a,141b}, A.R. Didenko ⁴⁰, M. Didenko ¹⁷⁰, E.B. Diehl ¹⁰⁹, S. Díez Cornell ⁴⁹, C. Diez Pardos ¹⁴⁸, C. Dimitriadi ¹⁵¹, A. Dimitrievska ²¹, A. Dimri ¹⁵², J. Dingfelder ²⁵, T. Dingley ¹³⁰, I-M. Dinu ^{28b}, S.J. Dittmeier ^{64b}, F. Dittus ³⁷, M. Divisek ¹³⁷, B. Dixit ⁹⁵, F. Djama ¹⁰⁵, T. Djobava ^{156b}, C. Doglioni ^{104,101}, A. Dohnalova ^{29a}, Z. Dolezal ¹³⁷, K. Domijan ^{87a}, K.M. Dona ⁴¹, M. Donadelli ^{84d}, B. Dong ¹¹⁰, J. Donini ⁴², A. D'Onofrio ^{73a,73b}, M. D'Onofrio ⁹⁵, J. Dopke ¹³⁸, A. Doria ^{73a}, N. Dos Santos Fernandes ^{134a}, P. Dougan ¹⁰⁴, M.T. Dova ⁹³, A.T. Doyle ⁶⁰, M.A. Draguet ¹³⁰, M.P. Drescher ⁵⁶, E. Dreyer ¹⁷⁶, I. Drivas-koulouris ¹⁰, M. Drnevich ¹²¹, M. Drozdova ⁵⁷, D. Du ⁶³, T.A. du Pree ¹¹⁸, F. Dubinin ³⁹, M. Dubovsky ^{29a}, E. Duchovni ¹⁷⁶, G. Duckeck ¹¹², P.K. Duckett ⁹⁹, O.A. Ducu ^{28b}, D. Duda ⁵³, A. Dudarev ³⁷, E.R. Duden ²⁷, M. D'uffizi ¹⁰⁴, L. Duflost ⁶⁷, M. Dührssen ³⁷, I. Duminica ^{28g}, A.E. Dumitriu ^{28b}, M. Dunford ^{64a}, S. Dungs ⁵⁰, K. Dunne ^{48a,48b}, A. Duperrin ¹⁰⁵, H. Duran Yildiz ^{3a}, M. Düren ⁵⁹, A. Durglishvili ^{156b}, D. Duvnjak ³⁵, B.L. Dwyer ¹¹⁹, G.I. Dyckes ^{18a}, M. Dyndal ^{87a}, B.S. Dziedzic ³⁷, Z.O. Earnshaw ¹⁵³, G.H. Eberwein ¹³⁰, B. Eckerova ^{29a}, S. Eggebrecht ⁵⁶, E. Egidio Purcino De Souza ^{84e}, G. Eigen ¹⁷, K. Einsweiler ^{18a}, T. Ekelof ¹⁶⁸, P.A. Ekman ¹⁰¹, S. El Farkh ^{36b}, Y. El Ghazali ⁶³, H. El Jarrari ³⁷, A. El Moussaouy ^{36a}, V. Ellajosyula ¹⁶⁸, M. Ellert ¹⁶⁸, F. Ellinghaus ¹⁷⁸, N. Ellis ³⁷, J. Elmsheuser ³⁰, M. Elsayy ^{120a}, M. Elsing ³⁷, D. Emelianov ¹³⁸, Y. Enari ⁸⁵, I. Ene ^{18a}, S. Epari ¹³, D. Ernani Martins Neto ⁸⁸, M. Errenst ¹⁷⁸, M. Escalier ⁶⁷, C. Escobar ¹⁷⁰, E. Etzion ¹⁵⁸, G. Evans ^{134a,134b}, H. Evans ⁶⁹, L.S. Evans ⁹⁸, A. Ezhilov ³⁹, S. Ezzarqtouni ^{36a}, F. Fabbri ^{24b,24a}, L. Fabbri ^{24b,24a}, G. Facini ⁹⁹, V. Fadeyev ¹⁴⁰, R.M. Fakhruddinov ³⁹,

D. Fakoudis [ID103](#), S. Falciano [ID76a](#), L.F. Falda Ulhoa Coelho [ID134a](#), F. Fallavollita [ID113](#),
 G. Falsetti [ID45b,45a](#), J. Faltova [ID137](#), C. Fan [ID169](#), K.Y. Fan [ID65b](#), Y. Fan [ID14](#), Y. Fang [ID14,115c](#),
 M. Fanti [ID72a,72b](#), M. Faraj [ID70a,70b](#), Z. Farazpay [ID100](#), A. Farbin [ID8](#), A. Farilla [ID78a](#), T. Farooque [ID110](#),
 J.N. Farr [ID179](#), S.M. Farrington [ID138,53](#), F. Fassi [ID36e](#), D. Fassouliotis [ID9](#), L. Fayard [ID67](#), P. Federic [ID137](#),
 P. Federicova [ID135](#), O.L. Fedin [ID39,a](#), M. Feickert [ID177](#), L. Feligioni [ID105](#), D.E. Fellers [ID18a](#),
 C. Feng [ID144a](#), Z. Feng [ID118](#), M.J. Fenton [ID166](#), L. Ferencz [ID49](#), P. Fernandez Martinez [ID68](#),
 M.J.V. Fernoux [ID105](#), J. Ferrando [ID94](#), A. Ferrari [ID168](#), P. Ferrari [ID118,117](#), R. Ferrari [ID74a](#), D. Ferrere [ID57](#),
 C. Ferretti [ID109](#), M.P. Fewell [ID1](#), D. Fiacco [ID76a,76b](#), F. Fiedler [ID103](#), P. Fiedler [ID136](#), S. Filimonov [ID39](#),
 A. Filipčić [ID96](#), E.K. Filmer [ID163a](#), F. Filthaut [ID117](#), M.C.N. Fiolhais [ID134a,134c,c](#), L. Fiorini [ID170](#),
 W.C. Fisher [ID110](#), T. Fitschen [ID104](#), P.M. Fitzhugh [ID139](#), I. Fleck [ID148](#), P. Fleischmann [ID109](#), T. Flick [ID178](#),
 M. Flores [ID34d,ad](#), L.R. Flores Castillo [ID65a](#), L. Flores Sanz De Acedo [ID37](#), F.M. Follega [ID79a,79b](#),
 N. Fomin [ID33](#), J.H. Foo [ID162](#), A. Formica [ID139](#), A.C. Forti [ID104](#), E. Fortin [ID37](#), A.W. Fortman [ID18a](#),
 L. Fountas [ID9j](#), D. Fournier [ID67](#), H. Fox [ID94](#), P. Francavilla [ID75a,75b](#), S. Francescato [ID62](#),
 S. Franchellucci [ID57](#), M. Franchini [ID24b,24a](#), S. Franchino [ID64a](#), D. Francis [ID37](#), L. Franco [ID117](#),
 V. Franco Lima [ID37](#), L. Franconi [ID49](#), M. Franklin [ID62](#), G. Frattari [ID27](#), Y.Y. Frid [ID158](#), J. Friend [ID60](#),
 N. Fritzsche [ID37](#), A. Froch [ID57](#), D. Froidevaux [ID37](#), J.A. Frost [ID130](#), Y. Fu [ID110](#),
 S. Fuenzalida Garrido [ID141f](#), M. Fujimoto [ID105](#), K.Y. Fung [ID65a](#), E. Furtado De Simas Filho [ID84e](#),
 M. Furukawa [ID160](#), J. Fuster [ID170](#), A. Gaa [ID56](#), A. Gabrielli [ID24b,24a](#), A. Gabrielli [ID162](#), P. Gadow [ID37](#),
 G. Gagliardi [ID58b,58a](#), L.G. Gagnon [ID18a](#), S. Gaid [ID89b](#), S. Galantzan [ID158](#), J. Gallagher [ID1](#),
 E.J. Gallas [ID130](#), A.L. Gallen [ID168](#), B.J. Gallop [ID138](#), K.K. Gan [ID123](#), S. Ganguly [ID160](#), Y. Gao [ID53](#),
 A. Garabaglu [ID143](#), F.M. Garay Walls [ID141a,141b](#), B. Garcia [ID30](#), C. García [ID170](#), A. Garcia Alonso [ID118](#),
 A.G. Garcia Caffaro [ID179](#), J.E. García Navarro [ID170](#), M. Garcia-Sciveres [ID18a](#), G.L. Gardner [ID132](#),
 R.W. Gardner [ID41](#), N. Garelli [ID165](#), R.B. Garg [ID150](#), J.M. Gargan [ID53](#), C.A. Garner [ID162](#), C.M. Garvey [ID34a](#),
 V.K. Gassmann [ID165](#), G. Gaudio [ID74a](#), V. Gautam [ID13](#), P. Gauzzi [ID76a,76b](#), J. Gavranovic [ID96](#),
 I.L. Gavrilenko [ID39](#), A. Gavrilyuk [ID39](#), C. Gay [ID171](#), G. Gaycken [ID127](#), E.N. Gazis [ID10](#), A. Gekow [ID123](#),
 C. Gemme [ID58b](#), M.H. Genest [ID61](#), A.D. Gentry [ID116](#), S. George [ID98](#), W.F. George [ID21](#), T. Geralis [ID47](#),
 A.A. Gerwin [ID124](#), P. Gessinger-Befurt [ID37](#), M.E. Geyik [ID178](#), M. Ghani [ID174](#), K. Ghorbanian [ID97](#),
 A. Ghosal [ID148](#), A. Ghosh [ID166](#), A. Ghosh [ID7](#), B. Giacobbe [ID24b](#), S. Giagu [ID76a,76b](#), T. Giani [ID118](#),
 A. Giannini [ID63](#), S.M. Gibson [ID98](#), M. Gignac [ID140](#), D.T. Gil [ID87b](#), A.K. Gilbert [ID87a](#), B.J. Gilbert [ID43](#),
 D. Gillberg [ID35](#), G. Gilles [ID118](#), L. Ginabat [ID131](#), D.M. Gingrich [ID2,ag](#), M.P. Giordani [ID70a,70c](#),
 P.F. Giraud [ID139](#), G. Giugliarelli [ID70a,70c](#), D. Giugni [ID72a](#), F. Giuli [ID77a,77b](#), I. Gkialas [ID9j](#),
 L.K. Gladilin [ID39](#), C. Glasman [ID102](#), G. Glemža [ID49](#), M. Glisic [ID127](#), I. Gnesi [ID45b](#), Y. Go [ID30](#),
 M. Goblirsch-Kolb [ID37](#), B. Gocke [ID50](#), D. Godin [ID111](#), B. Gokturk [ID22a](#), S. Goldfarb [ID108](#), T. Golling [ID57](#),
 M.G.D. Gololo [ID34c](#), D. Golubkov [ID39](#), J.P. Gombas [ID110](#), A. Gomes [ID134a,134b](#), G. Gomes Da Silva [ID148](#),
 A.J. Gomez Delegido [ID170](#), R. Gonçalo [ID134a](#), L. Gonella [ID21](#), A. Gongadze [ID156c](#), F. Gonnella [ID21](#),
 J.L. Gonski [ID150](#), R.Y. González Andana [ID53](#), S. González de la Hoz [ID170](#), R. Gonzalez Lopez [ID95](#),
 C. Gonzalez Renteria [ID18a](#), M.V. Gonzalez Rodrigues [ID49](#), R. Gonzalez Suarez [ID168](#),
 S. Gonzalez-Sevilla [ID57](#), L. Goossens [ID37](#), B. Gorini [ID37](#), E. Gorini [ID71a,71b](#), A. Gorišek [ID96](#),
 T.C. Gosart [ID132](#), A.T. Goshaw [ID52](#), M.I. Gostkin [ID40](#), S. Goswami [ID125](#), C.A. Gottardo [ID37](#),
 S.A. Gotz [ID112](#), M. Gouighri [ID36b](#), A.G. Goussiou [ID143](#), N. Govender [ID34c](#), R.P. Grabarczyk [ID130](#),
 I. Grabowska-Bold [ID87a](#), K. Graham [ID35](#), E. Gramstad [ID129](#), S. Grancagnolo [ID71a,71b](#), C.M. Grant [ID1,139](#),
 P.M. Gravila [ID28f](#), F.G. Gravili [ID71a,71b](#), H.M. Gray [ID18a](#), M. Greco [ID113](#), M.J. Green [ID1](#), C. Grefe [ID25](#),
 A.S. Grefsrud [ID17](#), I.M. Gregor [ID49](#), K.T. Greif [ID166](#), P. Grenier [ID150](#), S.G. Grewe [ID113](#), A.A. Grillo [ID140](#),
 K. Grimm [ID32](#), S. Grinstein [ID13,x](#), J.-F. Grivaz [ID67](#), E. Gross [ID176](#), J. Grosse-Knetter [ID56](#), L. Guan [ID109](#),
 G. Guerrieri [ID37](#), R. Gugel [ID103](#), J.A.M. Guhit [ID109](#), A. Guida [ID19](#), E. Guilloton [ID174](#), S. Guindon [ID37](#),
 F. Guo [ID14,115c](#), J. Guo [ID145a](#), L. Guo [ID49](#), L. Guo [ID115b,v](#), Y. Guo [ID109](#), A. Gupta [ID50](#), R. Gupta [ID133](#),
 S. Gurbuz [ID25](#), S.S. Gurdasani [ID49](#), G. Gustavino [ID76a,76b](#), P. Gutierrez [ID124](#),

L.F. Gutierrez Zagazeta ¹³², M. Gutsche ⁵¹, C. Gutschow ⁹⁹, C. Gwenlan ¹³⁰, C.B. Gwilliam ⁹⁵, E.S. Haaland ¹²⁹, A. Haas ¹²¹, M. Habedank ⁶⁰, C. Haber ^{18a}, H.K. Hadavand ⁸, A. Haddad ⁴², A. Hadeef ⁵¹, A.I. Hagan ⁹⁴, J.J. Hahn ¹⁴⁸, E.H. Haines ⁹⁹, M. Haleem ¹⁷³, J. Haley ¹²⁵, G.D. Hallewell ¹⁰⁵, L. Halser ²⁰, K. Hamano ¹⁷², M. Hamer ²⁵, S.E.D. Hammoud ⁶⁷, E.J. Hampshire ⁹⁸, J. Han ^{144a}, L. Han ^{115a}, L. Han ⁶³, S. Han ^{18a}, K. Hanagaki ⁸⁵, M. Hance ¹⁴⁰, D.A. Hangal ⁴³, H. Hanif ¹⁴⁹, M.D. Hank ¹³², J.B. Hansen ⁴⁴, P.H. Hansen ⁴⁴, D. Harada ⁵⁷, T. Harenberg ¹⁷⁸, S. Harkusha ¹⁸⁰, M.L. Harris ¹⁰⁶, Y.T. Harris ²⁵, J. Harrison ¹³, N.M. Harrison ¹²³, P.F. Harrison ¹⁷⁴, N.M. Hartman ¹¹³, N.M. Hartmann ¹¹², R.Z. Hasan ^{98,138}, Y. Hasegawa ¹⁴⁷, F. Haslbeck ¹³⁰, S. Hassan ¹⁷, R. Hauser ¹¹⁰, C.M. Hawkes ²¹, R.J. Hawkings ³⁷, Y. Hayashi ¹⁶⁰, D. Hayden ¹¹⁰, C. Hayes ¹⁰⁹, R.L. Hayes ¹¹⁸, C.P. Hays ¹³⁰, J.M. Hays ⁹⁷, H.S. Hayward ⁹⁵, F. He ⁶³, M. He ^{14,115c}, Y. He ⁴⁹, Y. He ⁹⁹, N.B. Heatley ⁹⁷, V. Hedberg ¹⁰¹, A.L. Heggelund ¹²⁹, C. Heidegger ⁵⁵, K.K. Heidegger ⁵⁵, J. Heilman ³⁵, S. Heim ⁴⁹, T. Heim ^{18a}, J.G. Heinlein ¹³², J.J. Heinrich ¹²⁷, L. Heinrich ^{113,ae}, J. Hejbal ¹³⁵, A. Held ¹⁷⁷, S. Hellesund ¹⁷, C.M. Helling ¹⁷¹, S. Hellman ^{48a,48b}, L. Henkelmann ³³, A.M. Henriques Correia ³⁷, H. Herde ¹⁰¹, Y. Hernández Jiménez ¹⁵², L.M. Herrmann ²⁵, T. Herrmann ⁵¹, G. Herten ⁵⁵, R. Hertenberger ¹¹², L. Hervas ³⁷, M.E. Hesping ¹⁰³, N.P. Hessey ^{163a}, J. Hessler ¹¹³, M. Hidaoui ^{36b}, N. Hidic ¹³⁷, E. Hill ¹⁶², S.J. Hillier ²¹, J.R. Hinds ¹¹⁰, F. Hinterkeuser ²⁵, M. Hirose ¹²⁸, S. Hirose ¹⁶⁴, D. Hirschbuehl ¹⁷⁸, T.G. Hitchings ¹⁰⁴, B. Hiti ⁹⁶, J. Hobbs ¹⁵², R. Hobincu ^{28e}, N. Hod ¹⁷⁶, M.C. Hodgkinson ¹⁴⁶, B.H. Hodgkinson ¹³⁰, A. Hoecker ³⁷, D.D. Hofer ¹⁰⁹, J. Hofer ¹⁷⁰, M. Holzbock ³⁷, L.B.A.H. Hommels ³³, B.P. Honan ¹⁰⁴, J.J. Hong ⁶⁹, J. Hong ^{145a}, T.M. Hong ¹³³, B.H. Hooberman ¹⁶⁹, W.H. Hopkins ⁶, M.C. Hoppesch ¹⁶⁹, Y. Horii ¹¹⁴, M.E. Horstmann ¹¹³, S. Hou ¹⁵⁵, M.R. Housenga ¹⁶⁹, A.S. Howard ⁹⁶, J. Howarth ⁶⁰, J. Hoya ⁶, M. Hrabovsky ¹²⁶, T. Hryn'ova ⁴, P.J. Hsu ⁶⁶, S.-C. Hsu ¹⁴³, T. Hsu ⁶⁷, M. Hu ^{18a}, Q. Hu ⁶³, S. Huang ³³, X. Huang ^{14,115c}, Y. Huang ¹³⁷, Y. Huang ^{115b}, Y. Huang ¹⁰³, Y. Huang ¹⁴, Z. Huang ¹⁰⁴, Z. Hubacek ¹³⁶, M. Huebner ²⁵, F. Huegging ²⁵, T.B. Huffman ¹³⁰, M. Hufnagel Maranha De Faria ^{84a}, C.A. Hugli ⁴⁹, M. Huhtinen ³⁷, S.K. Huiberts ¹⁷, R. Hulsken ¹⁰⁷, C.E. Hultquist ^{18a}, N. Huseynov ^{12,g}, J. Huston ¹¹⁰, J. Huth ⁶², R. Hyneman ⁷, G. Iacobucci ⁵⁷, G. Iakovidis ³⁰, L. Iconomidou-Fayard ⁶⁷, J.P. Iddon ³⁷, P. Iengo ^{73a,73b}, R. Iguchi ¹⁶⁰, Y. Iiyama ¹⁶⁰, T. Iizawa ¹³⁰, Y. Ikegami ⁸⁵, D. Iliadis ¹⁵⁹, N. Ilic ¹⁶², H. Imam ^{84c}, G. Inacio Goncalves ^{84d}, S.A. Infante Cabanas ^{141c}, T. Ingebretsen Carlson ^{48a,48b}, J.M. Inglis ⁹⁷, G. Introzzi ^{74a,74b}, M. Iodice ^{78a}, V. Ippolito ^{76a,76b}, R.K. Irwin ⁹⁵, M. Ishino ¹⁶⁰, W. Islam ¹⁷⁷, C. Issever ¹⁹, S. Istin ^{22a,al}, H. Ito ¹⁷⁵, R. Iuppa ^{79a,79b}, A. Ivina ¹⁷⁶, V. Izzo ^{73a}, P. Jacka ¹³⁵, P. Jackson ¹, P. Jain ⁴⁹, K. Jakobs ⁵⁵, T. Jakoubek ¹⁷⁶, J. Jamieson ⁶⁰, W. Jang ¹⁶⁰, M. Javurkova ¹⁰⁶, P. Jawahar ¹⁰⁴, L. Jeanty ¹²⁷, J. Jejelava ^{156a}, P. Jenni ^{55,f}, C.E. Jessiman ³⁵, C. Jia ^{144a}, H. Jia ¹⁷¹, J. Jia ¹⁵², X. Jia ^{14,115c}, Z. Jia ^{115a}, C. Jiang ⁵³, Q. Jiang ^{65b}, S. Jiggins ⁴⁹, J. Jimenez Pena ¹³, S. Jin ^{115a}, A. Jinaru ^{28b}, O. Jinnouchi ¹⁴², P. Johansson ¹⁴⁶, K.A. Johns ⁷, J.W. Johnson ¹⁴⁰, F.A. Jolly ⁴⁹, D.M. Jones ¹⁵³, E. Jones ⁴⁹, K.S. Jones ⁸, P. Jones ³³, R.W.L. Jones ⁹⁴, T.J. Jones ⁹⁵, H.L. Joos ^{56,37}, R. Joshi ¹²³, J. Jovicevic ¹⁶, X. Ju ^{18a}, J.J. Junggeburth ³⁷, T. Junkermann ^{64a}, A. Juste Rozas ^{13,x}, M.K. Juzek ⁸⁸, S. Kabana ^{141e}, A. Kaczmarzka ⁸⁸, M. Kado ¹¹³, H. Kagan ¹²³, M. Kagan ¹⁵⁰, A. Kahn ¹³², C. Kahra ¹⁰³, T. Kaji ¹⁶⁰, E. Kajomovitz ¹⁵⁷, N. Kakati ¹⁷⁶, I. Kalaitzidou ⁵⁵, N.J. Kang ¹⁴⁰, D. Kar ^{34g}, K. Karava ¹³⁰, E. Karentzos ²⁵, O. Karkout ¹¹⁸, S.N. Karpov ⁴⁰, Z.M. Karpova ⁴⁰, V. Kartvelishvili ⁹⁴, A.N. Karyukhin ³⁹, E. Kasimi ¹⁵⁹, J. Katzy ⁴⁹, S. Kaur ³⁵, K. Kawade ¹⁴⁷, M.P. Kawale ¹²⁴, C. Kawamoto ⁹⁰, T. Kawamoto ⁶³, E.F. Kay ³⁷, F.I. Kaya ¹⁶⁵, S. Kazakos ¹¹⁰, V.F. Kazanin ³⁹, Y. Ke ¹⁵², J.M. Keaveney ^{34a}, R. Keeler ¹⁷², G.V. Kehris ⁶², J.S. Keller ³⁵, J.J. Kempster ¹⁵³, O. Kepka ¹³⁵, J. Kerr ^{163b}, B.P. Kerridge ¹³⁸,

B.P. Kerševan [ID⁹⁶](#), L. Keszeghova [ID^{29a}](#), R.A. Khan [ID¹³³](#), A. Khanov [ID¹²⁵](#), A.G. Kharlamov [ID³⁹](#),
 T. Kharlamova [ID³⁹](#), E.E. Khoda [ID¹⁴³](#), M. Kholodenko [ID^{134a}](#), T.J. Khoo [ID¹⁹](#), G. Khorauli [ID¹⁷³](#),
 J. Khubua [ID^{156b,*}](#), Y.A.R. Khwaira [ID¹³¹](#), B. Kibirige^{34g}, D. Kim [ID⁶](#), D.W. Kim [ID^{48a,48b}](#), Y.K. Kim [ID⁴¹](#),
 N. Kimura [ID⁹⁹](#), M.K. Kingston [ID⁵⁶](#), A. Kirchhoff [ID⁵⁶](#), C. Kirfel [ID²⁵](#), F. Kirfel [ID²⁵](#), J. Kirk [ID¹³⁸](#),
 A.E. Kiryunin [ID¹¹³](#), S. Kita [ID¹⁶⁴](#), C. Kitsaki [ID¹⁰](#), O. Kivernyk [ID²⁵](#), M. Klassen [ID¹⁶⁵](#), C. Klein [ID³⁵](#),
 L. Klein [ID¹⁷³](#), M.H. Klein [ID⁴⁶](#), S.B. Klein [ID⁵⁷](#), U. Klein [ID⁹⁵](#), A. Klimentov [ID³⁰](#), T. Klioutchnikova [ID³⁷](#),
 P. Kluit [ID¹¹⁸](#), S. Kluth [ID¹¹³](#), E. Kneringer [ID⁸⁰](#), T.M. Knight [ID¹⁶²](#), A. Knue [ID⁵⁰](#), D. Kobylanskii [ID¹⁷⁶](#),
 S.F. Koch [ID¹³⁰](#), M. Kocian [ID¹⁵⁰](#), P. Kodyš [ID¹³⁷](#), D.M. Koeck [ID¹²⁷](#), P.T. Koenig [ID²⁵](#), T. Koffas [ID³⁵](#),
 O. Kolay [ID⁵¹](#), I. Koletsou [ID⁴](#), T. Komarek [ID⁸⁸](#), K. Köneke [ID⁵⁶](#), A.X.Y. Kong [ID¹](#), T. Kono [ID¹²²](#),
 N. Konstantinidis [ID⁹⁹](#), P. Kontaxakis [ID⁵⁷](#), B. Konya [ID¹⁰¹](#), R. Kopeliansky [ID⁴³](#), S. Koperny [ID^{87a}](#),
 K. Korcyl [ID⁸⁸](#), K. Kordas [ID^{159,e}](#), A. Korn [ID⁹⁹](#), S. Korn [ID⁵⁶](#), I. Korolkov [ID¹³](#), N. Korotkova [ID³⁹](#),
 B. Kortman [ID¹¹⁸](#), O. Kortner [ID¹¹³](#), S. Kortner [ID¹¹³](#), W.H. Kostecka [ID¹¹⁹](#), V.V. Kostyukhin [ID¹⁴⁸](#),
 A. Kotsokechagia [ID³⁷](#), A. Kotwal [ID⁵²](#), A. Koulouris [ID³⁷](#), A. Kourkoumeli-Charalampidi [ID^{74a,74b}](#),
 C. Kourkoumelis [ID⁹](#), E. Kourlitis [ID^{113,ae}](#), O. Kovanda [ID¹²⁷](#), R. Kowalewski [ID¹⁷²](#), W. Kozanecki [ID¹²⁷](#),
 A.S. Kozhin [ID³⁹](#), V.A. Kramarenko [ID³⁹](#), G. Kramberger [ID⁹⁶](#), P. Kramer [ID²⁵](#), M.W. Krasny [ID¹³¹](#),
 A. Krasznahorkay [ID¹⁰⁶](#), A.C. Kraus [ID¹¹⁹](#), J.W. Kraus [ID¹⁷⁸](#), J.A. Kremer [ID⁴⁹](#), N.B. Krengel [ID¹⁴⁸](#),
 T. Kresse [ID⁵¹](#), L. Kretschmann [ID¹⁷⁸](#), J. Kretschmar [ID⁹⁵](#), K. Kreul [ID¹⁹](#), P. Krieger [ID¹⁶²](#), K. Krizka [ID²¹](#),
 K. Kroeninger [ID⁵⁰](#), H. Kroha [ID¹¹³](#), J. Kroll [ID¹³⁵](#), J. Kroll [ID¹³²](#), K.S. Krowpman [ID¹¹⁰](#), U. Kruchonak [ID⁴⁰](#),
 H. Krüger [ID²⁵](#), N. Krumnack⁸², M.C. Kruse [ID⁵²](#), O. Kuchinskaia [ID³⁹](#), S. Kuday [ID^{3a}](#), S. Kuehn [ID³⁷](#),
 R. Kuesters [ID⁵⁵](#), T. Kuhl [ID⁴⁹](#), V. Kukhtin [ID⁴⁰](#), Y. Kulchitsky [ID⁴⁰](#), S. Kuleshov [ID^{141d,141b}](#), M. Kumar [ID^{34g}](#),
 N. Kumari [ID⁴⁹](#), P. Kumari [ID^{163b}](#), A. Kupco [ID¹³⁵](#), T. Kupfer⁵⁰, A. Kupich [ID³⁹](#), O. Kuprash [ID⁵⁵](#),
 H. Kurashige [ID⁸⁶](#), L.L. Kurchaninov [ID^{163a}](#), O. Kurdysh [ID⁴](#), Y.A. Kurochkin [ID³⁸](#), A. Kurova [ID³⁹](#),
 M. Kuze [ID¹⁴²](#), A.K. Kvam [ID¹⁰⁶](#), J. Kvita [ID¹²⁶](#), N.G. Kyriacou [ID¹⁰⁹](#), L.A.O. Laatu [ID¹⁰⁵](#), C. Lacasta [ID¹⁷⁰](#),
 F. Lacava [ID^{76a,76b}](#), H. Lacker [ID¹⁹](#), D. Lacour [ID¹³¹](#), N.N. Lad [ID⁹⁹](#), E. Ladygin [ID⁴⁰](#), A. Lafarge [ID⁴²](#),
 B. Laforge [ID¹³¹](#), T. Lagouri [ID¹⁷⁹](#), F.Z. Lahbabi [ID^{36a}](#), S. Lai [ID⁵⁶](#), J.E. Lambert [ID¹⁷²](#), S. Lammers [ID⁶⁹](#),
 W. Lampl [ID⁷](#), C. Lampoudis [ID^{159,e}](#), G. Lamprinoudis [ID¹⁰³](#), A.N. Lancaster [ID¹¹⁹](#), E. Lançon [ID³⁰](#),
 U. Landgraf [ID⁵⁵](#), M.P.J. Landon [ID⁹⁷](#), V.S. Lang [ID⁵⁵](#), O.K.B. Langrekken [ID¹²⁹](#), A.J. Lankford [ID¹⁶⁶](#),
 F. Lanni [ID³⁷](#), K. Lantzsch [ID²⁵](#), A. Lanza [ID^{74a}](#), M. Lanzac Berrocal [ID¹⁷⁰](#), J.F. Laporte [ID¹³⁹](#), T. Lari [ID^{72a}](#),
 D. Larsen [ID¹⁷](#), F. Lasagni Manghi [ID^{24b}](#), M. Lassnig [ID³⁷](#), V. Latonova [ID¹³⁵](#), S.D. Lawlor [ID¹⁴⁶](#),
 Z. Lawrence [ID¹⁰⁴](#), R. Lazaridou¹⁷⁴, M. Lazzaroni [ID^{72a,72b}](#), H.D.M. Le [ID¹¹⁰](#), E.M. Le Boulicaut [ID¹⁷⁹](#),
 L.T. Le Pottier [ID^{18a}](#), B. Leban [ID^{24b,24a}](#), M. LeBlanc [ID¹⁰⁴](#), F. Ledroit-Guillon [ID⁶¹](#), S.C. Lee [ID¹⁵⁵](#),
 T.F. Lee [ID⁹⁵](#), L.L. Leeuw [ID^{34c,aj}](#), M. Lefebvre [ID¹⁷²](#), C. Leggett [ID^{18a}](#), G. Lehmann Miotto [ID³⁷](#),
 M. Leigh [ID⁵⁷](#), W.A. Leight [ID¹⁰⁶](#), W. Leinonen [ID¹¹⁷](#), A. Leisos [ID^{159,u}](#), M.A.L. Leite [ID^{84c}](#),
 C.E. Leitgeb [ID¹⁹](#), R. Leitner [ID¹³⁷](#), K.J.C. Leney [ID⁴⁶](#), T. Lenz [ID²⁵](#), S. Leone [ID^{75a}](#), C. Leonidopoulos [ID⁵³](#),
 A. Leopold [ID¹⁵¹](#), J.H. Lepage Bourbonnais [ID³⁵](#), R. Les [ID¹¹⁰](#), C.G. Lester [ID³³](#), M. Levchenko [ID³⁹](#),
 J. Levêque [ID⁴](#), L.J. Levinson [ID¹⁷⁶](#), G. Levirini [ID^{24b,24a}](#), M.P. Lewicki [ID⁸⁸](#), C. Lewis [ID¹⁴³](#), D.J. Lewis [ID⁴](#),
 L. Lewitt [ID¹⁴⁶](#), A. Li [ID³⁰](#), B. Li [ID^{144a}](#), C. Li¹⁰⁹, C-Q. Li [ID¹¹³](#), H. Li [ID⁶³](#), H. Li [ID^{144a}](#), H. Li [ID¹⁰⁴](#),
 H. Li [ID¹⁵](#), H. Li [ID^{144a}](#), J. Li [ID^{145a}](#), K. Li [ID¹⁴](#), L. Li [ID^{145a}](#), R. Li [ID¹⁷⁹](#), S. Li [ID^{14,115c}](#), S. Li [ID^{145b,145a,d}](#),
 T. Li [ID⁵](#), X. Li [ID¹⁰⁷](#), Z. Li [ID¹⁶⁰](#), Z. Li [ID^{14,115c}](#), Z. Li [ID⁶³](#), S. Liang [ID^{14,115c}](#), Z. Liang [ID¹⁴](#),
 M. Liberatore [ID¹³⁹](#), B. Liberti [ID^{77a}](#), K. Lie [ID^{65c}](#), J. Lieber Marin [ID^{84e}](#), H. Lien [ID⁶⁹](#), H. Lin [ID¹⁰⁹](#),
 L. Linden [ID¹¹²](#), R.E. Lindley [ID⁷](#), J.H. Lindon [ID²](#), J. Ling [ID⁶²](#), E. Lipeles [ID¹³²](#), A. Lipniacka [ID¹⁷](#),
 A. Lister [ID¹⁷¹](#), J.D. Little [ID⁶⁹](#), B. Liu [ID¹⁴](#), B.X. Liu [ID^{115b}](#), D. Liu [ID^{145b,145a}](#), E.H.L. Liu [ID²¹](#),
 J.K.K. Liu [ID³³](#), K. Liu [ID^{145b}](#), K. Liu [ID^{145b,145a}](#), M. Liu [ID⁶³](#), M.Y. Liu [ID⁶³](#), P. Liu [ID¹⁴](#),
 Q. Liu [ID^{145b,143,145a}](#), X. Liu [ID⁶³](#), X. Liu [ID^{144a}](#), Y. Liu [ID^{115b,115c}](#), Y.L. Liu [ID^{144a}](#), Y.W. Liu [ID⁶³](#),
 S.L. Lloyd [ID⁹⁷](#), E.M. Lobodzinska [ID⁴⁹](#), P. Loch [ID⁷](#), E. Lodhi [ID¹⁶²](#), T. Lohse [ID¹⁹](#), K. Lohwasser [ID¹⁴⁶](#),
 E. Loiacono [ID⁴⁹](#), J.D. Lomas [ID²¹](#), J.D. Long [ID⁴³](#), I. Longarini [ID¹⁶⁶](#), R. Longo [ID¹⁶⁹](#), A. Lopez Solis [ID⁴⁹](#),
 N.A. Lopez-canelas [ID⁷](#), N. Lorenzo Martinez [ID⁴](#), A.M. Lory [ID¹¹²](#), M. Losada [ID^{120a}](#),


G. Löschcke Centeno [id](#)¹⁵³, O. Loseva [id](#)³⁹, X. Lou [id](#)^{48a,48b}, X. Lou [id](#)^{14,115c}, A. Lounis [id](#)⁶⁷, P.A. Love [id](#)⁹⁴, G. Lu [id](#)^{14,115c}, M. Lu [id](#)⁶⁷, S. Lu [id](#)¹³², Y.J. Lu [id](#)¹⁵⁵, H.J. Lubatti [id](#)¹⁴³, C. Luci [id](#)^{76a,76b}, F.L. Lucio Alves [id](#)^{115a}, F. Luehring [id](#)⁶⁹, B.S. Lunday [id](#)¹³², O. Lundberg [id](#)¹⁵¹, B. Lund-Jensen [id](#)^{151,*}, N.A. Luongo [id](#)⁶, M.S. Lutz [id](#)³⁷, A.B. Lux [id](#)²⁶, D. Lynn [id](#)³⁰, R. Lysak [id](#)¹³⁵, E. Lytken [id](#)¹⁰¹, V. Lyubushkin [id](#)⁴⁰, T. Lyubushkina [id](#)⁴⁰, M.M. Lyukova [id](#)¹⁵², M.Firdaus M. Soberi [id](#)⁵³, H. Ma [id](#)³⁰, K. Ma [id](#)⁶³, L.L. Ma [id](#)^{144a}, W. Ma [id](#)⁶³, Y. Ma [id](#)¹²⁵, J.C. MacDonald [id](#)¹⁰³, P.C. Machado De Abreu Farias [id](#)^{84e}, R. Madar [id](#)⁴², T. Madula [id](#)⁹⁹, J. Maeda [id](#)⁸⁶, T. Maeno [id](#)³⁰, P.T. Mafa [id](#)^{34c,k}, H. Maguire [id](#)¹⁴⁶, V. Maiboroda [id](#)¹³⁹, A. Maio [id](#)^{134a,134b,134d}, K. Maj [id](#)^{87a}, O. Majersky [id](#)⁴⁹, S. Majewski [id](#)¹²⁷, R. Makhmanazarov [id](#)³⁹, N. Makovec [id](#)⁶⁷, V. Maksimovic [id](#)¹⁶, B. Malaescu [id](#)¹³¹, Pa. Malecki [id](#)⁸⁸, V.P. Maleev [id](#)³⁹, F. Malek [id](#)^{61,p}, M. Mali [id](#)⁹⁶, D. Malito [id](#)⁹⁸, U. Mallik [id](#)^{81,*}, S. Maltezos¹⁰, S. Malyukov⁴⁰, J. Mamuzic [id](#)¹³, G. Mancini [id](#)⁵⁴, M.N. Mancini [id](#)²⁷, G. Manco [id](#)^{74a,74b}, J.P. Mandalia [id](#)⁹⁷, S.S. Mandarry [id](#)¹⁵³, I. Mandić [id](#)⁹⁶, L. Manhaes de Andrade Filho [id](#)^{84a}, I.M. Maniatis [id](#)¹⁷⁶, J. Manjarres Ramos [id](#)⁹², D.C. Mankad [id](#)¹⁷⁶, A. Mann [id](#)¹¹², S. Manzoni [id](#)³⁷, L. Mao [id](#)^{145a}, X. Mapekula [id](#)^{34c}, A. Marantis [id](#)^{159,u}, G. Marchiori [id](#)⁵, M. Marcisovsky [id](#)¹³⁵, C. Marcon [id](#)^{72a}, M. Marinescu [id](#)²¹, S. Marium [id](#)⁴⁹, M. Marjanovic [id](#)¹²⁴, A. Markhoos [id](#)⁵⁵, M. Markovitch [id](#)⁶⁷, M.K. Maroun [id](#)¹⁰⁶, E.J. Marshall [id](#)⁹⁴, Z. Marshall [id](#)^{18a}, S. Marti-Garcia [id](#)¹⁷⁰, J. Martin [id](#)⁹⁹, T.A. Martin [id](#)¹³⁸, V.J. Martin [id](#)⁵³, B. Martin dit Latour [id](#)¹⁷, L. Martinelli [id](#)^{76a,76b}, M. Martinez [id](#)^{13,x}, P. Martinez Agullo [id](#)¹⁷⁰, V.I. Martinez Outschoorn [id](#)¹⁰⁶, P. Martinez Suarez [id](#)¹³, S. Martin-Haugh [id](#)¹³⁸, G. Martinovicova [id](#)¹³⁷, V.S. Martoiu [id](#)^{28b}, A.C. Martyniuk [id](#)⁹⁹, A. Marzin [id](#)³⁷, D. Mascione [id](#)^{79a,79b}, L. Masetti [id](#)¹⁰³, J. Masik [id](#)¹⁰⁴, A.L. Maslennikov [id](#)⁴⁰, S.L. Mason [id](#)⁴³, P. Massarotti [id](#)^{73a,73b}, P. Mastrandrea [id](#)^{75a,75b}, A. Mastroberardino [id](#)^{45b,45a}, T. Masubuchi [id](#)¹²⁸, T.T. Mathew [id](#)¹²⁷, J. Matousek [id](#)¹³⁷, D.M. Mattern [id](#)⁵⁰, J. Maurer [id](#)^{28b}, T. Maurin [id](#)⁶⁰, A.J. Maury [id](#)⁶⁷, B. Maček [id](#)⁹⁶, D.A. Maximov [id](#)³⁹, A.E. May [id](#)¹⁰⁴, E. Mayer [id](#)⁴², R. Mazini [id](#)^{34g}, I. Maznas [id](#)¹¹⁹, M. Mazza [id](#)¹¹⁰, S.M. Mazza [id](#)¹⁴⁰, E. Mazzeo [id](#)^{72a,72b}, J.P. Mc Gowan [id](#)¹⁷², S.P. Mc Kee [id](#)¹⁰⁹, C.A. Mc Lean [id](#)⁶, C.C. McCracken [id](#)¹⁷¹, E.F. McDonald [id](#)¹⁰⁸, A.E. McDougall [id](#)¹¹⁸, L.F. Mcelhinney [id](#)⁹⁴, J.A. Mcfayden [id](#)¹⁵³, R.P. McGovern [id](#)¹³², R.P. Mckenzie [id](#)^{34g}, T.C. Mclachlan [id](#)⁴⁹, D.J. Mclaughlin [id](#)⁹⁹, S.J. McMahon [id](#)¹³⁸, C.M. Mcpartland [id](#)⁹⁵, R.A. McPherson [id](#)^{172,ab}, S. Mehlhase [id](#)¹¹², A. Mehta [id](#)⁹⁵, D. Melini [id](#)¹⁷⁰, B.R. Mellado Garcia [id](#)^{34g}, A.H. Melo [id](#)⁵⁶, F. Meloni [id](#)⁴⁹, A.M. Mendes Jacques Da Costa [id](#)¹⁰⁴, H.Y. Meng [id](#)¹⁶², L. Meng [id](#)⁹⁴, S. Menke [id](#)¹¹³, M. Mentink [id](#)³⁷, E. Meoni [id](#)^{45b,45a}, G. Mercado [id](#)¹¹⁹, S. Merianos [id](#)¹⁵⁹, C. Merlassino [id](#)^{70a,70c}, C. Meroni [id](#)^{72a,72b}, J. Metcalfe [id](#)⁶, A.S. Mete [id](#)⁶, E. Meuser [id](#)¹⁰³, C. Meyer [id](#)⁶⁹, J-P. Meyer [id](#)¹³⁹, R.P. Middleton [id](#)¹³⁸, L. Mijović [id](#)⁵³, G. Mikenberg [id](#)¹⁷⁶, M. Mikestikova [id](#)¹³⁵, M. Mikuž [id](#)⁹⁶, H. Mildner [id](#)¹⁰³, A. Milic [id](#)³⁷, D.W. Miller [id](#)⁴¹, E.H. Miller [id](#)¹⁵⁰, L.S. Miller [id](#)³⁵, A. Milov [id](#)¹⁷⁶, D.A. Milstead^{48a,48b}, T. Min^{115a}, A.A. Minaenko [id](#)³⁹, I.A. Minashvili [id](#)^{156b}, A.I. Mincer [id](#)¹²¹, B. Mindur [id](#)^{87a}, M. Mineev [id](#)⁴⁰, Y. Mino [id](#)⁹⁰, L.M. Mir [id](#)¹³, M. Miralles Lopez [id](#)⁶⁰, M. Mironova [id](#)^{18a}, M.C. Missio [id](#)¹¹⁷, A. Mitra [id](#)¹⁷⁴, V.A. Mitsou [id](#)¹⁷⁰, Y. Mitsumori [id](#)¹¹⁴, O. Miu [id](#)¹⁶², P.S. Miyagawa [id](#)⁹⁷, T. Mkrtychyan [id](#)^{64a}, M. Mlinarevic [id](#)⁹⁹, T. Mlinarevic [id](#)⁹⁹, M. Mlynarikova [id](#)³⁷, S. Mobius [id](#)²⁰, P. Mogg [id](#)¹¹², M.H. Mohamed Farook [id](#)¹¹⁶, A.F. Mohammed [id](#)^{14,115c}, S. Mohapatra [id](#)⁴³, S. Mohiuddin [id](#)¹²⁵, G. Mokgatitwane [id](#)^{34g}, L. Moleri [id](#)¹⁷⁶, B. Mondal [id](#)¹⁴⁸, S. Mondal [id](#)¹³⁶, K. Mönig [id](#)⁴⁹, E. Monnier [id](#)¹⁰⁵, L. Monsonis Romero¹⁷⁰, J. Montejo Berlingen [id](#)¹³, A. Montella [id](#)^{48a,48b}, M. Montella [id](#)¹²³, F. Montekali [id](#)^{78a,78b}, F. Monticelli [id](#)⁹³, S. Monzani [id](#)^{70a,70c}, A. Morancho Tarda [id](#)⁴⁴, N. Morange [id](#)⁶⁷, A.L. Moreira De Carvalho [id](#)⁴⁹, M. Moreno Llácer [id](#)¹⁷⁰, C. Moreno Martinez [id](#)⁵⁷, J.M. Moreno Perez^{23b}, P. Morettini [id](#)^{58b}, S. Morgenstern [id](#)³⁷, M. Morii [id](#)⁶², M. Morinaga [id](#)¹⁶⁰, M. Moritsu [id](#)⁹¹, F. Morodei [id](#)^{76a,76b}, P. Moschovakos [id](#)³⁷, B. Moser [id](#)¹³⁰, M. Mosidze [id](#)^{156b}, T. Moskalets [id](#)⁴⁶, P. Moskvitina [id](#)¹¹⁷, J. Moss [id](#)^{32,m}, P. Moszkowicz [id](#)^{87a}, A. Moussa [id](#)^{36d}, Y. Moyal [id](#)¹⁷⁶, E.J.W. Moyse [id](#)¹⁰⁶, O. Mtintsilana [id](#)^{34g}, S. Muanza [id](#)¹⁰⁵, J. Mueller [id](#)¹³³, R. Müller [id](#)³⁷,

G.A. Mullier ¹⁶⁸, A.J. Mullin³³, J.J. Mullin⁵², A.E. Mulski ⁶², D.P. Mungo ¹⁶², D. Munoz Perez ¹⁷⁰, F.J. Munoz Sanchez ¹⁰⁴, M. Murin ¹⁰⁴, W.J. Murray ^{174,138}, M. Muškinja ⁹⁶, C. Mwewa ³⁰, A.G. Myagkov ^{39,a}, A.J. Myers ⁸, G. Myers ¹⁰⁹, M. Myska ¹³⁶, B.P. Nachman ^{18a}, K. Nagai ¹³⁰, K. Nagano ⁸⁵, R. Nagasaka¹⁶⁰, J.L. Nagle ^{30,ai}, E. Nagy ¹⁰⁵, A.M. Nairz ³⁷, Y. Nakahama ⁸⁵, K. Nakamura ⁸⁵, K. Nakkalil ⁵, H. Nanjo ¹²⁸, E.A. Narayanan ⁴⁶, Y. Narukawa ¹⁶⁰, I. Naryshkin ³⁹, L. Nasella ^{72a,72b}, S. Nasri ^{120b}, C. Nass ²⁵, G. Navarro ^{23a}, J. Navarro-Gonzalez ¹⁷⁰, A. Nayaz ¹⁹, P.Y. Nechaeva ³⁹, S. Nechaeva ^{24b,24a}, F. Nechansky ¹³⁵, L. Nedic ¹³⁰, T.J. Neep ²¹, A. Negri ^{74a,74b}, M. Negrini ^{24b}, C. Nellist ¹¹⁸, C. Nelson ¹⁰⁷, K. Nelson ¹⁰⁹, S. Nemecek ¹³⁵, M. Nessi ^{37,h}, M.S. Neubauer ¹⁶⁹, F. Neuhaus ¹⁰³, J. Newell ⁹⁵, P.R. Newman ²¹, Y.W.Y. Ng ¹⁶⁹, B. Ngair ^{120a}, H.D.N. Nguyen ¹¹¹, R.B. Nickerson ¹³⁰, R. Nicolaidou ¹³⁹, J. Nielsen ¹⁴⁰, M. Niemeyer ⁵⁶, J. Niermann ³⁷, N. Nikiforou ³⁷, V. Nikolaenko ^{39,a}, I. Nikolic-Audit ¹³¹, P. Nilsson ³⁰, I. Ninca ⁴⁹, G. Ninio ¹⁵⁸, A. Nisati ^{76a}, N. Nishu ², R. Nisius ¹¹³, N. Nitika ^{70a,70c}, J-E. Nitschke ⁵¹, E.K. Nkadimeng ^{34g}, T. Nobe ¹⁶⁰, T. Nommensen ¹⁵⁴, M.B. Norfolk ¹⁴⁶, B.J. Norman ³⁵, M. Noury ^{36a}, J. Novak ⁹⁶, T. Novak ⁹⁶, R. Novotny ¹¹⁶, L. Nozka ¹²⁶, K. Ntekas ¹⁶⁶, N.M.J. Nunes De Moura Junior ^{84b}, J. Ocariz ¹³¹, A. Ochi ⁸⁶, I. Ochoa ^{134a}, S. Oerdek ^{49,y}, J.T. Offermann ⁴¹, A. Ogrodnik ¹³⁷, A. Oh ¹⁰⁴, C.C. Ohm ¹⁵¹, H. Oide ⁸⁵, R. Oishi ¹⁶⁰, M.L. Ojeda ³⁷, Y. Okumura ¹⁶⁰, L.F. Oleiro Seabra ^{134a}, I. Oleksiyuk ⁵⁷, S.A. Olivares Pino ^{141d}, G. Oliveira Correa ¹³, D. Oliveira Damazio ³⁰, J.L. Oliver ¹⁶⁶, Ö.O. Öncel ⁵⁵, A.P. O'Neill ²⁰, A. Onofre ^{134a,134e}, P.U.E. Onyisi ¹¹, M.J. Oreglia ⁴¹, D. Orestano ^{78a,78b}, R.S. Orr ¹⁶², L.M. Osojnak ¹³², Y. Osumi¹¹⁴, G. Otero y Garzon ³¹, H. Otono ⁹¹, G.J. Ottino ^{18a}, M. Ouchrif ^{36d}, F. Ould-Saada ¹²⁹, T. Ovsianikova ¹⁴³, M. Owen ⁶⁰, R.E. Owen ¹³⁸, V.E. Ozcan ^{22a}, F. Ozturk ⁸⁸, N. Ozturk ⁸, S. Ozturk ⁸³, H.A. Pacey ¹³⁰, K. Pachal ^{163a}, A. Pacheco Pages ¹³, C. Padilla Aranda ¹³, G. Padovano ^{76a,76b}, S. Pagan Griso ^{18a}, G. Palacino ⁶⁹, A. Palazzo ^{71a,71b}, J. Pampel ²⁵, J. Pan ¹⁷⁹, T. Pan ^{65a}, D.K. Panchal ¹¹, C.E. Pandini ¹¹⁸, J.G. Panduro Vazquez ¹³⁸, H.D. Pandya ¹, H. Pang ¹³⁹, P. Pani ⁴⁹, G. Panizzo ^{70a,70c}, L. Panwar ¹³¹, L. Paolozzi ⁵⁷, S. Parajuli ¹⁶⁹, A. Paramonov ⁶, C. Paraskevopoulos ⁵⁴, D. Paredes Hernandez ^{65b}, A. Pareti ^{74a,74b}, K.R. Park ⁴³, T.H. Park ¹¹³, F. Parodi ^{58b,58a}, J.A. Parsons ⁴³, U. Parzefall ⁵⁵, B. Pascual Dias ⁴², L. Pascual Dominguez ¹⁰², E. Pasqualucci ^{76a}, S. Passaggio ^{58b}, F. Pastore ⁹⁸, P. Patel ⁸⁸, U.M. Patel ⁵², J.R. Pater ¹⁰⁴, T. Pauly ³⁷, F. Pauwels ¹³⁷, C.I. Pazos ¹⁶⁵, M. Pedersen ¹²⁹, R. Pedro ^{134a}, S.V. Peleganchuk ³⁹, O. Penc ³⁷, E.A. Pender ⁵³, S. Peng ¹⁵, G.D. Penn ¹⁷⁹, K.E. Penski ¹¹², M. Penzin ³⁹, B.S. Peralva ^{84d}, A.P. Pereira Peixoto ¹⁴³, L. Pereira Sanchez ¹⁵⁰, D.V. Perepelitsa ^{30,ai}, G. Perera ¹⁰⁶, E. Perez Codina ^{163a}, M. Perganti ¹⁰, H. Pernegger ³⁷, S. Perrella ^{76a,76b}, O. Perrin ⁴², K. Peters ⁴⁹, R.F.Y. Peters ¹⁰⁴, B.A. Petersen ³⁷, T.C. Petersen ⁴⁴, E. Petit ¹⁰⁵, V. Petousis ¹³⁶, A.R. Petri^{72a,72b}, C. Petridou ^{159,e}, T. Petru ¹³⁷, A. Petrukhin ¹⁴⁸, M. Pettee ^{18a}, A. Petukhov ⁸³, K. Petukhova ³⁷, R. Pezoa ^{141f}, L. Pezzotti ^{24b,24a}, G. Pezzullo ¹⁷⁹, L. Pfaffenbichler ³⁷, A.J. Pflieger ³⁷, T.M. Pham ¹⁷⁷, T. Pham ¹⁰⁸, P.W. Phillips ¹³⁸, G. Piacquadio ¹⁵², E. Pianori ^{18a}, F. Piazza ¹²⁷, R. Piegaia ³¹, D. Pietreanu ^{28b}, A.D. Pilkington ¹⁰⁴, M. Pinamonti ^{70a,70c}, J.L. Pinfeld ², B.C. Pinheiro Pereira ^{134a}, J. Pinol Bel ¹³, A.E. Pinto Pinoargote ¹³⁹, L. Pintucci ^{70a,70c}, K.M. Piper ¹⁵³, A. Pirttikoski ⁵⁷, D.A. Pizzi ³⁵, L. Pizzimento ^{65b}, M.-A. Pleier ³⁰, V. Pleskot ¹³⁷, E. Plotnikova⁴⁰, G. Poddar ⁹⁷, R. Poettgen ¹⁰¹, L. Poggioli ¹³¹, S. Polacek ¹³⁷, G. Polesello ^{74a}, A. Poley ^{149,163a}, A. Polini ^{24b}, C.S. Pollard ¹⁷⁴, Z.B. Pollock ¹²³, E. Pompa Pacchi ¹²⁴, N.I. Pond ⁹⁹, D. Ponomarenko ⁶⁹, L. Pontecorvo ³⁷, S. Popa ^{28a}, G.A. Popeneciu ^{28d}, A. Poreba ³⁷, D.M. Portillo Quintero ^{163a}, S. Pospisil ¹³⁶, M.A. Postill ¹⁴⁶, P. Postolache ^{28c}, K. Potamianos ¹⁷⁴, P.A. Potepa ^{87a}, I.N. Potrap ⁴⁰, C.J. Potter ³³, H. Potti ¹⁵⁴, J. Poveda ¹⁷⁰, M.E. Pozo Astigarraga ³⁷, A. Prades Ibanez ^{77a,77b},

J. Pretel ¹⁷², D. Price ¹⁰⁴, M. Primavera ^{71a}, L. Primomo ^{70a,70c}, M.A. Principe Martin ¹⁰²,
 R. Privara ¹²⁶, T. Procter ⁶⁰, M.L. Proffitt ¹⁴³, N. Proklova ¹³², K. Prokofiev ^{65c}, G. Proto ¹¹³,
 J. Proudfoot ⁶, M. Przybycien ^{87a}, W.W. Przygoda ^{87b}, A. Psallidas ⁴⁷, J.E. Puddefoot ¹⁴⁶,
 D. Pudzha ⁵⁵, D. Pyatiizbyantseva ¹¹⁷, J. Qian ¹⁰⁹, R. Qian ¹¹⁰, D. Qichen ¹⁰⁴, Y. Qin ¹³,
 T. Qiu ⁵³, A. Quadt ⁵⁶, M. Queitsch-Maitland ¹⁰⁴, G. Quetant ⁵⁷, R.P. Quinn ¹⁷¹,
 G. Rabanal Bolanos ⁶², D. Rafanoharana ⁵⁵, F. Raffaeli ^{77a,77b}, F. Ragusa ^{72a,72b}, J.L. Rainbolt ⁴¹,
 J.A. Raine ⁵⁷, S. Rajagopalan ³⁰, E. Ramakoti ³⁹, L. Rambelli ^{58b,58a}, I.A. Ramirez-Berend ³⁵,
 K. Ran ^{49,115c}, D.S. Rankin ¹³², N.P. Rapheeha ^{34g}, H. Rasheed ^{28b}, V. Raskina ¹³¹,
 D.F. Rassloff ^{64a}, A. Rastogi ^{18a}, S. Rave ¹⁰³, S. Ravera ^{58b,58a}, B. Ravina ³⁷, I. Ravinovich ¹⁷⁶,
 M. Raymond ³⁷, A.L. Read ¹²⁹, N.P. Readioff ¹⁴⁶, D.M. Rebutti ^{74a,74b}, A.S. Reed ¹¹³,
 K. Reeves ²⁷, J.A. Reidelsturz ¹⁷⁸, D. Reikher ¹²⁷, A. Rej ⁵⁰, C. Rembser ³⁷, H. Ren ⁶³,
 M. Renda ^{28b}, F. Renner ⁴⁹, A.G. Rennie ¹⁶⁶, A.L. Rescia ⁴⁹, S. Resconi ^{72a},
 M. Ressegotti ^{58b,58a}, S. Rettie ³⁷, W.F. Rettie ³⁵, J.G. Reyes Rivera ¹¹⁰, E. Reynolds ^{18a},
 O.L. Rezanova ⁴⁰, P. Reznicek ¹³⁷, H. Riani ^{36d}, N. Ribaric ⁵², E. Ricci ^{79a,79b}, R. Richter ¹¹³,
 S. Richter ^{48a,48b}, E. Richter-Was ^{87b}, M. Ridel ¹³¹, S. Ridouani ^{36d}, P. Rieck ¹²¹, P. Riedler ³⁷,
 E.M. Riefel ^{48a,48b}, J.O. Rieger ¹¹⁸, M. Rijssenbeek ¹⁵², M. Rimoldi ³⁷, L. Rinaldi ^{24b,24a},
 P. Rincke ^{56,168}, G. Ripellino ¹⁶⁸, I. Riu ¹³, J.C. Rivera Vergara ¹⁷², F. Rizatdinova ¹²⁵,
 E. Rizvi ⁹⁷, B.R. Roberts ^{18a}, S.S. Roberts ¹⁴⁰, D. Robinson ³³, M. Robles Manzano ¹⁰³,
 A. Robson ⁶⁰, A. Rocchi ^{77a,77b}, C. Roda ^{75a,75b}, S. Rodriguez Bosca ³⁷, Y. Rodriguez Garcia ^{23a},
 A.M. Rodríguez Vera ¹¹⁹, S. Roe ³⁷, J.T. Roemer ³⁷, O. Røhne ¹²⁹, C.P.A. Roland ¹³¹, J. Roloff ³⁰,
 A. Romaniouk ⁸⁰, E. Romano ^{74a,74b}, M. Romano ^{24b}, A.C. Romero Hernandez ¹⁶⁹,
 N. Rompotis ⁹⁵, L. Roos ¹³¹, S. Rosati ^{76a}, B.J. Rosser ⁴¹, E. Rossi ¹³⁰, E. Rossi ^{73a,73b},
 L.P. Rossi ⁶², L. Rossini ⁵⁵, R. Rosten ¹²³, M. Rotaru ^{28b}, B. Rottler ⁵⁵, D. Rousseau ⁶⁷,
 D. Rousso ⁴⁹, S. Roy-Garand ¹⁶², A. Rozanov ¹⁰⁵, Z.M.A. Rozario ⁶⁰, Y. Rozen ¹⁵⁷,
 A. Rubio Jimenez ¹⁷⁰, V.H. Ruelas Rivera ¹⁹, T.A. Ruggeri ¹, A. Ruggiero ¹³⁰,
 A. Ruiz-Martinez ¹⁷⁰, A. Rummler ³⁷, Z. Rurikova ⁵⁵, N.A. Rusakovich ⁴⁰, H.L. Russell ¹⁷²,
 G. Russo ^{76a,76b}, J.P. Rutherford ⁷, S. Rutherford Colmenares ³³, M. Rybar ¹³⁷, E.B. Rye ¹²⁹,
 A. Ryzhov ⁴⁶, J.A. Sabater Iglesias ⁵⁷, H.F.W. Sadrozinski ¹⁴⁰, F. Safai Tehrani ^{76a}, S. Saha ¹,
 M. Sahinsoy ⁸³, A. Saibel ¹⁷⁰, B.T. Saifuddin ¹²⁴, M. Saimpert ¹³⁹, M. Saito ¹⁶⁰, T. Saito ¹⁶⁰,
 A. Sala ^{72a,72b}, D. Salamani ³⁷, A. Salnikov ¹⁵⁰, J. Salt ¹⁷⁰, A. Salvador Salas ¹⁵⁸,
 D. Salvatore ^{45b,45a}, F. Salvatore ¹⁵³, A. Salzburger ³⁷, D. Sammel ⁵⁵, E. Sampson ⁹⁴,
 D. Sampsonidis ^{159,e}, D. Sampsonidou ¹²⁷, J. Sánchez ¹⁷⁰, V. Sanchez Sebastian ¹⁷⁰,
 H. Sandaker ¹²⁹, C.O. Sander ⁴⁹, J.A. Sandesara ¹⁰⁶, M. Sandhoff ¹⁷⁸, C. Sandoval ^{23b},
 L. Sanfilippo ^{64a}, D.P.C. Sankey ¹³⁸, T. Sano ⁹⁰, A. Sansoni ⁵⁴, L. Santi ³⁷, C. Santoni ⁴²,
 H. Santos ^{134a,134b}, A. Santra ¹⁷⁶, E. Sanzani ^{24b,24a}, K.A. Saoucha ^{89b}, J.G. Saraiva ^{134a,134d},
 J. Sardain ⁷, O. Sasaki ⁸⁵, K. Sato ¹⁶⁴, C. Sauer ³⁷, E. Sauvan ⁴, P. Savard ^{162,ag}, R. Sawada ¹⁶⁰,
 C. Sawyer ¹³⁸, L. Sawyer ¹⁰⁰, C. Sbarra ^{24b}, A. Sbrizzi ^{24b,24a}, T. Scanlon ⁹⁹,
 J. Schaarschmidt ¹⁴³, U. Schäfer ¹⁰³, A.C. Schaffer ^{67,46}, D. Schaile ¹¹², R.D. Schamberger ¹⁵²,
 C. Scharf ¹⁹, M.M. Schefer ²⁰, V.A. Schegelsky ³⁹, D. Scheirich ¹³⁷, M. Schernau ^{141e},
 C. Scheulen ⁵⁷, C. Schiavi ^{58b,58a}, M. Schioppa ^{45b,45a}, B. Schlag ¹⁵⁰, S. Schlenker ³⁷,
 J. Schmeing ¹⁷⁸, M.A. Schmidt ¹⁷⁸, K. Schmieden ¹⁰³, C. Schmitt ¹⁰³, N. Schmitt ¹⁰³,
 S. Schmitt ⁴⁹, L. Schoeffel ¹³⁹, A. Schoening ^{64b}, P.G. Scholer ³⁵, E. Schopf ¹⁴⁸, M. Schott ²⁵,
 S. Schramm ⁵⁷, T. Schroer ⁵⁷, H-C. Schultz-Coulon ^{64a}, M. Schumacher ⁵⁵, B.A. Schumm ¹⁴⁰,
 Ph. Schune ¹³⁹, H.R. Schwartz ¹⁴⁰, A. Schwartzman ¹⁵⁰, T.A. Schwarz ¹⁰⁹, Ph. Schwemling ¹³⁹,
 R. Schwienhorst ¹¹⁰, F.G. Sciacca ²⁰, A. Sciandra ³⁰, G. Sciolla ²⁷, F. Scuri ^{75a},
 C.D. Sebastiani ³⁷, K. Sedlaczek ¹¹⁹, S.C. Seidel ¹¹⁶, A. Seiden ¹⁴⁰, B.D. Seidlitz ⁴³,
 C. Seitz ⁴⁹, J.M. Seixas ^{84b}, G. Sekhniaidze ^{73a}, L. Selem ⁶¹, N. Semprini-Cesari ^{24b,24a},

A. Semushin ^{180,39}, D. Sengupta ⁵⁷, V. Senthilkumar ¹⁷⁰, L. Serin ⁶⁷, M. Sessa ^{77a,77b},
 H. Severini ¹²⁴, F. Sforza ^{58b,58a}, A. Sfyrla ⁵⁷, Q. Sha ¹⁴, E. Shabalina ⁵⁶, H. Shaddix ¹¹⁹,
 A.H. Shah ³³, R. Shaheen ¹⁵¹, J.D. Shahinian ¹³², D. Shaked Renous ¹⁷⁶, M. Shamim ³⁷,
 L.Y. Shan ¹⁴, M. Shapiro ^{18a}, A. Sharma ³⁷, A.S. Sharma ¹⁷¹, P. Sharma ³⁰, P.B. Shatalov ³⁹,
 K. Shaw ¹⁵³, S.M. Shaw ¹⁰⁴, Q. Shen ^{145a}, D.J. Sheppard ¹⁴⁹, P. Sherwood ⁹⁹, L. Shi ⁹⁹,
 X. Shi ¹⁴, S. Shimizu ⁸⁵, C.O. Shimmin ¹⁷⁹, I.P.J. Shipsey ^{130,*}, S. Shirabe ⁹¹,
 M. Shiyakova ^{40,z}, M.J. Shochet ⁴¹, D.R. Shope ¹²⁹, B. Shrestha ¹²⁴, S. Shrestha ^{123,ak},
 I. Shreyber ³⁹, M.J. Shroff ¹⁷², P. Sicho ¹³⁵, A.M. Sickles ¹⁶⁹, E. Sideras Haddad ^{34g,167},
 A.C. Sidley ¹¹⁸, A. Sidoti ^{24b}, F. Siegert ⁵¹, Dj. Sijacki ¹⁶, F. Sili ⁹³, J.M. Silva ⁵³,
 I. Silva Ferreira ^{84b}, M.V. Silva Oliveira ³⁰, S.B. Silverstein ^{48a}, S. Simion ⁶⁷, R. Simoniello ³⁷,
 E.L. Simpson ¹⁰⁴, H. Simpson ¹⁵³, L.R. Simpson ¹⁰⁹, S. Simsek ⁸³, S. Sindhu ⁵⁶, P. Sinervo ¹⁶²,
 S.N. Singh ²⁷, S. Singh ³⁰, S. Sinha ⁴⁹, S. Sinha ¹⁰⁴, M. Sioli ^{24b,24a}, K. Sioulas ⁹, I. Siral ³⁷,
 E. Sitnikova ⁴⁹, J. Sjölin ^{48a,48b}, A. Skaf ⁵⁶, E. Skorda ²¹, P. Skubic ¹²⁴, M. Slawinska ⁸⁸,
 I. Slazyk ¹⁷, V. Smakhtin ¹⁷⁶, B.H. Smart ¹³⁸, S.Yu. Smirnov ^{141b}, Y. Smirnov ³⁹,
 L.N. Smirnova ^{39,a}, O. Smirnova ¹⁰¹, A.C. Smith ⁴³, D.R. Smith ¹⁶⁶, E.A. Smith ⁴¹, J.L. Smith ¹⁰⁴,
 M.B. Smith ³⁵, R. Smith ¹⁵⁰, H. Smitmanns ¹⁰³, M. Smizanska ⁹⁴, K. Smolek ¹³⁶,
 A.A. Snesarev ⁴⁰, H.L. Snoek ¹¹⁸, S. Snyder ³⁰, R. Sobie ^{172,ab}, A. Soffer ¹⁵⁸,
 C.A. Solans Sanchez ³⁷, E.Yu. Soldatov ⁴⁰, U. Soldevila ¹⁷⁰, A.A. Solodkov ^{34g}, S. Solomon ²⁷,
 A. Soloshenko ⁴⁰, K. Solovieva ⁵⁵, O.V. Solovyanov ⁴², P. Sommer ⁵¹, A. Sonay ¹³,
 W.Y. Song ^{163b}, A. Sopczak ¹³⁶, A.L. Soppio ⁵³, F. Sopkova ^{29b}, J.D. Sorenson ¹¹⁶,
 I.R. Sotarriva Alvarez ¹⁴², V. Sothilingam ^{64a}, O.J. Soto Sandoval ^{141c,141b}, S. Sottocornola ⁶⁹,
 R. Soualah ^{89b}, Z. Soumami ^{36e}, D. South ⁴⁹, N. Soybelman ¹⁷⁶, S. Spagnolo ^{71a,71b},
 M. Spalla ¹¹³, D. Sperlich ⁵⁵, B. Spisso ^{73a,73b}, D.P. Spiteri ⁶⁰, M. Spousta ¹³⁷, E.J. Staats ³⁵,
 R. Stamen ^{64a}, E. Stanecka ⁸⁸, W. Stanek-Maslouska ⁴⁹, M.V. Stange ⁵¹, B. Stanislaus ^{18a},
 M.M. Stanitzki ⁴⁹, B. Stapf ⁴⁹, E.A. Starchenko ³⁹, G.H. Stark ¹⁴⁰, J. Stark ⁹², P. Staroba ¹³⁵,
 P. Starovoitov ^{89b}, R. Staszewski ⁸⁸, G. Stavropoulos ⁴⁷, A. Steff ³⁷, P. Steinberg ³⁰,
 B. Stelzer ^{149,163a}, H.J. Stelzer ¹³³, O. Stelzer-Chilton ^{163a}, H. Stenzel ⁵⁹, T.J. Stevenson ¹⁵³,
 G.A. Stewart ³⁷, J.R. Stewart ¹²⁵, M.C. Stockton ³⁷, G. Stoicea ^{28b}, M. Stolarski ^{134a},
 S. Stonjek ¹¹³, A. Straessner ⁵¹, J. Strandberg ¹⁵¹, S. Strandberg ^{48a,48b}, M. Stratmann ¹⁷⁸,
 M. Strauss ¹²⁴, T. Strebler ¹⁰⁵, P. Strizenec ^{29b}, R. Ströhmer ¹⁷³, D.M. Strom ¹²⁷,
 R. Stroynowski ⁴⁶, A. Strubig ^{48a,48b}, S.A. Stucci ³⁰, B. Stugu ¹⁷, J. Stupak ¹²⁴, N.A. Styles ⁴⁹,
 D. Su ¹⁵⁰, S. Su ⁶³, W. Su ^{145b}, X. Su ⁶³, D. Suchy ^{29a}, K. Sugizaki ¹³², V.V. Sulin ³⁹,
 M.J. Sullivan ⁹⁵, D.M.S. Sultan ¹³⁰, L. Sultanaliyeva ³⁹, S. Sultansoy ^{3b}, S. Sun ¹⁷⁷, W. Sun ¹⁴,
 O. Sunneborn Gudnadottir ¹⁶⁸, N. Sur ¹⁰⁵, M.R. Sutton ¹⁵³, H. Suzuki ¹⁶⁴, M. Svatos ¹³⁵,
 P.N. Swallow ³³, M. Swiatlowski ^{163a}, T. Swirski ¹⁷³, I. Sykora ^{29a}, M. Sykora ¹³⁷,
 T. Sykora ¹³⁷, D. Ta ¹⁰³, K. Tackmann ^{49,y}, A. Taffard ¹⁶⁶, R. Tafirout ^{163a}, J.S. Tafoya Vargas ⁶⁷,
 Y. Takubo ⁸⁵, M. Talby ¹⁰⁵, A.A. Talyshev ³⁹, K.C. Tam ^{65b}, N.M. Tamir ¹⁵⁸, A. Tanaka ¹⁶⁰,
 J. Tanaka ¹⁶⁰, R. Tanaka ⁶⁷, M. Tanasini ¹⁵², Z. Tao ¹⁷¹, S. Tapia Araya ^{141f}, S. Tapprogge ¹⁰³,
 A. Tarek Abouelfadl Mohamed ¹¹⁰, S. Tarem ¹⁵⁷, K. Tariq ¹⁴, G. Tarna ^{28b}, G.F. Tartarelli ^{72a},
 M.J. Tartarin ⁹², P. Tas ¹³⁷, M. Tasevsky ¹³⁵, E. Tassi ^{45b,45a}, A.C. Tate ¹⁶⁹, G. Tateno ¹⁶⁰,
 Y. Tayalati ^{36e,aa}, G.N. Taylor ¹⁰⁸, W. Taylor ^{163b}, A.S. Tegetmeier ⁹², P. Teixeira-Dias ⁹⁸,
 J.J. Teoh ¹⁶², K. Terashi ¹⁶⁰, J. Terron ¹⁰², S. Terzo ¹³, M. Testa ⁵⁴, R.J. Teuscher ^{162,ab},
 A. Thaler ⁸⁰, O. Theiner ⁵⁷, T. Theveneaux-Pelzer ¹⁰⁵, O. Thielmann ¹⁷⁸, D.W. Thomas ⁹⁸,
 J.P. Thomas ²¹, E.A. Thompson ^{18a}, P.D. Thompson ²¹, E. Thomson ¹³², R.E. Thornberry ⁴⁶,
 C. Tian ⁶³, Y. Tian ⁵⁷, V. Tikhomirov ^{39,a}, Yu.A. Tikhonov ³⁹, S. Timoshenko ³⁹, D. Timoshyn ¹³⁷,
 E.X.L. Ting ¹, P. Tipton ¹⁷⁹, A. Tishelman-Charny ³⁰, S.H. Tlou ^{34g}, K. Todome ¹⁴²,
 S. Todorova-Nova ¹³⁷, S. Todt ⁵¹, L. Toffolin ^{70a,70c}, M. Togawa ⁸⁵, J. Tojo ⁹¹, S. Tokár ^{29a},

O. Toldaiev ⁶⁹, G. Tolkachev ¹⁰⁵, M. Tomoto ^{85,114}, L. Tompkins ^{150,o}, E. Torrence ¹²⁷, H. Torres ⁹², E. Torró Pastor ¹⁷⁰, M. Toscani ³¹, C. Toscirci ⁴¹, M. Tost ¹¹, D.R. Tovey ¹⁴⁶, T. Trefzger ¹⁷³, A. Tricoli ³⁰, I.M. Trigger ^{163a}, S. Trincaz-Duvoid ¹³¹, D.A. Trischuk ²⁷, A. Tropina ⁴⁰, L. Truong ^{34c}, M. Trzebinski ⁸⁸, A. Trzupiek ⁸⁸, F. Tsai ¹⁵², M. Tsai ¹⁰⁹, A. Tsiamis ¹⁵⁹, P.V. Tsiareshka ⁴⁰, S. Tsigaridas ^{163a}, A. Tsirigotis ^{159,u}, V. Tsiskaridze ¹⁶², E.G. Tskhadadze ^{156a}, M. Tsopoulou ¹⁵⁹, Y. Tsujikawa ⁹⁰, I.I. Tsukerman ³⁹, V. Tsulaia ^{18a}, S. Tsuno ⁸⁵, K. Tsuru ¹²², D. Tsybychev ¹⁵², Y. Tu ^{65b}, A. Tudorache ^{28b}, V. Tudorache ^{28b}, S. Turchikhin ^{58b,58a}, I. Turk Cakir ^{3a}, R. Turra ^{72a}, T. Turtuvshin ⁴⁰, P.M. Tuts ⁴³, S. Tzamarias ^{159,e}, E. Tzovara ¹⁰³, F. Ukegawa ¹⁶⁴, P.A. Ulloa Poblete ^{141c,141b}, E.N. Umaka ³⁰, G. Unal ³⁷, A. Undrus ³⁰, G. Unel ¹⁶⁶, J. Urban ^{29b}, P. Urrejola ^{141a}, G. Usai ⁸, R. Ushioda ¹⁶¹, M. Usman ¹¹¹, F. Ustuner ⁵³, Z. Uysal ⁸³, V. Vacek ¹³⁶, B. Vachon ¹⁰⁷, T. Vafeiadis ³⁷, A. Vaitkus ⁹⁹, C. Valderanis ¹¹², E. Valdes Santurio ^{48a,48b}, M. Valente ^{163a}, S. Valentinetti ^{24b,24a}, A. Valero ¹⁷⁰, E. Valiente Moreno ¹⁷⁰, A. Vallier ⁹², J.A. Valls Ferrer ¹⁷⁰, D.R. Van Arneeman ¹¹⁸, T.R. Van Daalen ¹⁴³, A. Van Der Graaf ⁵⁰, H.Z. Van Der Schyf ^{34g}, P. Van Gemmeren ⁶, M. Van Rijnbach ³⁷, S. Van Stroud ⁹⁹, I. Van Vulpen ¹¹⁸, P. Vana ¹³⁷, M. Vanadia ^{77a,77b}, U.M. Vande Voorde ¹⁵¹, W. Vandelli ³⁷, E.R. Vandewall ¹²⁵, D. Vannicola ¹⁵⁸, L. Vannoli ⁵⁴, R. Vari ^{76a}, E.W. Varnes ⁷, C. Varni ^{18b}, D. Varouchas ⁶⁷, L. Varriale ¹⁷⁰, K.E. Varvell ¹⁵⁴, M.E. Vasile ^{28b}, L. Vaslin ⁸⁵, A. Vasyukov ⁴⁰, L.M. Vaughan ¹²⁵, R. Vavricka ¹³⁷, T. Vazquez Schroeder ¹³, J. Veatch ³², V. Vecchio ¹⁰⁴, M.J. Veen ¹⁰⁶, I. Veliscek ³⁰, L.M. Veloce ¹⁶², F. Veloso ^{134a,134c}, S. Veneziano ^{76a}, A. Ventura ^{71a,71b}, S. Ventura Gonzalez ¹³⁹, A. Verbytskyi ¹¹³, M. Verducci ^{75a,75b}, C. Vergis ⁹⁷, M. Verissimo De Araujo ^{84b}, W. Verkerke ¹¹⁸, J.C. Vermeulen ¹¹⁸, C. Vernieri ¹⁵⁰, M. Vessella ¹⁶⁶, M.C. Vetterli ^{149,ag}, A. Vgenopoulos ¹⁰³, N. Viaux Maira ^{141f}, T. Vickey ¹⁴⁶, O.E. Vickey Boeriu ¹⁴⁶, G.H.A. Viehhauser ¹³⁰, L. Vigani ^{64b}, M. Vigl ¹¹³, M. Villa ^{24b,24a}, M. Villaplana Perez ¹⁷⁰, E.M. Villhauer ⁵³, E. Vilucchi ⁵⁴, M.G. Vincter ³⁵, A. Visibile ¹¹⁸, C. Vittori ³⁷, I. Vivarelli ^{24b,24a}, E. Voevodina ¹¹³, F. Vogel ¹¹², J.C. Voigt ⁵¹, P. Vokac ¹³⁶, Yu. Volkotrub ^{87b}, E. Von Toerne ²⁵, B. Vormwald ³⁷, K. Vorobev ³⁹, M. Vos ¹⁷⁰, K. Voss ¹⁴⁸, M. Vozak ³⁷, L. Vozdecky ¹²⁴, N. Vranjes ¹⁶, M. Vranjes Milosavljevic ¹⁶, M. Vreeswijk ¹¹⁸, N.K. Vu ^{145b,145a}, R. Vuillermet ³⁷, O. Vujinovic ¹⁰³, I. Vukotic ⁴¹, I.K. Vyas ³⁵, S. Wada ¹⁶⁴, C. Wagner ¹⁵⁰, J.M. Wagner ^{18a}, W. Wagner ¹⁷⁸, S. Wahdan ¹⁷⁸, H. Wahlberg ⁹³, C.H. Waits ¹²⁴, J. Walder ¹³⁸, R. Walker ¹¹², W. Walkowiak ¹⁴⁸, A. Wall ¹³², E.J. Wallin ¹⁰¹, T. Wamorkar ^{18a}, A.Z. Wang ¹⁴⁰, C. Wang ¹⁰³, C. Wang ¹¹, H. Wang ^{18a}, J. Wang ^{65c}, P. Wang ¹⁰⁴, P. Wang ⁹⁹, R. Wang ⁶², R. Wang ⁶, S.M. Wang ¹⁵⁵, S. Wang ¹⁴, T. Wang ⁶³, T. Wang ⁶³, W.T. Wang ⁸¹, W. Wang ¹⁴, X. Wang ¹⁶⁹, X. Wang ^{145a}, X. Wang ⁴⁹, Y. Wang ^{115a}, Y. Wang ⁶³, Z. Wang ¹⁰⁹, Z. Wang ^{145b,52,145a}, Z. Wang ¹⁰⁹, C. Wanotayaroj ⁸⁵, A. Warburton ¹⁰⁷, R.J. Ward ²¹, A.L. Warnerbring ¹⁴⁸, N. Warrack ⁶⁰, S. Waterhouse ⁹⁸, A.T. Watson ²¹, H. Watson ⁵³, M.F. Watson ²¹, E. Watton ⁶⁰, G. Watts ¹⁴³, B.M. Waugh ⁹⁹, J.M. Webb ⁵⁵, C. Weber ³⁰, H.A. Weber ¹⁹, M.S. Weber ²⁰, S.M. Weber ^{64a}, C. Wei ⁶³, Y. Wei ⁵⁵, A.R. Weidberg ¹³⁰, E.J. Weik ¹²¹, J. Weingarten ⁵⁰, C. Weiser ⁵⁵, C.J. Wells ⁴⁹, T. Wenaus ³⁰, B. Wendland ⁵⁰, T. Wengler ³⁷, N.S. Wenke ¹¹³, N. Wermes ²⁵, M. Wessels ^{64a}, A.M. Wharton ⁹⁴, A.S. White ⁶², A. White ⁸, M.J. White ¹, D. Whiteson ¹⁶⁶, L. Wickremasinghe ¹²⁸, W. Wiedenmann ¹⁷⁷, M. Wielers ¹³⁸, C. Wigglesworth ⁴⁴, D.J. Wilbern ¹²⁴, H.G. Wilkens ³⁷, J.J.H. Wilkinson ³³, D.M. Williams ⁴³, H.H. Williams ¹³², S. Williams ³³, S. Willocq ¹⁰⁶, B.J. Wilson ¹⁰⁴, D.J. Wilson ¹⁰⁴, P.J. Windischhofer ⁴¹, F.I. Winkel ³¹, F. Winklmeier ¹²⁷, B.T. Winter ⁵⁵, M. Wittgen ¹⁵⁰, M. Wobisch ¹⁰⁰, T. Wojtkowski ⁶¹, Z. Wolffs ¹¹⁸, J. Wollrath ³⁷, M.W. Wolter ⁸⁸, H. Wolters ^{134a,134c}, M.C. Wong ¹⁴⁰, E.L. Woodward ⁴³, S.D. Worm ⁴⁹, B.K. Wosiek ⁸⁸, K.W. Woźniak ⁸⁸, S. Wozniowski ⁵⁶, K. Wraight ⁶⁰, C. Wu ²¹, M. Wu ^{115b}, M. Wu ¹¹⁷, S.L. Wu ¹⁷⁷, X. Wu ⁵⁷,

X. Wu , Y. Wu , Z. Wu , J. Wuerzinger ^{113,ae}, T.R. Wyatt ¹⁰⁴, B.M. Wynne ⁵³, S. Xella ⁴⁴, L. Xia ^{115a}, M. Xia ¹⁵, M. Xie ⁶³, A. Xiong ¹²⁷, J. Xiong ^{18a}, D. Xu ¹⁴, H. Xu ⁶³, L. Xu ⁶³, R. Xu ¹³², T. Xu ¹⁰⁹, Y. Xu ¹⁴³, Z. Xu ⁵³, Z. Xu ^{115a}, B. Yabsley ¹⁵⁴, S. Yacoob ^{34a}, Y. Yamaguchi ⁸⁵, E. Yamashita ¹⁶⁰, H. Yamauchi ¹⁶⁴, T. Yamazaki ^{18a}, Y. Yamazaki ⁸⁶, S. Yan ⁶⁰, Z. Yan ¹⁰⁶, H.J. Yang ^{145a,145b}, H.T. Yang ⁶³, S. Yang ⁶³, T. Yang ^{65c}, X. Yang ³⁷, X. Yang ¹⁴, Y. Yang ⁴⁶, Y. Yang ⁶³, W-M. Yao ^{18a}, C.L. Yardley ¹⁵³, H. Ye ⁵⁶, J. Ye ¹⁴, S. Ye ³⁰, X. Ye ⁶³, Y. Yeh ⁹⁹, I. Yeletsikh ⁴⁰, B. Yeo ^{18b}, M.R. Yexley ⁹⁹, T.P. Yildirim ¹³⁰, P. Yin ⁴³, K. Yorita ¹⁷⁵, S. Younas ^{28b}, C.J.S. Young ³⁷, C. Young ¹⁵⁰, N.D. Young ¹²⁷, Y. Yu ⁶³, J. Yuan ^{14,115c}, M. Yuan ¹⁰⁹, R. Yuan ^{145b,145a}, L. Yue ⁹⁹, M. Zaazoua ⁶³, B. Zabinski ⁸⁸, I. Zahir ^{36a}, Z.K. Zak ⁸⁸, T. Zakareishvili ¹⁷⁰, S. Zambito ⁵⁷, J.A. Zamora Saa ^{141d,141b}, J. Zang ¹⁶⁰, D. Zanzi ⁵⁵, R. Zanzottera ^{72a,72b}, O. Zaplatilek ¹³⁶, C. Zeitnitz ¹⁷⁸, H. Zeng ¹⁴, J.C. Zeng ¹⁶⁹, D.T. Zenger Jr ²⁷, O. Zenin ³⁹, T. Ženiš ^{29a}, S. Zenz ⁹⁷, S. Zerradi ^{36a}, D. Zerwas ⁶⁷, M. Zhai ^{14,115c}, D.F. Zhang ¹⁴⁶, J. Zhang ^{144a}, J. Zhang ⁶, K. Zhang ^{14,115c}, L. Zhang ⁶³, L. Zhang ^{115a}, P. Zhang ^{14,115c}, R. Zhang ¹⁷⁷, S. Zhang ⁹², T. Zhang ¹⁶⁰, X. Zhang ^{145a}, Y. Zhang ¹⁴³, Y. Zhang ⁹⁹, Y. Zhang ⁶³, Y. Zhang ^{115a}, Z. Zhang ^{18a}, Z. Zhang ^{144a}, Z. Zhang ⁶⁷, H. Zhao ¹⁴³, T. Zhao ^{144a}, Y. Zhao ³⁵, Z. Zhao ⁶³, Z. Zhao ⁶³, A. Zhemchugov ⁴⁰, J. Zheng ^{115a}, K. Zheng ¹⁶⁹, X. Zheng ⁶³, Z. Zheng ¹⁵⁰, D. Zhong ¹⁶⁹, B. Zhou ¹⁰⁹, H. Zhou ⁷, N. Zhou ^{145a}, Y. Zhou ¹⁵, Y. Zhou ^{115a}, Y. Zhou ⁷, C.G. Zhu ^{144a}, J. Zhu ¹⁰⁹, X. Zhu ^{145b}, Y. Zhu ^{145a}, Y. Zhu ⁶³, X. Zhuang ¹⁴, K. Zhukov ⁶⁹, N.I. Zimine ⁴⁰, J. Zinsser ^{64b}, M. Ziolkowski ¹⁴⁸, L. Živković ¹⁶, A. Zoccoli ^{24b,24a}, K. Zoch ⁶², T.G. Zorbas ¹⁴⁶, O. Zormpa ⁴⁷, W. Zou ⁴³, L. Zwalinski ³⁷.

¹Department of Physics, University of Adelaide, Adelaide; Australia.

²Department of Physics, University of Alberta, Edmonton AB; Canada.

³(^a)Department of Physics, Ankara University, Ankara; (^b)Division of Physics, TOBB University of Economics and Technology, Ankara; Türkiye.

⁴LAPP, Université Savoie Mont Blanc, CNRS/IN2P3, Annecy; France.

⁵APC, Université Paris Cité, CNRS/IN2P3, Paris; France.

⁶High Energy Physics Division, Argonne National Laboratory, Argonne IL; United States of America.

⁷Department of Physics, University of Arizona, Tucson AZ; United States of America.

⁸Department of Physics, University of Texas at Arlington, Arlington TX; United States of America.

⁹Physics Department, National and Kapodistrian University of Athens, Athens; Greece.

¹⁰Physics Department, National Technical University of Athens, Zografou; Greece.

¹¹Department of Physics, University of Texas at Austin, Austin TX; United States of America.

¹²Institute of Physics, Azerbaijan Academy of Sciences, Baku; Azerbaijan.

¹³Institut de Física d'Altes Energies (IFAE), Barcelona Institute of Science and Technology, Barcelona; Spain.

¹⁴Institute of High Energy Physics, Chinese Academy of Sciences, Beijing; China.

¹⁵Physics Department, Tsinghua University, Beijing; China.

¹⁶Institute of Physics, University of Belgrade, Belgrade; Serbia.

¹⁷Department for Physics and Technology, University of Bergen, Bergen; Norway.

¹⁸(^a)Physics Division, Lawrence Berkeley National Laboratory, Berkeley CA; (^b)University of California, Berkeley CA; United States of America.

¹⁹Institut für Physik, Humboldt Universität zu Berlin, Berlin; Germany.

²⁰Albert Einstein Center for Fundamental Physics and Laboratory for High Energy Physics, University of Bern, Bern; Switzerland.

²¹School of Physics and Astronomy, University of Birmingham, Birmingham; United Kingdom.

- ^{22(a)}Department of Physics, Bogazici University, Istanbul;^(b)Department of Physics Engineering, Gaziantep University, Gaziantep;^(c)Department of Physics, Istanbul University, Istanbul; Türkiye.
- ^{23(a)}Facultad de Ciencias y Centro de Investigaciones, Universidad Antonio Nariño, Bogotá;^(b)Departamento de Física, Universidad Nacional de Colombia, Bogotá; Colombia.
- ^{24(a)}Dipartimento di Fisica e Astronomia A. Righi, Università di Bologna, Bologna;^(b)INFN Sezione di Bologna; Italy.
- ²⁵Physikalisches Institut, Universität Bonn, Bonn; Germany.
- ²⁶Department of Physics, Boston University, Boston MA; United States of America.
- ²⁷Department of Physics, Brandeis University, Waltham MA; United States of America.
- ^{28(a)}Transilvania University of Brasov, Brasov;^(b)Horia Hulubei National Institute of Physics and Nuclear Engineering, Bucharest;^(c)Department of Physics, Alexandru Ioan Cuza University of Iasi, Iasi;^(d)National Institute for Research and Development of Isotopic and Molecular Technologies, Physics Department, Cluj-Napoca;^(e)National University of Science and Technology Politehnica, Bucharest;^(f)West University in Timisoara, Timisoara;^(g)Faculty of Physics, University of Bucharest, Bucharest; Romania.
- ^{29(a)}Faculty of Mathematics, Physics and Informatics, Comenius University, Bratislava;^(b)Department of Subnuclear Physics, Institute of Experimental Physics of the Slovak Academy of Sciences, Kosice; Slovak Republic.
- ³⁰Physics Department, Brookhaven National Laboratory, Upton NY; United States of America.
- ³¹Universidad de Buenos Aires, Facultad de Ciencias Exactas y Naturales, Departamento de Física, y CONICET, Instituto de Física de Buenos Aires (IFIBA), Buenos Aires; Argentina.
- ³²California State University, CA; United States of America.
- ³³Cavendish Laboratory, University of Cambridge, Cambridge; United Kingdom.
- ^{34(a)}Department of Physics, University of Cape Town, Cape Town;^(b)iThemba Labs, Western Cape;^(c)Department of Mechanical Engineering Science, University of Johannesburg, Johannesburg;^(d)National Institute of Physics, University of the Philippines Diliman (Philippines);^(e)University of South Africa, Department of Physics, Pretoria;^(f)University of Zululand, KwaDlangezwa;^(g)School of Physics, University of the Witwatersrand, Johannesburg; South Africa.
- ³⁵Department of Physics, Carleton University, Ottawa ON; Canada.
- ^{36(a)}Faculté des Sciences Ain Chock, Université Hassan II de Casablanca;^(b)Faculté des Sciences, Université Ibn-Tofail, Kénitra;^(c)Faculté des Sciences Semailia, Université Cadi Ayyad, LPHEA-Marrakech;^(d)LPMR, Faculté des Sciences, Université Mohamed Premier, Oujda;^(e)Faculté des sciences, Université Mohammed V, Rabat;^(f)Institute of Applied Physics, Mohammed VI Polytechnic University, Ben Guerir; Morocco.
- ³⁷CERN, Geneva; Switzerland.
- ³⁸Affiliated with an institute formerly covered by a cooperation agreement with CERN.
- ³⁹Affiliated with an institute covered by a cooperation agreement with CERN.
- ⁴⁰Affiliated with an international laboratory covered by a cooperation agreement with CERN.
- ⁴¹Enrico Fermi Institute, University of Chicago, Chicago IL; United States of America.
- ⁴²LPC, Université Clermont Auvergne, CNRS/IN2P3, Clermont-Ferrand; France.
- ⁴³Nevis Laboratory, Columbia University, Irvington NY; United States of America.
- ⁴⁴Niels Bohr Institute, University of Copenhagen, Copenhagen; Denmark.
- ^{45(a)}Dipartimento di Fisica, Università della Calabria, Rende;^(b)INFN Gruppo Collegato di Cosenza, Laboratori Nazionali di Frascati; Italy.
- ⁴⁶Physics Department, Southern Methodist University, Dallas TX; United States of America.
- ⁴⁷National Centre for Scientific Research "Demokritos", Agia Paraskevi; Greece.
- ^{48(a)}Department of Physics, Stockholm University;^(b)Oskar Klein Centre, Stockholm; Sweden.
- ⁴⁹Deutsches Elektronen-Synchrotron DESY, Hamburg and Zeuthen; Germany.

- ⁵⁰Fakultät Physik , Technische Universität Dortmund, Dortmund; Germany.
- ⁵¹Institut für Kern- und Teilchenphysik, Technische Universität Dresden, Dresden; Germany.
- ⁵²Department of Physics, Duke University, Durham NC; United States of America.
- ⁵³SUPA - School of Physics and Astronomy, University of Edinburgh, Edinburgh; United Kingdom.
- ⁵⁴INFN e Laboratori Nazionali di Frascati, Frascati; Italy.
- ⁵⁵Physikalisches Institut, Albert-Ludwigs-Universität Freiburg, Freiburg; Germany.
- ⁵⁶II. Physikalisches Institut, Georg-August-Universität Göttingen, Göttingen; Germany.
- ⁵⁷Département de Physique Nucléaire et Corpusculaire, Université de Genève, Genève; Switzerland.
- ⁵⁸(^a)Dipartimento di Fisica, Università di Genova, Genova;(^b)INFN Sezione di Genova; Italy.
- ⁵⁹II. Physikalisches Institut, Justus-Liebig-Universität Giessen, Giessen; Germany.
- ⁶⁰SUPA - School of Physics and Astronomy, University of Glasgow, Glasgow; United Kingdom.
- ⁶¹LPSC, Université Grenoble Alpes, CNRS/IN2P3, Grenoble INP, Grenoble; France.
- ⁶²Laboratory for Particle Physics and Cosmology, Harvard University, Cambridge MA; United States of America.
- ⁶³Department of Modern Physics and State Key Laboratory of Particle Detection and Electronics, University of Science and Technology of China, Hefei; China.
- ⁶⁴(^a)Kirchhoff-Institut für Physik, Ruprecht-Karls-Universität Heidelberg, Heidelberg;(^b)Physikalisches Institut, Ruprecht-Karls-Universität Heidelberg, Heidelberg; Germany.
- ⁶⁵(^a)Department of Physics, Chinese University of Hong Kong, Shatin, N.T., Hong Kong;(^b)Department of Physics, University of Hong Kong, Hong Kong;(^c)Department of Physics and Institute for Advanced Study, Hong Kong University of Science and Technology, Clear Water Bay, Kowloon, Hong Kong; China.
- ⁶⁶Department of Physics, National Tsing Hua University, Hsinchu; Taiwan.
- ⁶⁷IJCLab, Université Paris-Saclay, CNRS/IN2P3, 91405, Orsay; France.
- ⁶⁸Centro Nacional de Microelectrónica (IMB-CNM-CSIC), Barcelona; Spain.
- ⁶⁹Department of Physics, Indiana University, Bloomington IN; United States of America.
- ⁷⁰(^a)INFN Gruppo Collegato di Udine, Sezione di Trieste, Udine;(^b)ICTP, Trieste;(^c)Dipartimento Politecnico di Ingegneria e Architettura, Università di Udine, Udine; Italy.
- ⁷¹(^a)INFN Sezione di Lecce;(^b)Dipartimento di Matematica e Fisica, Università del Salento, Lecce; Italy.
- ⁷²(^a)INFN Sezione di Milano;(^b)Dipartimento di Fisica, Università di Milano, Milano; Italy.
- ⁷³(^a)INFN Sezione di Napoli;(^b)Dipartimento di Fisica, Università di Napoli, Napoli; Italy.
- ⁷⁴(^a)INFN Sezione di Pavia;(^b)Dipartimento di Fisica, Università di Pavia, Pavia; Italy.
- ⁷⁵(^a)INFN Sezione di Pisa;(^b)Dipartimento di Fisica E. Fermi, Università di Pisa, Pisa; Italy.
- ⁷⁶(^a)INFN Sezione di Roma;(^b)Dipartimento di Fisica, Sapienza Università di Roma, Roma; Italy.
- ⁷⁷(^a)INFN Sezione di Roma Tor Vergata;(^b)Dipartimento di Fisica, Università di Roma Tor Vergata, Roma; Italy.
- ⁷⁸(^a)INFN Sezione di Roma Tre;(^b)Dipartimento di Matematica e Fisica, Università Roma Tre, Roma; Italy.
- ⁷⁹(^a)INFN-TIFPA;(^b)Università degli Studi di Trento, Trento; Italy.
- ⁸⁰Universität Innsbruck, Department of Astro and Particle Physics, Innsbruck; Austria.
- ⁸¹University of Iowa, Iowa City IA; United States of America.
- ⁸²Department of Physics and Astronomy, Iowa State University, Ames IA; United States of America.
- ⁸³Istinye University, Sariyer, Istanbul; Türkiye.
- ⁸⁴(^a)Departamento de Engenharia Elétrica, Universidade Federal de Juiz de Fora (UFJF), Juiz de Fora;(^b)Universidade Federal do Rio De Janeiro COPPE/EE/IF, Rio de Janeiro;(^c)Instituto de Física, Universidade de São Paulo, São Paulo;(^d)Rio de Janeiro State University, Rio de Janeiro;(^e)Federal University of Bahia, Bahia; Brazil.
- ⁸⁵KEK, High Energy Accelerator Research Organization, Tsukuba; Japan.

- ⁸⁶Graduate School of Science, Kobe University, Kobe; Japan.
- ⁸⁷(^a) AGH University of Krakow, Faculty of Physics and Applied Computer Science, Krakow; (^b) Marian Smoluchowski Institute of Physics, Jagiellonian University, Krakow; Poland.
- ⁸⁸Institute of Nuclear Physics Polish Academy of Sciences, Krakow; Poland.
- ⁸⁹(^a) Khalifa University of Science and Technology, Abu Dhabi; (^b) University of Sharjah, Sharjah; United Arab Emirates.
- ⁹⁰Faculty of Science, Kyoto University, Kyoto; Japan.
- ⁹¹Research Center for Advanced Particle Physics and Department of Physics, Kyushu University, Fukuoka ; Japan.
- ⁹²L2IT, Université de Toulouse, CNRS/IN2P3, UPS, Toulouse; France.
- ⁹³Instituto de Física La Plata, Universidad Nacional de La Plata and CONICET, La Plata; Argentina.
- ⁹⁴Physics Department, Lancaster University, Lancaster; United Kingdom.
- ⁹⁵Oliver Lodge Laboratory, University of Liverpool, Liverpool; United Kingdom.
- ⁹⁶Department of Experimental Particle Physics, Jožef Stefan Institute and Department of Physics, University of Ljubljana, Ljubljana; Slovenia.
- ⁹⁷School of Physics and Astronomy, Queen Mary University of London, London; United Kingdom.
- ⁹⁸Department of Physics, Royal Holloway University of London, Egham; United Kingdom.
- ⁹⁹Department of Physics and Astronomy, University College London, London; United Kingdom.
- ¹⁰⁰Louisiana Tech University, Ruston LA; United States of America.
- ¹⁰¹Fysiska institutionen, Lunds universitet, Lund; Sweden.
- ¹⁰²Departamento de Física Teórica C-15 and CIAFF, Universidad Autónoma de Madrid, Madrid; Spain.
- ¹⁰³Institut für Physik, Universität Mainz, Mainz; Germany.
- ¹⁰⁴School of Physics and Astronomy, University of Manchester, Manchester; United Kingdom.
- ¹⁰⁵CPPM, Aix-Marseille Université, CNRS/IN2P3, Marseille; France.
- ¹⁰⁶Department of Physics, University of Massachusetts, Amherst MA; United States of America.
- ¹⁰⁷Department of Physics, McGill University, Montreal QC; Canada.
- ¹⁰⁸School of Physics, University of Melbourne, Victoria; Australia.
- ¹⁰⁹Department of Physics, University of Michigan, Ann Arbor MI; United States of America.
- ¹¹⁰Department of Physics and Astronomy, Michigan State University, East Lansing MI; United States of America.
- ¹¹¹Group of Particle Physics, University of Montreal, Montreal QC; Canada.
- ¹¹²Fakultät für Physik, Ludwig-Maximilians-Universität München, München; Germany.
- ¹¹³Max-Planck-Institut für Physik (Werner-Heisenberg-Institut), München; Germany.
- ¹¹⁴Graduate School of Science and Kobayashi-Maskawa Institute, Nagoya University, Nagoya; Japan.
- ¹¹⁵(^a) Department of Physics, Nanjing University, Nanjing; (^b) School of Science, Shenzhen Campus of Sun Yat-sen University; (^c) University of Chinese Academy of Science (UCAS), Beijing; China.
- ¹¹⁶Department of Physics and Astronomy, University of New Mexico, Albuquerque NM; United States of America.
- ¹¹⁷Institute for Mathematics, Astrophysics and Particle Physics, Radboud University/Nikhef, Nijmegen; Netherlands.
- ¹¹⁸Nikhef National Institute for Subatomic Physics and University of Amsterdam, Amsterdam; Netherlands.
- ¹¹⁹Department of Physics, Northern Illinois University, DeKalb IL; United States of America.
- ¹²⁰(^a) New York University Abu Dhabi, Abu Dhabi; (^b) United Arab Emirates University, Al Ain; United Arab Emirates.
- ¹²¹Department of Physics, New York University, New York NY; United States of America.
- ¹²²Ochanomizu University, Otsuka, Bunkyo-ku, Tokyo; Japan.

- ¹²³Ohio State University, Columbus OH; United States of America.
- ¹²⁴Homer L. Dodge Department of Physics and Astronomy, University of Oklahoma, Norman OK; United States of America.
- ¹²⁵Department of Physics, Oklahoma State University, Stillwater OK; United States of America.
- ¹²⁶Palacký University, Joint Laboratory of Optics, Olomouc; Czech Republic.
- ¹²⁷Institute for Fundamental Science, University of Oregon, Eugene, OR; United States of America.
- ¹²⁸Graduate School of Science, Osaka University, Osaka; Japan.
- ¹²⁹Department of Physics, University of Oslo, Oslo; Norway.
- ¹³⁰Department of Physics, Oxford University, Oxford; United Kingdom.
- ¹³¹LPNHE, Sorbonne Université, Université Paris Cité, CNRS/IN2P3, Paris; France.
- ¹³²Department of Physics, University of Pennsylvania, Philadelphia PA; United States of America.
- ¹³³Department of Physics and Astronomy, University of Pittsburgh, Pittsburgh PA; United States of America.
- ¹³⁴(^a) Laboratório de Instrumentação e Física Experimental de Partículas - LIP, Lisboa; (^b) Departamento de Física, Faculdade de Ciências, Universidade de Lisboa, Lisboa; (^c) Departamento de Física, Universidade de Coimbra, Coimbra; (^d) Centro de Física Nuclear da Universidade de Lisboa, Lisboa; (^e) Departamento de Física, Universidade do Minho, Braga; (^f) Departamento de Física Teórica y del Cosmos, Universidad de Granada, Granada (Spain); (^g) Departamento de Física, Instituto Superior Técnico, Universidade de Lisboa, Lisboa; Portugal.
- ¹³⁵Institute of Physics of the Czech Academy of Sciences, Prague; Czech Republic.
- ¹³⁶Czech Technical University in Prague, Prague; Czech Republic.
- ¹³⁷Charles University, Faculty of Mathematics and Physics, Prague; Czech Republic.
- ¹³⁸Particle Physics Department, Rutherford Appleton Laboratory, Didcot; United Kingdom.
- ¹³⁹IRFU, CEA, Université Paris-Saclay, Gif-sur-Yvette; France.
- ¹⁴⁰Santa Cruz Institute for Particle Physics, University of California Santa Cruz, Santa Cruz CA; United States of America.
- ¹⁴¹(^a) Departamento de Física, Pontificia Universidad Católica de Chile, Santiago; (^b) Millennium Institute for Subatomic physics at high energy frontier (SAPHIR), Santiago; (^c) Instituto de Investigación Multidisciplinario en Ciencia y Tecnología, y Departamento de Física, Universidad de La Serena; (^d) Universidad Andres Bello, Department of Physics, Santiago; (^e) Instituto de Alta Investigación, Universidad de Tarapacá, Arica; (^f) Departamento de Física, Universidad Técnica Federico Santa María, Valparaíso; Chile.
- ¹⁴²Department of Physics, Institute of Science, Tokyo; Japan.
- ¹⁴³Department of Physics, University of Washington, Seattle WA; United States of America.
- ¹⁴⁴(^a) Institute of Frontier and Interdisciplinary Science and Key Laboratory of Particle Physics and Particle Irradiation (MOE), Shandong University, Qingdao; (^b) School of Physics, Zhengzhou University; China.
- ¹⁴⁵(^a) School of Physics and Astronomy, Shanghai Jiao Tong University, Key Laboratory for Particle Astrophysics and Cosmology (MOE), SKLPPC, Shanghai; (^b) Tsung-Dao Lee Institute, Shanghai; China.
- ¹⁴⁶Department of Physics and Astronomy, University of Sheffield, Sheffield; United Kingdom.
- ¹⁴⁷Department of Physics, Shinshu University, Nagano; Japan.
- ¹⁴⁸Department Physik, Universität Siegen, Siegen; Germany.
- ¹⁴⁹Department of Physics, Simon Fraser University, Burnaby BC; Canada.
- ¹⁵⁰SLAC National Accelerator Laboratory, Stanford CA; United States of America.
- ¹⁵¹Department of Physics, Royal Institute of Technology, Stockholm; Sweden.
- ¹⁵²Departments of Physics and Astronomy, Stony Brook University, Stony Brook NY; United States of America.
- ¹⁵³Department of Physics and Astronomy, University of Sussex, Brighton; United Kingdom.

- ¹⁵⁴School of Physics, University of Sydney, Sydney; Australia.
- ¹⁵⁵Institute of Physics, Academia Sinica, Taipei; Taiwan.
- ¹⁵⁶(^a) E. Andronikashvili Institute of Physics, Iv. Javakhishvili Tbilisi State University, Tbilisi; (^b) High Energy Physics Institute, Tbilisi State University, Tbilisi; (^c) University of Georgia, Tbilisi; Georgia.
- ¹⁵⁷Department of Physics, Technion, Israel Institute of Technology, Haifa; Israel.
- ¹⁵⁸Raymond and Beverly Sackler School of Physics and Astronomy, Tel Aviv University, Tel Aviv; Israel.
- ¹⁵⁹Department of Physics, Aristotle University of Thessaloniki, Thessaloniki; Greece.
- ¹⁶⁰International Center for Elementary Particle Physics and Department of Physics, University of Tokyo, Tokyo; Japan.
- ¹⁶¹Graduate School of Science and Technology, Tokyo Metropolitan University, Tokyo; Japan.
- ¹⁶²Department of Physics, University of Toronto, Toronto ON; Canada.
- ¹⁶³(^a) TRIUMF, Vancouver BC; (^b) Department of Physics and Astronomy, York University, Toronto ON; Canada.
- ¹⁶⁴Division of Physics and Tomonaga Center for the History of the Universe, Faculty of Pure and Applied Sciences, University of Tsukuba, Tsukuba; Japan.
- ¹⁶⁵Department of Physics and Astronomy, Tufts University, Medford MA; United States of America.
- ¹⁶⁶Department of Physics and Astronomy, University of California Irvine, Irvine CA; United States of America.
- ¹⁶⁷University of West Attica, Athens; Greece.
- ¹⁶⁸Department of Physics and Astronomy, University of Uppsala, Uppsala; Sweden.
- ¹⁶⁹Department of Physics, University of Illinois, Urbana IL; United States of America.
- ¹⁷⁰Instituto de Física Corpuscular (IFIC), Centro Mixto Universidad de Valencia - CSIC, Valencia; Spain.
- ¹⁷¹Department of Physics, University of British Columbia, Vancouver BC; Canada.
- ¹⁷²Department of Physics and Astronomy, University of Victoria, Victoria BC; Canada.
- ¹⁷³Fakultät für Physik und Astronomie, Julius-Maximilians-Universität Würzburg, Würzburg; Germany.
- ¹⁷⁴Department of Physics, University of Warwick, Coventry; United Kingdom.
- ¹⁷⁵Waseda University, Tokyo; Japan.
- ¹⁷⁶Department of Particle Physics and Astrophysics, Weizmann Institute of Science, Rehovot; Israel.
- ¹⁷⁷Department of Physics, University of Wisconsin, Madison WI; United States of America.
- ¹⁷⁸Fakultät für Mathematik und Naturwissenschaften, Fachgruppe Physik, Bergische Universität Wuppertal, Wuppertal; Germany.
- ¹⁷⁹Department of Physics, Yale University, New Haven CT; United States of America.
- ¹⁸⁰Yerevan Physics Institute, Yerevan; Armenia.
- ^a Also Affiliated with an institute covered by a cooperation agreement with CERN.
- ^b Also at An-Najah National University, Nablus; Palestine.
- ^c Also at Borough of Manhattan Community College, City University of New York, New York NY; United States of America.
- ^d Also at Center for High Energy Physics, Peking University; China.
- ^e Also at Center for Interdisciplinary Research and Innovation (CIRI-AUTH), Thessaloniki; Greece.
- ^f Also at CERN, Geneva; Switzerland.
- ^g Also at CMD-AC UNEC Research Center, Azerbaijan State University of Economics (UNEC); Azerbaijan.
- ^h Also at Département de Physique Nucléaire et Corpusculaire, Université de Genève, Genève; Switzerland.
- ⁱ Also at Departament de Física de la Universitat Autònoma de Barcelona, Barcelona; Spain.
- ^j Also at Department of Financial and Management Engineering, University of the Aegean, Chios; Greece.
- ^k Also at Department of Mathematical Sciences, University of South Africa, Johannesburg; South Africa.

- ^l Also at Department of Physics, Bolu Abant Izzet Baysal University, Bolu; Türkiye.
- ^m Also at Department of Physics, California State University, Sacramento; United States of America.
- ⁿ Also at Department of Physics, King's College London, London; United Kingdom.
- ^o Also at Department of Physics, Stanford University, Stanford CA; United States of America.
- ^p Also at Department of Physics, Stellenbosch University; South Africa.
- ^q Also at Department of Physics, University of Fribourg, Fribourg; Switzerland.
- ^r Also at Department of Physics, University of Thessaly; Greece.
- ^s Also at Department of Physics, Westmont College, Santa Barbara; United States of America.
- ^t Also at Faculty of Physics, Sofia University, 'St. Kliment Ohridski', Sofia; Bulgaria.
- ^u Also at Hellenic Open University, Patras; Greece.
- ^v Also at Henan University; China.
- ^w Also at Imam Mohammad Ibn Saud Islamic University; Saudi Arabia.
- ^x Also at Institutio Catalana de Recerca i Estudis Avancats, ICREA, Barcelona; Spain.
- ^y Also at Institut für Experimentalphysik, Universität Hamburg, Hamburg; Germany.
- ^z Also at Institute for Nuclear Research and Nuclear Energy (INRNE) of the Bulgarian Academy of Sciences, Sofia; Bulgaria.
- ^{aa} Also at Institute of Applied Physics, Mohammed VI Polytechnic University, Ben Guerir; Morocco.
- ^{ab} Also at Institute of Particle Physics (IPP); Canada.
- ^{ac} Also at Institute of Physics, Azerbaijan Academy of Sciences, Baku; Azerbaijan.
- ^{ad} Also at National Institute of Physics, University of the Philippines Diliman (Philippines); Philippines.
- ^{ae} Also at Technical University of Munich, Munich; Germany.
- ^{af} Also at The Collaborative Innovation Center of Quantum Matter (CICQM), Beijing; China.
- ^{ag} Also at TRIUMF, Vancouver BC; Canada.
- ^{ah} Also at Università di Napoli Parthenope, Napoli; Italy.
- ^{ai} Also at University of Colorado Boulder, Department of Physics, Colorado; United States of America.
- ^{aj} Also at University of the Western Cape; South Africa.
- ^{ak} Also at Washington College, Chestertown, MD; United States of America.
- ^{al} Also at Yeditepe University, Physics Department, Istanbul; Türkiye.
- * Deceased